

Understanding the role of the Sonic Hedgehog signaling pathway in cerebellar development
and medulloblastoma genesis

Joyoti Dey

A dissertation
submitted in partial fulfillment of the
requirements for the degree of

Doctor of Philosophy

University of Washington

2012

Reading Committee:

Dr. James M. Olson, Chair

Dr. Leo J. Pallanck

Dr. Stephen J. Tapscott

Program authorized to offer degree
Molecular and Cellular Biology

University of Washington

Abstract

Understanding the role of the Sonic Hedgehog signaling pathway in cerebellar development and medulloblastoma genesis

Joyoti Dey

Chair of Supervisory Committee
Professor James M. Olson
Department of Pediatrics

Medulloblastoma is a developmental cancer of the cerebellum. It continues to be the most common pediatric brain cancer associated with dire survival and impaired quality of life. In order to develop therapeutic interventions, it is necessary to bridge the gaps in knowledge about cerebellar development and understand how aberrations in developmental pathways lead to cancer. The Sonic hedgehog pathway (Shh) plays a pivotal role in cerebellar development and mutations leading to hyperactive signaling cause medulloblastoma. Although the fundamentals of the pathway mechanics are known, and have led to the development of mouse models to study the human disease, there are critical questions that remain to be answered. Based on pathway signatures medulloblastomas are categorized into subgroups, Shh-driven being one such subgroup. However there is significant heterogeneity even among Shh-driven medulloblastomas that necessitates understanding key differences between the various mutations and differential regulation of downstream effectors. Through the characterization of a novel mouse model of medulloblastoma, SmoA2 and comparative

analyses with the existing SmoA1 model, I have demonstrated salient molecular and cellular differences between two activating mutations in the same region of a single gene. While the SmoA1 mutation leads to medulloblastoma in adult mice, in addition to cancer, the SmoA2 mutation causes severe defects early in cerebellar development. The transcriptional profiles downstream of these two mutations and biological processes affected are distinct. An unexpected finding from the SmoA2 model is the preservation of normal cerebellar function despite a completely disrupted cytoarchitecture challenging the notion that stereotypical organization of the cerebellum is critical for its function. My second aim was to identify molecules that interact with the Shh pathway in development and disease. Toward this goal, I discovered a previously unknown expression pattern of MyoD in the proliferative phase of the developing cerebellum as well as in mouse medulloblastoma. MyoD, a myogenic differentiation factor has been known to be exclusive to the skeletal muscle lineage. I demonstrate MyoD functions as a novel haploinsufficient tumor suppressor in the context of medulloblastoma with potential clinical significance.

TABLE OF CONTENTS

LIST OF FIGURES	ii
LIST OF TABLES	iii
Chapter 1: Introduction	1
The Cerebellum and its Development.....	1
Cells of the Cerebellum	1
Neuronal migration in the cerebellum	3
Bi-directional cellular interactions in the cerebellum	4
Foliation and Cerebellar Circuitry	5
Signal transduction pathways in cerebellar development.....	6
Sonic hedgehog pathway in granule neuron precursor proliferation and foliation.....	7
Mechanics of the vertebrate Sonic Hedgehog pathway	8
Medulloblastoma.....	11
Sonic hedgehog-driven medulloblastoma.....	12
Mouse models of medulloblastoma	18
Aim of my Dissertation Research	20
Chapter 2: Oncogenic mutation in Smoothened causes severe cerebellar developmental defects and medulloblastoma in mice	22
Abstract	22
Introduction.....	22
Results:.....	25
Discussion	49
Materials and Methods.....	53
Chapter 3: A novel role of MyoD, a muscle differentiation factor, as a tumor suppressor in mouse models of medulloblastoma.....	57
Abstract	57
Introduction.....	58
Results.....	61
Discussion	78
Materials and Methods.....	86
Chapter 4: Role of extrinsic Sonic Hedgehog signaling in the tumor microenvironment for the growth and maintenance of non-Sonic Hedgehog driven medulloblastomas.....	90
Introduction.....	90
Results.....	92
Conclusions.....	94
Chapter 5: Conclusions and Future Directions	97
Bibliography	100

LIST OF FIGURES

Figure Number		Page
1.1	Mechanics of the vertebrate Shh signaling pathway	10
2.1	Distinct effects of SmoA1 and SmoA2 on mouse cerebellar development	27
2.2	Comparative histopathology of SmoA2 and SmoA1 medulloblastomas	29
2.3	Independent effects of SmoA2 on proliferation and migration	31
2.4	SmoA2 induced aberrations in neuronal and glial organization	33
2.5	Transcriptional profiles of SmoA1 and SmoA2 cerebella	39
3.1	MyoD expression in mouse models of medulloblastoma	63
3.2	Cerebellar tumor cells undergoing proliferation express MyoD	65
3.3	MyoD expression in the proliferative phase of early cerebellar development	67
3.4	Progenitor cells undergoing proliferation express MyoD	68
3.5	Loss of MyoD accelerates tumor onset in SmoA1 and SmoA2 mice	70
3.6	MyoD mediated regulation of muscle differentiation program genes in tumors	71
3.7	Loss of MyoD leads to increased Id3 transcription	74
3.8	Inverse correlation between MyoD and Id3 supported by metaGEO analysis	75
3.9	MyoD induces myogenic differentiation in human medulloblastoma line	77
4.1	Determination of best-tolerated dose of IPI-926	93
4.2	Response of Ptch F/F-Math1-Cre allograft tumors to IPI-926	95
4.3	Response of human medulloblastoma xenograft tumors to IPI-926	96

LIST OF TABLES

Table Number		Page
2.1	Measures of Neurobehavioral Assessment	36
2.2	Genes up-regulated in P5 SmoA2 vs WT cerebella	40
2.3	Genes down-regulated in P5 SmoA2 vs WT cerebella	42
2.4	Genes up-regulated in P5 SmoA1 vs WT cerebella	44
2.5	Genes down-regulated in P5 SmoA1 vs WT cerebella	45
2.6	Genes up-regulated in both P5 SmoA2 and SmoA1 vs WT cerebella	46
2.7	Genes down-regulated in both P5 SmoA2 and SmoA1 vs WT cerebella	48
3.1	Assessment of <i>MyoD</i> mRNA in a subset of human medulloblastomas	62

ACKNOWLEDGEMENTS

I consider myself privileged to have Jim as my mentor in the truest sense of the word. My deepest gratitude to him for being such an excellent and patient teacher, and for instilling in me the passion to touch lives, even if in the smallest possible way. His invaluable guidance and insights will always remain with me, not only for my scientific career but for my journey through life as well.

My sincerest thanks to my committee members, Dr. Stephen Tapscott for guiding me through a significant part of my thesis project, Dr. Leo Pallanck, Dr. Jonathan Cooper and Dr. Charles Laird for their esteemed advice during my entire tenure through graduate school.

I wish to thank Dr. Barbara Wakimoto and the Developmental Biology Training Grant for supporting my research work. I am indebted to Dr. Michael Emerman, MaryEllin Robinson and Diane Darling in the Molecular and Cellular Biology program for everything they have done in making my research career smooth and exciting.

The encouragement, comradeship and the continued patient support of my wonderful friends and coworkers in the lab specially Sally Ditzler, Stacey Hansen, Michelle Lee, Beryl Hatton, Beth Villavicencio, Kyle Pedro, Andrew Richardson, Barbara Pullar, Andy Strand, Mark Stroud, Sue Heiner, Chris Hubert and Phil Olsen, who have made my work meaningful and so much more fun.

I wish to thank the Tapscott Lab, Kyle Macquarrie, Lauren Snider, Yi Cao, Abraham Fong in particular, Dr. Olga Klezovitch, Dr. Michael Le Blanc, and Dr. Richard Klinghoffer for their intellectual inputs and technical assistance.

My deepest thanks also go to FHCRC/UW Shared Resources, FHCRC Animal Health Resources, Ying-tzang Tien at University of Washington Histopathology, Dr. Julie Randolph-Habecker, Kimberly Melton and the FHCRC Experimental Histopathology team, Dr. Sue Knoublaugh, Dr. Julio Vasquez and Dave McDonald at FHCRC Scientific Imaging, Deborah Anderson at CDS-CS, without whose help, this work would not have been possible.

My sincerest gratitude to Michele and Yiorgos Karantsavelos, for being my loving family away from home, and to all my other friends whom I might have failed to mention here.

Lastly but certainly not the least, I cannot adequately thank my parents and my younger sister Ayona – a budding scientist in her own right- for being my inexhaustible source of strength and encouragement, for believing in me and for being there for me, always!

DEDICATION

To the brave children and their families who have let us share their battle against cancer

Chapter 1

Introduction

The Cerebellum and its Development

The cerebellum (Latin: *little brain*) constitutes only 10% of the total brain in volume yet consists of more than half the total number of neurons. This reflects its neuronal complexity as well as functional importance as a central nervous system structure (Wang and Zoghbi, 2001). In addition to its classic functions in motor coordination and balance, recent studies reveal a role for the cerebellum in higher cognitive processes that include sensory-motor learning, speech and spatial memory (Hatten and Roussel, 2011). The development of the cerebellum is unique compared to the rest of the brain. It consists of distinct prenatal and postnatal phases that include intricately regulated processes of cell specification, proliferation, differentiation, regression and migration (Selvadurai and Mason, 2011).

Cells of the Cerebellum

The cerebellum has a unique laminar cytoarchitecture consisting of the outermost molecular layer, the Purkinje cell monolayer, the internal granule layer (IGL) and an inner most region of white matter. The cells of the cerebellum arise from two germinal matrices – the Purkinje cells, cells of the deep cerebellar nuclei and the modulatory neurons (stellate, Golgi and basket) originate from the ventricular zone while the granule neuron precursors (GNPs) and some cells of the deep cerebellar nuclei are born in the rhombic lip (Wang and Zoghbi, 2001). The granule neurons and the Purkinje cells function as the cerebellar sensory input and motor output respectively. The granule neurons transmit sensory information from

the periphery to the Purkinje cells (Wang and Zoghbi, 2001). The Purkinje cells via the deep cerebellar nuclei transmit this information to the motor cortex for fine-tuning of movement and balance. The other neuronal types modulate the activity of the Purkinje cells (Wang and Zoghbi, 2001). Although the above is a simplistic representation, this basic circuitry underlies the function of the cerebellum as a motor coordination center.

Granule neuron precursors are born around embryonic day (E)10.5 in mice and migrate circumferentially along the cerebellar anlage between E12.5-E15.5 to form the transient external granule layer (EGL) (Zindy et al., 2006). In the postnatal phase, the GNPs undergo massive expansion in response to the mitogen Sonic hedgehog (Shh) secreted by the overlying Purkinje cells. The GNPs reach their peak of proliferation between postnatal day (P) 5-P8 in mice (Fujita, 1967). This unique protracted proliferative phase predisposes the cerebellum to various developmental anomalies as well as neoplastic changes (Wang and Zoghbi, 2001). The cells in the inner EGL then exit the cell cycle and undergo inward radial migration to form the IGL of the adult cerebellum. This process is complete by about P21 in mice and a year after birth in humans (Wang and Zoghbi, 2001).

The Purkinje cells are born around E13, exit mitosis by E14 and migrate along radial glia into the cerebellar anlage (Wang and Zoghbi, 2001). The cells then become suspended beneath the EGL. Initially the Purkinje cells are organized into a multi-layered structure but around the time of birth disperse into a single monolayer (Sillitoe and Joyner, 2007). This layer undergoes further maturation developing extensive dendritic arbors and making appropriate synaptic connections with incoming afferents, a process that is complete by P15 (Wang and Zoghbi, 2001; Sillitoe and Joyner, 2007).

Neuronal migration in the cerebellum

The defined cytoarchitecture, limited diversity in neuronal types and the protracted postnatal development make the cerebellum an excellent model system for studying neuronal migration which include circumferential, radial and tangential migration pathways (Goldowitz and Hamre, 1998). In this section, I present an overview of some of the major neuronal migration systems involving granule neurons and Purkinje cell, that play key roles in the developing cerebellum.

The GNPs in the rhombic lip proliferate and then begin to migrate dorsally over the roof of the cerebellar anlage to form the EGL between E12-E15 (Wang and Zoghbi, 2001; Hatten, 2002). UNC6/Netrin1 and its receptors are critical for early cell migration events in the cerebellum, acting as a chemorepellant for the EGL cells and a chemoattractant for the precerebellar nuclei progenitors (Hatten, 2002). GNPs in the outer EGL undergo massive expansion and then migrate into the inner EGL where they are in a post mitotic state. At this stage, the GNPs undergo tangential migration, possibly to ensure appropriate distribution across parasagittal compartments of the expanding cerebellar cortex (Komuro et al., 2001). The chemokine Cxcl12/Stromal derived growth factor (Sdf)-1 α secreted from the pia mater (*one of the three meninges lining the central nervous system*) and its receptor Cxcr-4 expressed in the EGL help in retaining the GNPs in the EGL thereby preventing premature migration (Klein et al., 2001).

The next phase involves GNP migration to the IGL under the guidance of radial glial (Bergmann glia) fibers. One of the factors shown to be important in preparing the cells for this phase is N-methyl-D-aspartate (NMDA) subtype of glutamate receptors-mediated depolarization followed by compensatory hyperpolarization by inward rectifying K⁺ channel,

GIRK2 (Wang and Zoghbi, 2001). During glial-guided migration, the cytoskeletal organization of the cells is also critical (Hatten, 2002). In addition, several proteins play key roles in the glia-guided migration of GNPs including Astrotactin (acts as a heterophilic ligand for glial binding), Thrombospondin (involved in axon extension during migration), Tenascin (promotes neurite outgrowth and migration) and Neuregulin (expressed in GNPs that bind to ErbB4 on the glial cell during migration) (Wang and Zoghbi, 2001).

The proper migration of the Purkinje cells depends on the Reelin pathway, a protein secreted by cells in the EGL. Mutations in the *Reelin* gene or any of the downstream components in its signaling pathway cause various cerebellar migration defects as observed in the *reeler* and *scrambler* neurological mouse mutants (Rice and Curran, 1999).

Bi-directional cellular interactions in the cerebellum

The final maturation phase of the Purkinje cells when they develop extensive dendritic arbors and synapse onto granule neurons depends on signals from the latter (Wang and Zoghbi, 2001). In mutants such as *weaver* that lack granule neurons, the dendritic trees of Purkinje cells do not form (Rakic and Sidman, 1973) and in *in vitro* experiments, Purkinje cells need to be co-cultured with granule neurons for proper development (Baptista et al., 1994). Granule neurons with mutations in the Netrin receptor migrate to ectopic locations and attract Purkinje cells and other cell types resulting in abnormal migration of the latter as well (Goldowitz and Hamre, 1998). Whether the influence of granule neurons on Purkinje cells is via specific molecules or through electrical activity or a combination of both is yet to be fully understood. Although the migration of Purkinje cells depends on signals from GNPs, the differentiation program is independent of granule neurons, since mutants that lack GNPs,

have normally differentiated Purkinje cells (Jensen et al., 2002). On the other hand, perturbation of Purkinje cells lead to loss in granule neuron numbers (Smeyne et al., 1995). In *reeler* and *scrambler* mutants, the abnormal migration of Purkinje cells compromises granule cell numbers and subsequently affects foliation (Rice and Curran, 1999).

Bidirectional interactions also exist between radial glia and granule neurons which include neuron-glial trophic signals as well as glial-neuron buffering of the surrounding environment (Goldowitz and Hamre, 1998).

Foliation and Cerebellar Circuitry

The cerebellum has a unique morphological structure consisting of folia with fissures separating its anterior-posterior extent into lobules (Sillitoe and Joyner, 2007). The folia putatively serve as a platform for organizing cerebellar circuits (Sudarov and Joyner, 2007). Specific gene expression patterns in the Purkinje cells along parasagittal stripes molecularly code each lobule along the medial-lateral axis (Sudarov and Joyner, 2007). Afferent inputs from outside the cerebellum via climbing fibers and from within the cerebellum via granule neurons axon synapse onto the Purkinje cells (Chizhikov and Millen, 2003). The current understanding of cerebellar function is that these afferents carrying synchronized sensory-motor information terminate onto specific parasagittal domains in a pattern that mirrors the Purkinje cell molecular coding thereby compartmentalizing the cerebellum into distinct functional modules (Chizhikov and Millen, 2003; Sillitoe and Joyner, 2007).

Cerebellar foliation is genetically determined and results from coordinated cell movements and structural changes (Sudarov and Joyner, 2007). The process can be divided into two stages – the embryonic stage which involves formation of fissures at ~ E17 dividing

the cerebellum into cardinal lobes (Sillitoe and Joyner, 2007). By birth a rudimentary set of synaptic connections are established that are topographically organized in the context of the anterior-posterior folds and the medial-lateral molecular coding (Sillitoe and Joyner, 2007). The second postnatal stage involves extensive outgrowth of the cardinal lobes and further subdivision into lobules and sub lobules (Sudarov and Joyner, 2007). By P15, the cellular layers and the complete set of ten folia in mice (designated as I to X) are fully formed with specific cerebellar circuits that correlate the lobular morphology with the molecular domains (Sillitoe and Joyner, 2007).

The cellular and genetic basis of foliation initiation is not well understood. According to a new cellular model proposed by Sudarov and Joyner, the GNPs are responsible for providing the physical force through the formation of multicellular “anchoring centers” at the base of each fissure that consists of Purkinje cells, GNPs and Bergmann glia, between E16.5-E18.5 (Sudarov and Joyner, 2007). The outgrowth of folia then continues through a self-sustaining process involving coordinated actions of GNPs and Bergmann glia (Sudarov and Joyner, 2007).

Signal transduction pathways in cerebellar development

A number of signal transduction pathways play critical roles in the cerebellum during normal development as well as pathological conditions. These pathways include Notch, Wnt/beta-catenin, Bone morphogenetic proteins (BMP) and Sonic hedgehog (Shh) (Hatten and Roussel, 2011). My dissertation research involves the Shh pathway, which I describe in detail in this section.

Sonic hedgehog pathway in granule neuron precursor proliferation and foliation

The Shh ligand secreted by the Purkinje cells around E17 is responsible for the high degree of proliferation of GNPs in the postnatal phase of cerebellar development in the EGL (Wechsler-Reya and Scott, 1999; Hatten and Roussel, 2011) that causes the cerebellum to increase over a 1000-fold in volume (Corrales et al., 2006) (Figure 1.1A). Perturbations to Purkinje cells can result in a devastating decline in granule neuron numbers as observed in various mutant mouse models (Goldowitz and Hamre, 1998). Interestingly, although Shh is expressed in the cerebellum throughout life, Shh-induced proliferation of GNPs occurs only in the early postnatal period exclusively in the EGL (Rubin et al., 2002). This mitogenic niche is created in part by the anatomic localization of factors like heparan sulphate proteoglycans (Rubin et al., 2002), Sdf-1 α (Klein et al., 2001), laminin and Notch2 that interact with the Shh pathway and are critical determinants of GNP expansion (Rubin et al., 2002). In addition, the Shh concentration gradient and the resulting dose-response to Shh-induced proliferation play a key role in this spatiotemporal regulation of GNP expansion (Rubin et al., 2002).

The Shh pathway is also important for development of Bergmann glia, a critical component in the migration of GNPs. Shh induces differentiation of Bergmann glia and aberrations in Shh signaling lead to disorganized glial fibers (Corrales et al., 2006; Vaillant and Monard, 2009).

The Shh pathway plays a critical role in cerebellar foliation by driving GNP proliferation (Corrales et al., 2004; Corrales et al., 2006). Graded increases in Shh signaling through genetic manipulations in mice show that in addition to a thicker and irregular IGL resulting from increased GNP proliferation, these mice show increased folia length,

additional bulges in the IGL and even an extra sub-lobule, the extent of foliation being proportional to the degree of Shh signaling (Corrales et al., 2006). Reducing Shh signaling by conditional knockout of Smo or Gli2, activators of the pathway, result in simpler foliation patterns (Corrales et al., 2006). In both cases, the patterns of foliation along the anteroposterior and mediolateral axes are the same as the conserved pattern which suggests that Shh does not determine the position of the fissures, but is a permissive factor for foliation (Sillitoe and Joyner, 2007).

Mechanics of the vertebrate Sonic Hedgehog pathway

The eukaryotic primary cilium, a microtubule based membrane extension assembled and maintained by bidirectional intraflagellar transport, plays a critical role in Shh signaling in vertebrate cells by aiding in the concentration of various components of the pathway (Rohatgi et al., 2007; Spassky et al., 2008; Wen et al., 2010). In vertebrates, Gli1, Gli2 and Gli3 are the main activators of the pathway. Gli2 and Gli3 when processed, can function as repressors when the Shh pathway is inactive (Wen et al., 2010). In the absence of the ligand Shh, Patched 1 (Ptch1), a twelve-transmembrane domain protein, located on the cell membrane in the cilia, represses the activity of the seven-transmembrane domain protein Smoothed (Smo) (Lum and Beachy, 2004; Cohen, 2010; Hui and Angers, 2011; Markant and Wechsler-Reya, 2011) presumably by preventing its cell surface localization from intercellular endosomes (Deneff et al., 2000; Rubin and de Sauvage, 2006) (Figure 1.1Bi). There are a few different models describing the mechanics of the Shh pathway. One model suggests that a yet uncharacterized small molecule agonist of Smo is potentially transported outside the cell by Ptch1 thereby preventing its binding to Smo (Rubin and de Sauvage,

2006). Additionally, various kinases phosphorylate Gli3 (Gli1, Gli2, Gli3: the activators of the pathway), which is then cleaved into a repressor form, Gli^R. Gli^R translocates to the nucleus and inhibits activation of downstream targets. Iguana and SUFU sequester the active form of Gli proteins (Gli^A) preventing nuclear translocation. In the presence of Shh, binding of the ligand to Ptch1 causes internalization and subsequent destabilization of Ptch1 (Figure 1.1Bii). The endogenous ligand of Smo then activates Smo (Rubin and de Sauvage, 2006) causing its translocation to the ciliary surface along with the unprocessed Gli proteins (Corbit et al., 2005; Wen et al., 2010). Intraflagellar transport proteins play a key role in this translocation (Huangfu and Anderson, 2006). Smo-mediated activation of the Gli proteins cause them to translocate from the cilia to the nucleus where Shh target genes are activated. Thus, Shh, Smo and Gli proteins activate the pathway whereas Ptch and SUFU function as repressors.

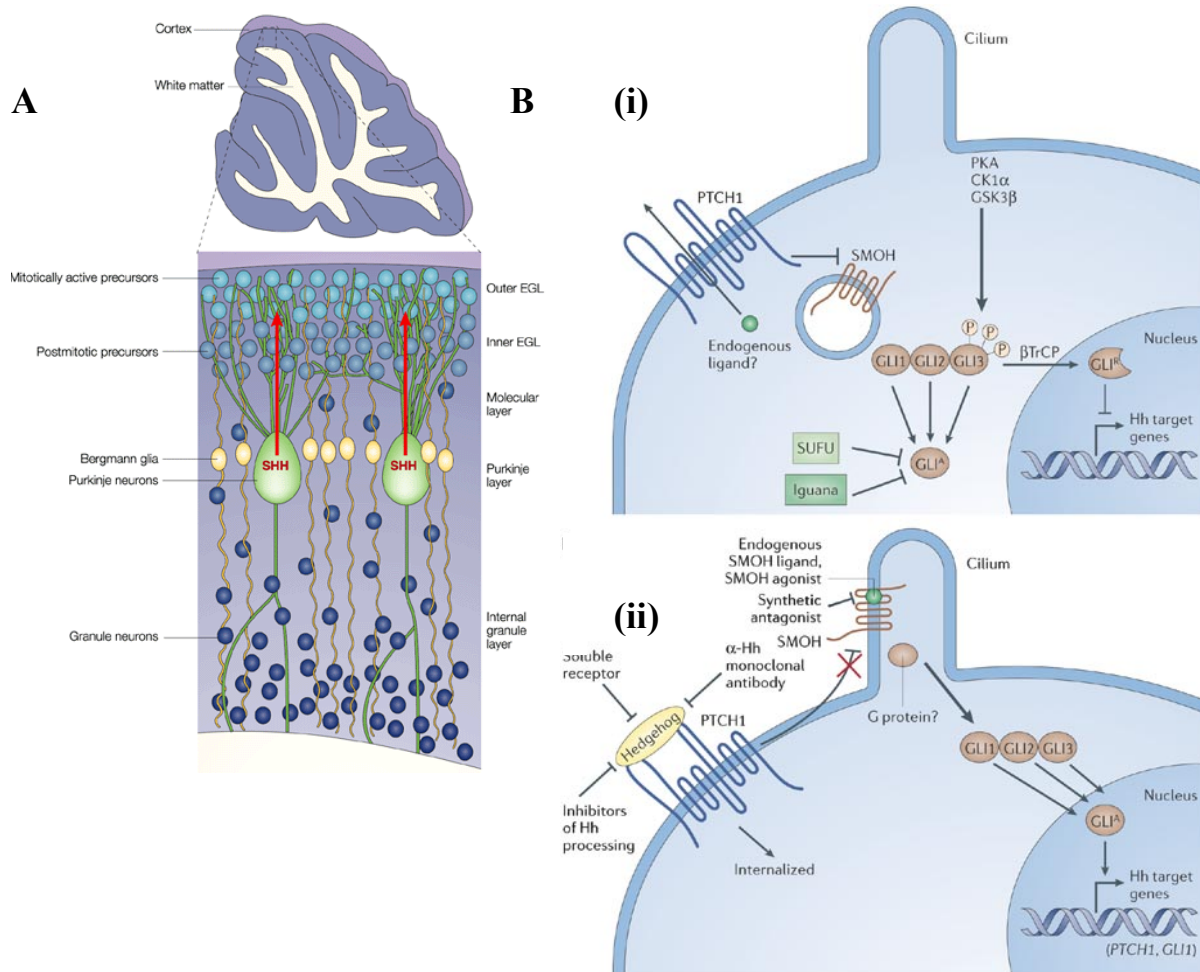


Figure 1.1

Mechanics of the vertebrate Shh signaling pathway

A. During early postnatal development of the mouse cerebellum, the Sonic hedgehog (Shh) protein secreted from the Purkinje cells promotes the proliferation of the granule neuron precursors in the outer external granule layer (EGL). The post mitotic GNPs then migrate from the inner EGL to the internal granule layer guided by radial glial processes (Bergmann glia). Shh also induces the maturation of Bergmann glia. Figure taken from (*Ruiz i Altaba et al., 2002*).

B (i) In the absence of Shh, its receptor Patched1 (Ptc1), located on the plasma membrane inhibits the G-protein coupled receptor, Smoothened (Smo) by possibly exporting an endogenous agonist of Smo outside the cell. Different kinases phosphorylate Gli2/3 creating a repressor form of this transcription factor (Gli^R). Iguana and SUFU prevent the active form of Gli (Gli^A) from trans activating Shh-responsive genes.

(ii) Upon binding of Shh, Ptc1 is internalized relieving the inhibition on Smo, which then translocates from the intracellular endosomes to the cilia of the plasma membrane. It then engages yet unknown components of the signaling pathway, which culminates in activating the Gli proteins, which regulate the expression of Shh target genes.

Figure taken from (*Rubin and de Sauvage, 2006*)

Medulloblastoma

Medulloblastoma is an embryonal tumor of the cerebellum and the most common pediatric brain malignancy (Gilbertson and Ellison, 2008). Although current treatment strategies including chemotherapy, radiation and surgical resection lead to significantly improved survival (Crawford et al., 2007), approximately one-third patients remain incurable and those who survive experience drastic neurocognitive sequelae (Wolfe-Christensen et al., 2007) (Saury and Emanuelson, 2011).

Medulloblastoma is a highly heterogeneous tumor that is classified into distinct histological subtypes which according to the 2007 WHO classification, are - classic, desmoplastic, anaplastic, large-cell medulloblastomas and medulloblastoma with extensive nodularity (Gilbertson and Ellison, 2008). A rare histological variant of medulloblastoma, medullomyoblastoma, that presents with myogenic differentiation, was first described in 1933 (Er et al., 2008). The molecular basis of this rare pathological feature is yet to be determined and is initiated by my work described in Chapter 3.

Gene expression studies of human medulloblastomas have led to identification of four distinct molecular subgroups (Thompson et al., 2006; Kool et al., 2008; Cho et al., 2011; Northcott et al., 2011a; Sengupta et al., 2011; Taylor et al., 2011). These subgroups are characterized by aberrations in (i) WNT signaling (ii) SHH signaling (iii) MYC amplification and a fourth heterogeneous group with yet unknown genetic determinants. Two distinct progenitor populations – GNPs (Schuller et al., 2008; Yang et al., 2008) and cells of the lower rhombic lip (Gibson et al., 2010) have been identified as cells of origin through lineage tracing and genetic analyses in mouse models of medulloblastoma. Medulloblastomas arising from GNPs frequently have mutations leading to constitutive SHH signaling (SHH-subtype)

while those that arise from the cells of the lower rhombic lip have activating mutations in the WNT pathway effector *CTNNB1* (WNT-subtype). There is also marked clinical difference between the WNT and SHH subgroup medulloblastomas. The WNT subtype medulloblastomas have classic histology, occur in older children and are highly curable as opposed to the SHH subtype tumors which includes desmoplastic as well as anaplastic large cell histology (Gibson et al., 2010; Sengupta et al., 2011), is predominant in babies and young adults with mixed prognosis (Taylor et al., 2011). My dissertation was aimed at furthering our understanding of the Shh pathway in cerebellar development and disease and hence I focus on the Shh-driven subgroup in the section below.

Sonic Hedgehog-driven medulloblastoma

The importance of the SHH pathway in medulloblastoma was first recognized following the discovery that patients with Gorlin's syndrome, a hereditary disease with increased incidence of basal cell carcinoma and medulloblastoma, carried heterozygous germline mutations in *PTCH1* (Goodrich et al., 1997). Sporadic mutations, which include inactivating mutations in *PTCH1*, *SUFU* and activating mutations in *SMO*, are observed in 20-30% of medulloblastoma cases predominantly in infants (< 3 years of age) and adults, but rarely in children showing heterogeneity in age of onset (Cho et al., 2011; Northcott et al., 2011a). The prognosis for the SHH-subtype of medulloblastoma is mixed (Gajjar et al., 2006; Thompson et al., 2006; Kool et al., 2008). Although, SHH-driven medulloblastomas have been associated with the desmoplastic histology (Pietsch et al., 1997; Pomeroy et al., 2002), this cannot be used as a prognostic indicator as shown by large-scale genomic studies where other histological variants may also present with SHH pathway signatures (Cho et al.,

2011; Markant and Wechsler-Reya, 2011; Northcott et al., 2011a).

GNPs with constitutive activation of Shh signaling are known to be the cellular source of Shh driven medulloblastomas (Gilbertson and Ellison, 2008). However, the histological heterogeneity makes it possible that different subpopulations of GNPs lead to distinct types of tumors even within the Shh driven class of medulloblastomas (Hatten and Roussel, 2011). Interestingly, studies from the GENSAT project, a large-scale CNS gene expression atlas that has generated more than 600 transgenic mouse lines expressing Enhanced Green Fluorescent Protein (EGFP) reporter genes in a variety of CNS cell types, have identified genes expressed in a subset of GNPs at specific developmental stages (Gong et al., 2003). This suggests the possibility that distinct subsets of GNPs that may have different susceptibilities to neoplastic transformations (Hatten and Roussel, 2011) that potentially contributes to the high degree of heterogeneity even in the same SHH subtype of medulloblastomas.

Co-acting pathways in Sonic Hedgehog driven Medulloblastoma

Activation of the Shh pathway alone does not explain medulloblastoma biology even within the SHH subgroup (Sengupta et al., 2011). The histological heterogeneity observed within the SHH group could be a result of different molecular mechanisms underlying tumorigenesis. The fact that medulloblastoma prone progenitor cells engineered to have constitutive Shh signaling can undergo normal cell cycle exit and differentiation and only a subset of these cells give rise to tumors suggests the presence of additional factors that keep the latter in a proliferative state (Ayrault et al., 2010). Only 14-20% of the preneoplastic lesions nullizygous for *Ptch1* develop into medulloblastomas in the *Ptch1* heterozygous

mouse model, underscores the importance of additional events that enhance the effect of the initial Shh pathway mutation and are necessary for tumorigenesis (Sengupta et al., 2011). The vast majority of molecules that functionally interact with the SHH pathway as tumor suppressors or oncogenes in medulloblastoma genesis are unknown and need to be identified to devise therapeutic strategies that take into account the molecular and cellular tumor heterogeneity (Markant and Wechsler-Reya, 2011). Outlined below are examples of some known pathways conserved in cerebellar development and tumorigenesis that functionally interact with the Shh pathway synergizing or antagonizing its effects.

CXCL12-CXCR4 pathway

The chemokine CXCL12/Stromal derived factor (SDF)-1 α secreted from the pia mater enhances SHH-induced proliferation of GNPs as well as proper migration during normal cerebellar development. A recent study by Sengupta *et al* shows that SHH driven medulloblastomas can be further subdivided into CXCR4 high and low expresser groups which have their distinct molecular, histological and epidemiological profiles (Sengupta et al., 2011). While CXCR4 potentiates Shh driven GNP as well as tumor growth, SHH modulates CXCR4 signaling by regulating its cell surface expression. The synergism between these two signaling pathways that lead to maximal tumor growth defines a new molecular subgroup within the SHH-driven medulloblastomas that may benefit from therapeutic interventions that target both pathways(Sengupta et al., 2011).

Hippo pathway/ Yes-associated protein (YAP)-1

Fernandez-L et al. demonstrate a functional interaction between the Hippo tumor suppressor pathway and Shh signaling. YAP1, that is normally repressed by the Hippo

pathway is overexpressed and amplified in both mouse and human medulloblastoma with aberrant Shh signaling (Fernandez et al., 2009). Shh induces YAP1 expression and nuclear localization that drive GNP proliferation during normal development as well as expansion of tumor cells in the perivascular niche where tumor re-populating cells persist (Fernandez et al., 2009)

Atoh1/Math1

Math1 (Atoh1), a basic helix loop helix transcription factor, is important for the generation of cerebellar granule neurons (Ben-Arie et al., 1997). It is expressed in the proliferating GNPs in the developing EGL and over-expressed in medulloblastomas that have increased Shh signaling. Although insufficient to support proliferation in the absence of Shh, by inhibiting neuronal differentiation genes, Math1 maintains GNPs in a Shh-responsive state and promotes Shh/Gli1 induced transformation of GNPs into medulloblastomas (Ayrault et al., 2010). However, Math1 is not purely a proliferation factor as demonstrated by Klisch et al., where Math1 is also necessary for the initiation of the differentiation program in the EGL cells (Klisch et al., 2011). Interestingly, Math1 promotes proliferation in the cerebellum and acts as an oncogene in medulloblastoma but enhances cell cycle exit and acts as a tumor suppressor in intestinal tumors (Klisch et al., 2011)

Insulin Growth Factor (IGF) signaling

IGF-2 synergizes the effect of Shh on proliferating GNPs (Hartmann et al., 2005) and is often upregulated in desmoplastic human medulloblastoma (Pomeroy et al., 2002). Mouse studies demonstrate that IGF-2 and the Shh pathway synergize to induce medulloblastoma formation (Hahn et al., 2000; Pomeroy et al., 2002; Rao et al., 2004)

Hypermethylated in cancer (HIC) 1

HIC1 is at the 17p13.3 chromosomal locus, a region frequently deleted in medulloblastoma (Ferretti et al., 2005). In mice, Hic cooperates with *Ptch1* to silence *Atoh1* which is important for GNP proliferation during cerebellar development. The loss of Hic1 accelerates tumor incidence in the *Ptch1* heterozygous medulloblastoma model (Briggs et al., 2008).

Fibroblast growth factor (FGF)

Fibroblast growth factor 2 (FGF-2) antagonizes the proliferative effect of Shh on GNPs, yet on its own stimulates proliferation (Wechsler-Reya and Scott, 1999; Fogarty et al., 2007). FGF has also been shown to impair growth of human medulloblastoma cells in vitro as well as in xenograft models (Duplan et al., 2002; Vachon et al., 2004)

Bone Morphogenetic Protein (BMP) signaling

A balance between the Shh and BMP signaling pathways regulate proliferation and differentiation of GNPs in the EGL. BMPs are important for initiating the granule neuron specification program in the cerebellum (Alder et al., 1999). BMP-2 and BMP-4 inhibit Shh-induced medulloblastoma (Alder et al., 1999) and BMP-2 regulates retinoid-induced apoptosis of medulloblastoma (Hallahan et al., 2003)

MicroRNAs in cerebellar development and medulloblastoma

microRNAs (miRNAs) are a class of non-coding small RNAs that regulate gene expression post-transcriptionally. miRNAs bind to the 3' UTRs of target mRNAs and inhibit subsequent transcription. miRNAs play critical roles in many aspects of development regulating proliferation and differentiation (Ferretti et al., 2008) including in the brain, which

is a major site of miRNA expression (Olsen et al., 2009; Hatten and Roussel, 2011). Various miRNAs have been implicated in neuronal morphogenesis, synaptic functions, neuronal differentiation, circadian clock modulation and Purkinje cell maintenance among others (Olsen et al., 2009).

Misregulations of miRNAs are linked to cancer (Calin and Croce, 2006). In medulloblastoma, various miRNAs have been shown to be up-regulated with potential oncogenic functions, while those that are down-regulated function as tumor suppressors (Hatten and Roussel, 2011). The miR 17~92 cluster has been shown to be upregulated by two independent studies although the targets remain to be identified (Northcott et al., 2009; Uziel et al., 2009). The up-regulation of miR 17~92 is also associated with a loss of a normal allele of *Ptch1* suggesting a functional interaction between the miR 17~92 cluster and Shh signaling in medulloblastomas genesis (Uziel et al., 2009). Another study with the help of high-throughput screening of miRNAs in distinct subsets of medulloblastomas, led to the identification of miRNAs involved in Shh signaling (Ferretti et al., 2008). miR-125b, miR-324-5p and miR-326 were found to be down regulated in Shh-driven medulloblastomas. The mRNA targets were shown to be the activators of the Shh signaling pathway – *SMO* and *GLII*. Interestingly, the same set of miRNAs is down regulated in normal proliferating GNPs where a high level of Shh signaling is required. As the GNPs differentiate, the miRNA levels increase to antagonize the Shh pathway and inhibit proliferation (Ferretti et al., 2008).

Although a large number of miRNAs are expressed in the brain, the function of most, remain to be elucidated. Several miRNAs are also associated with neurological and psychiatric diseases like schizophrenia (Hansen et al., 2007), Parkinson's disease (Kim et al., 2007), X-linked mental retardation suggesting that miRNAs are functionally important not

just in the developing nervous system, but in adulthood as well (Mehler and Mattick, 2006; Olsen et al., 2009). A study by Olsen et al. identified spatially restricted patterns of miRNA expression in the adult rat brain indicating their potential involvement in maintaining area-specific brain functions (Olsen et al., 2009). The cerebellum was shown to have either high enrichment for a set of miRNAs (miR-206 and miR-497) or depletion of others (miR-132, miR-212, miR-221 and miR-222). Intriguingly, miR-206 known to be an important skeletal-muscle specific miRNA (Rosenberg et al., 2006), has also been shown to function as a tumor suppressor in certain types of cancers (Kondo et al., 2008; Song et al., 2009; Taulli et al., 2009). miR-206 was also one of 24 miRNAs down regulated in proliferating mouse GNPs as well as medulloblastomas when compared to mature mouse cerebellum (Uziel et al., 2009). This finding is indicative of a potential tumor suppressor role of miR-206 in the cerebellum as well. The exact significance of miR-206 enrichment in the cerebellum remains to be determined.

These findings demonstrate that miRNAs play an important role in the nervous system both to modulate key developmental pathways (e.g. Shh signaling) as well as for maintaining critical functions in adulthood. Aberrations in miRNA expression and function can lead to cancer and neuropathological conditions.

Mouse models of medulloblastoma

The Shh-driven subtype of medulloblastoma is the most studied with the vast majority of the existing mouse models recapitulating this subtype (Hatten and Roussel, 2011). The *Ptch1*-heterozygous knock out model was the first genetically engineered mouse model of medulloblastoma (Goodrich et al., 1997). The existing models of medulloblastoma have

various genetic anomalies that lead to aberrant activation of Shh signaling. These include mutations in components directly involved in Shh signaling such as mutations in *Smo*, *Sufu*, loss of *Ptch1* alone or accompanied by loss of cell cycle regulators *p18^{INK4c}* or *p27^{Kip1}* as well as molecules not directly in the pathway such as loss of Rb, loss of DNA repair enzymes Brca2, Parp, Xrcc often in combination with the loss of Trp53 (Hatten and Roussel, 2011; Markant and Wechsler-Reya, 2011). The fact that mutations in molecules not directly involved in Shh signaling lead to tumors resembling Shh-driven tumors at a molecular level underscores the importance of this pathway in medulloblastoma genesis. It also implicates that some SHH-driven human medulloblastomas may be initiated by mutations in interacting pathways (Markant and Wechsler-Reya, 2011).

These mouse models have provided critical information about medulloblastoma biology and created opportunities to study the molecular and pathological basis of this cancer. The mouse model with activating mutation SmoA1 develops medulloblastoma and the Smo/Smo model (homozygous for activating mutation SmoA1) is the first to develop leptomeningeal dissemination (i.e. metastasis to the meninges covering the brain and the spinal cord) a feature common in human medulloblastoma (Hallahan et al., 2004; Hatton et al., 2006). The recent Ptch1 conditional knock out model has established that GNP cells are the cell of origin for Shh driven medulloblastomas (Yang et al., 2008). A 100% tumor incidence and a short time to tumor onset make this model ideal for preclinical trials. The Shh-medulloblastoma models have been invaluable in identifying cooperating pathways namely N-myc, IGF-1, Akt, Bcl-2, hepatocyte growth factor, Hippo pathway, CXCR4 among others thereby initiating efforts to therapeutically target multiple pathways for the most effective

inhibition of tumorigenesis (Briggs et al., 2008; Fernandez et al., 2009; Markant and Wechsler-Reya, 2011; Sengupta et al., 2011).

The Wnt driven medulloblastomas are recapitulated by a recent model which conditionally expresses activated beta-catenin in collaboration with the loss of Trp53 in cells of the cerebellar ventricular zone and lower rhombic lip (Gibson et al., 2010), the cell of origin for this subtype (Gilbertson and Ellison, 2008).

It is interesting to note that a number of mouse models of medulloblastoma require a loss of Trp53 (Hatten and Roussel, 2011) while only 10% of human medulloblastomas lack Trp53 (Thompson et al., 2006) suggesting that there might be certain molecular differences between mouse and human tumorigenesis (Hatten and Roussel, 2011).

Models representing the MYC subgroup, the most aggressive subtype of human medulloblastomas, as well as the unspecified genetic group, are yet to be established. A novel Non-Shh/Non-Wnt mouse model was recently developed by expressing MYCN in multiple cerebellar progenitors (Swartling et al., 2010). These mice develop aggressive tumors, the majority of which do not have a Shh pathway signature. The correlation of this model with the human medulloblastoma subgroups is yet to be determined.

Aim of my Dissertation Research

The goal of my dissertation research was to understand the molecular mechanisms underlying the roles played by the Shh pathway in cerebellar development and medulloblastoma. The two areas I have been interested in are (i) heterogeneity in Shh driven medulloblastomas and (ii) genes and/or pathways that interact with Shh signaling in development and medulloblastoma. Toward this goal, first, I aimed to characterize the

SmoA2 mouse model of medulloblastoma with hyperactive Shh signaling in the cerebellum. Through a comparative study with the SmoA1 model, I investigated if aberrant Shh signaling in the cerebellum stemming from different activating mutations have disparate effects on development and cancer. The findings from this study are described in Chapter 2. Toward my second aim, my finding that muscle differentiation factor, MyoD acts as a haploinsufficient tumor suppressor in Shh-driven mouse models of medulloblastoma, is described in Chapter 3. Finally, I aimed to understand the effect of extrinsic Shh signaling in the tumor microenvironment on medulloblastomas that are not caused by aberrant intrinsic Shh signaling. My findings are summarized in Chapter 4.

Chapter 2

Oncogenic mutation in *Smoothened* causes severe cerebellar developmental defects and medulloblastoma in mice

Abstract

Deregulated developmental processes in the cerebellum cause medulloblastoma, the most common malignant tumor of the central nervous system. About 25-30% of cases are caused by mutations increasing the activity of the Sonic hedgehog (Shh) pathway, a critical mitogen in cerebellar development. The proto-oncogene *Smoothened* (*Smo*) is a key transducer of the Shh pathway. Activating mutations in *Smo* that lead to constitutive activity of the Shh pathway have been identified in human medulloblastoma. To understand the molecular and cellular effects of *Smoothened* variants in normal development and medulloblastoma genesis, we generated the SmoA2 transgenic mouse model that expresses the transgene exclusively in granule neuron precursors and carried out a comparative analysis with our previous SmoA1 model. In this study, we demonstrate how two apparently similar point mutations in *Smo* can produce starkly different phenotypes. The SmoA2 mice have severe aberrations in cerebellar development whereas the SmoA1 mice are largely normal during development.

Medulloblastomas in the SmoA2 mice develop in the dysplastic cerebellar milieu. Despite disruptions in the stereotypic organization of the cerebellum, the SmoA2 mice do not exhibit any overt abnormalities in motor coordination. The differences in the global transcriptional profiles downstream of SmoA2 and SmoA1 further distinguish the two oncogenic *Smo* mutations. The SmoA2 model will enable investigation of the functional significance of the reiterative cerebellar circuitry as well as further our understanding of the Shh pathway in cerebellar development and oncogenesis.

Introduction

The protracted phase of extensive proliferation during cerebellar development makes it vulnerable to neoplastic transformation (Wang and Zoghbi, 2001). Medulloblastoma, a developmental cancer of the cerebellum, continues to be the most common pediatric brain cancer. Standard treatments result in neurocognitive impairment and adverse quality of life (Gilbertson and Ellison, 2008; Saury and Emanuelson, 2011).

Medulloblastomas are categorized based on histological characteristics and molecular signatures (Gilbertson and Ellison, 2008; Taylor et al., 2011). Genetic aberrations leading to hyperactive Shh signaling in granule neuron precursors (GNPs) cause 25-30% of medulloblastoma cases (Hatten and Roussel, 2011). The Shh pathway plays a pivotal role in cerebellar development by regulating proliferation of GNPs and foliation (Wechsler-Reya and Scott, 1999; Corrales et al., 2006). The Shh-subgroup has been widely studied with numerous mouse models recapitulating the human disease (Markant and Wechsler-Reya, 2011). The overall prognosis in patients with Shh-driven medulloblastomas, however, remains intermediate (Taylor et al., 2011).

Within the Shh-subgroup of human medulloblastoma there exists significant biological and clinical heterogeneity, the underlying molecular basis of which remain to be explored (Northcott et al., 2011b; Sengupta et al., 2011). Leptomeningeal dissemination observed uniquely in Smo/Smo mice and not other Shh-driven models (Hatton et al., 2008) demonstrate disparities in pathology. Inhibition of the Shh pathway by Smo antagonist, cyclopamine varies based on mutations driving hyperactive signaling (Berman et al., 2002; Chen et al., 2002) leading to differences in therapeutic responses. Aberrations in genes outside the Shh pathway also lead to medulloblastomas with Shh-signatures in mice

highlighting the widespread interactions of the Shh pathway with other networks (Markant and Wechsler-Reya, 2011). In several mouse models, medulloblastoma-prone progenitors exit cell cycle and undergo normal neuronal differentiation suggesting that factors in addition to initiating mutations contribute to tumorigenesis (Ayrault et al., 2010) and possibly tumor heterogeneity.

While broad molecular classifications are important, it is necessary to investigate the unique behavior of each driving mutation since the downstream effects may be distinct. Since medulloblastoma results from developmental aberrations (Marino, 2005), investigation of critical milestones in cerebellar development will provide valuable insights in this area. Toward this goal, we developed the SmoA2 mouse model of medulloblastoma and carried out a comparative analysis with the existing SmoA1 model. SmoA1 (W539L) and SmoA2 (S537N) mutations, originally identified in human cancer patients (Reifenberger et al., 1998; Xie et al., 1998) lie in the same transmembrane domain of Smo and cause constitutive activation of the Shh pathway (Taipale et al., 2000). While the SmoA1 mutation has been widely studied, very little is known about SmoA2.

Through characterization of the SmoA2 model, we show striking differences between the SmoA1 and SmoA2 mutations at a molecular and cellular level. While the SmoA1 mutation leads to medulloblastomas, the SmoA2 mutation causes severe defects in cerebellar development and medulloblastoma in adulthood. Early in development, the two mutations lead to distinct transcriptional profiles affecting different biological processes. Despite disruptions in the cytoarchitecture thought to be critical for cerebellar function, the SmoA2 mice intriguingly do not display signs of cerebellar malfunction.

Results:

Distinct mutations in the Smoothed receptor have vastly different effects on cerebellar development.

SmoA2 (S537N) and SmoA1 (W539L) are activating point mutations that lead to constitutive Shh signaling and were originally identified in human cancer cases of medulloblastoma and basal cell carcinoma respectively (Reifenberger et al., 1998; Xie et al., 1998; Taipale et al., 2000). In our previous studies, we have described the SmoA1 transgenic mouse medulloblastoma model which expresses the SmoA1 transgene driven by the GNP-specific fragment of the NeuroD2 (ND2) promoter causing constitutive Shh signaling exclusively in the cerebellum (Hallahan et al., 2004; Hatton et al., 2008)

In this study, we have characterized the SmoA2 transgenic mouse model with a similarly designed transgene expressing the SmoA2 mutation. Comparative histopathological analyses show striking differences in phenotypes - while SmoA1 mice have a largely normal development of the cerebellum (Figure 2.1 G-I) similar to wildtype (WT) (Figure 2.1 A-C), the SmoA2 mice have severe malformations (Figure 2.1D-F).

At postnatal day (P) 5, the SmoA2 cerebellum has an extended, undefined external granular layer (EGL) consisting of aberrantly migrating GNPs (Figure 2.1D). There is lack of normal foliation and ectopic progenitor-like cells in the adjacent parenchyma and along the pial surface (Figure 2.1D). At P14, the SmoA2 cerebellum continues to manifest extensive dysplasia with massive hypercellularity (Figure 2.1E). The dysplastic regions consist of normal progenitor cells and atypical cuboidal to spindle-shaped cells with indistinct cell borders, scant amount of eosinophilic fibrillar cytoplasm with irregularly round to fusiform nuclei, reminiscent of medulloblastoma. These features strongly suggest a primitive

phenotype and possible neoplastic transformation. However, the atypical cells in the SmoA2 P14 cerebellum also have morphological similarities to the normal GNPs remaining in the outer EGL of the WT P14 cerebellum that are still undergoing migration.

By P28, the WT cerebellum attains its mature size and shape (Figure 2.1C). Although a 100% of the SmoA2 cerebella remain dysplastic in adult mice, the cytoarchitecture is more mature compared to the hypercellular P14 stage (Figure 2.1F). The cells in the dysplasia are morphologically identical to the mature granule neurons in the WT cerebellum. At this stage, atypical cells if any, are exclusively positioned along the pial surface, clearly separate from the adjacent dysplastic regions.

To ensure that the phenotype observed is caused by the specific SmoA2 mutation and not consequent to disruptions caused by transgene integration, we analyzed two independent transgenic lines (221, 225). Both lines displayed cerebellar malformations, confirming that the phenotype observed stems from the SmoA2 mutation (Figure 2.1 J,K).

Medulloblastoma in the SmoA2 model develop in a dysplastic milieu

GNPs in the proliferative EGL are known to be the source of medulloblastomas caused by hyperactive Shh signaling (Goodrich et al., 1997; Oliver et al., 2005; Hatton et al., 2008; Schuller et al., 2008; Yang et al., 2008). The SmoA2 mice, as shown earlier, lack an organized EGL and the entire laminar cytoarchitecture of the cerebellum remains dysplastic throughout development (Figure 2.1 D-F). To understand the nature of tumor formation in these mice, we carried out a comparative histopathological analyses on SmoA2 and SmoA1 tumors. The histological criteria we used for tumor definition were the same as those established in our previous study (Hatton et al., 2008). Further to our initial report of

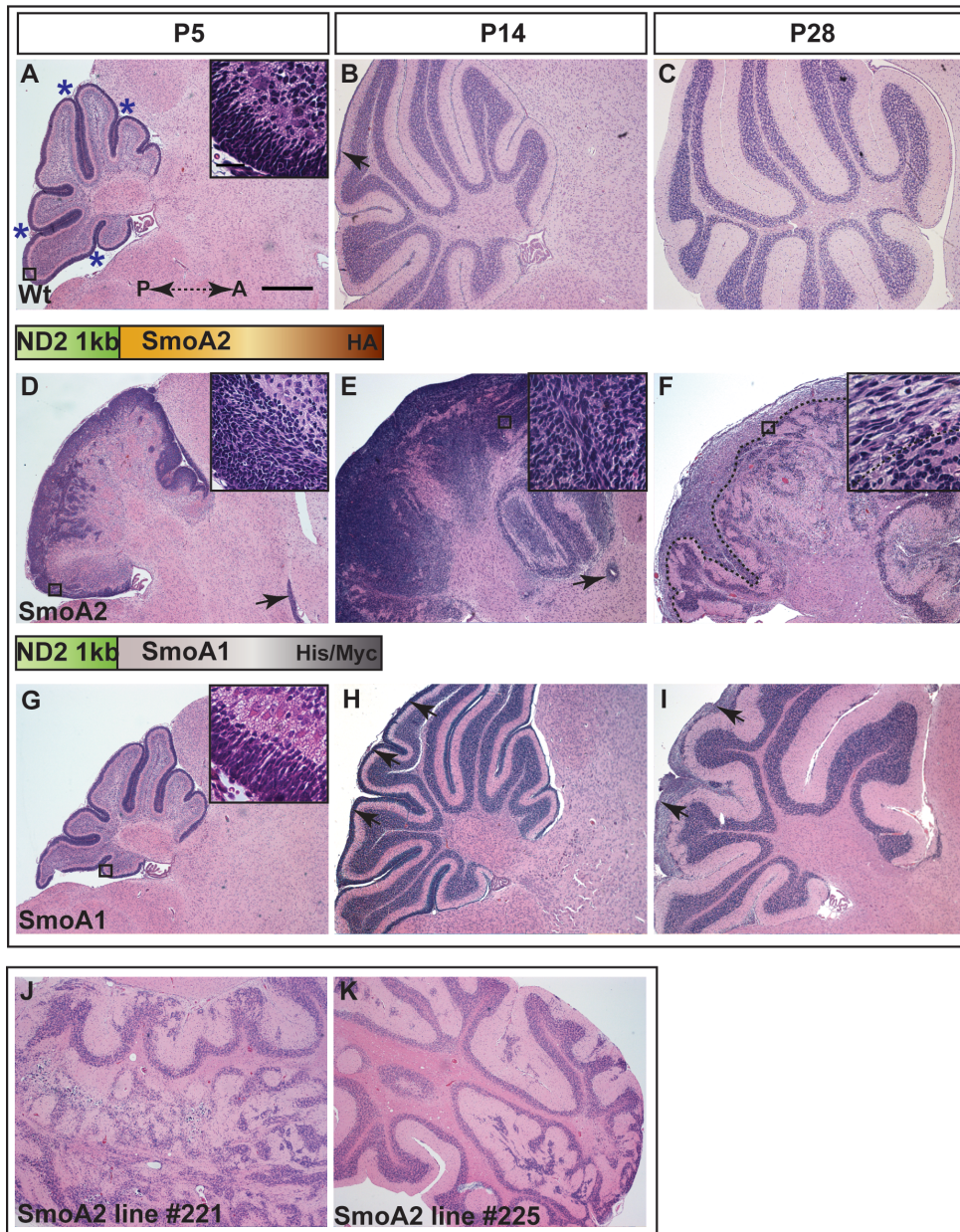


Figure 2.1 | The SmoA1 and SmoA2 mutations have vastly different effects on the development of mouse cerebellum. Hematoxylin-Eosin (H&E) staining of representative sagittal sections show development of the mouse cerebellum at P5, P14 and P28 in (A-C) WT, (D-F) SmoA2 and (G-I) SmoA1 mice. (A-C) Asterisks indicate fissure formation during foliation at P5 and dotted arrow denotes the anteroposterior (A-P) axis. At P14, formation of the molecular layer, Purkinje cell (PC) layer, Internal granular layer (IGL) near completion with remnants of the External granular layer (EGL) (arrow). At P28, the mature cerebellum is fully formed. (D-F) The SmoA2 cerebellum has an ill-defined expanded EGL with loss of foliation. Arrows point to ectopic clusters of cells at P5 and P14. In the P28 adult SmoA2 cerebellum, atypical cells with neoplastic morphology, if any, are concentrated along the superficial surface separated from the dysplastic region (dotted line). (G-I) The SmoA1 cerebellum closely parallels the development of the WT cerebellum except for a slight thickening of the EGL at P14 (H; arrows). In the P28 adult SmoA1 cerebellum, neoplastic cells, if any, localize to the superficial surface of the cerebellum (I; arrows). Insets in (A, D, G) show high magnification views of EGL and PC layers at P5, inset in (E) shows a mix of atypical and normal cells at P14 and inset in (F) shows concentration of atypical cells along the superficial surface. (J-K) H&E staining of horizontal sections from two independent SmoA2 transgenic lines 221 and 225 show disrupted cerebellar cytoarchitecture in adult mice from both lines (age ≥ 2 months). Scale bars (A-K) 500µm, insets 25µm

hyperplasia in the SmoA2 line, our subsequent experiments reveal tumorigenesis (Hallahan et al., 2004).

The SmoA2 mice develop cerebellar tumors in a dysplastic cerebellar milieu (Figure 2.2A) compared to the SmoA1 tumors which form in an otherwise normally developed cerebellum (Figure 2.2D) and are preceded by an expansion of the EGL at P14 (Hatton et al., 2008) (Figure 2.1H). The frank solid tumors are densely cellular with oval to spindle shaped cells (Figure 2.2B, F) arranged in undefined sheets, short streams and bundles supported on a scant fibrovascular stroma. Multifocally, neoplastic cells palisade along vessels and form numerous pseudorosettes. Although during development the entire SmoA2 cerebellum appears hypercellular with atypical cells and other features of neoplasia (Figure 2.2D-F), even in the absence of a defined EGL, the solid tumors are localized in anatomic regions along the pial surface (Fig 2.2A).

A natural history study to determine the clinical incidence of tumor formation in the SmoA2 mice (n=235) show 2% of the SmoA2 mice manifest clinical symptoms of tumor formation at 2 months of age, which increases to 46% by 4 months and 76% by 6 months (Figure 2.2G) similar to the SmoA1 model (Hatton et al., 2008). The main clinical symptoms, as previously described (Hatton et al., 2008) were weight loss, protruded head as a result of tumor formation beneath the skull, hunched posture or head tilt resulting from hydrocephalus or nerve impingement, and lethargy. Histological analyses using asymptomatic SmoA2 mice show 80% of the SmoA2 mice (n=15) have subclinical neoplastic lesions by 2 months, which increases to 100% by 4 months of age (n=16).

The presence of neoplastic features as early as P5 indicated that the SmoA2 mutation confers transformative potential to precursor cells early in development much before the

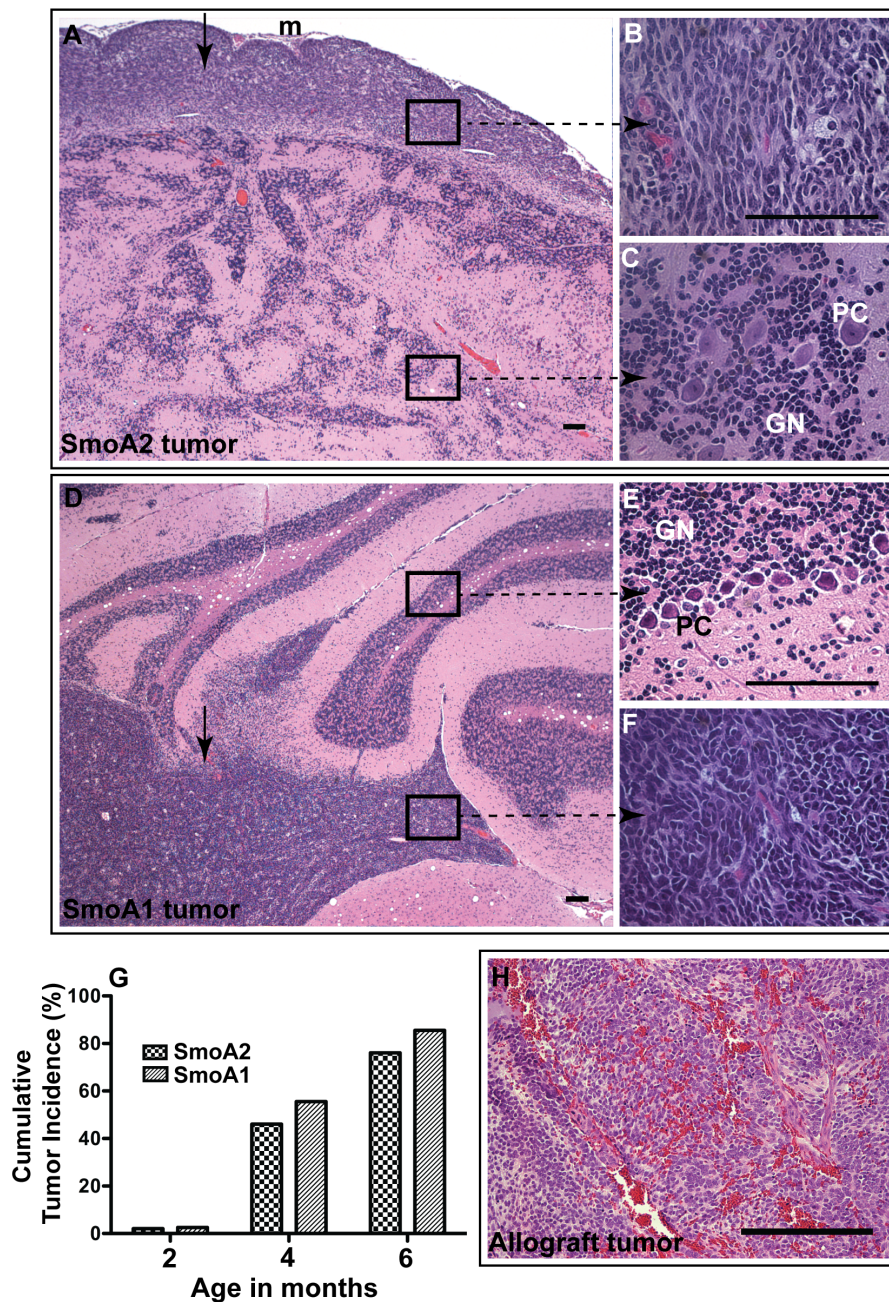


Figure 2.2

Comparative histopathology of SmoA2 and SmoA1 medulloblastomas

(A) Representative images from horizontal cerebellar sections show formation of SmoA2 tumors (arrow) in an aberrantly developed cerebellum on the superficial surface, m denotes meninges. (B) pleomorphic neoplastic cells with multifocal pseudorosettes are distinct from (C) uniformly round granule neurons (GN) and Purkinje cells (PC) in adjacent dysplasia. (D) SmoA1 tumors (arrow) form adjacent to a normally developed cerebellum also along the superficial surface. (E) Normal cellular morphology is distinct from (F) adjacent tumor cells. (G) Columns represent cumulative tumor incidence in SmoA2 and SmoA1 (Hatton et al., 2008) mice at 2, 4 and 6 months of age, based on manifestation of clinical symptoms. (H) Highly vascularized allograft tumor in athymic recipient mice (n=5) transplanted orthotopically with granule neuron precursor (GNP)-enriched cells from P5 SmoA2 donor mice. Scale bars (A-F, H) 100µm

onset of clinical disease. To investigate the oncogenic potential of SmoA2 precursors, we transplanted GNP-enriched cells isolated from P5 SmoA2 cerebella, orthotopically into immunocompromised recipient mice. All five recipients succumbed to aggressive tumors between 20-30 days after transplantation (Figure 2.2H) confirming that the SmoA2 expressing GNPs have neoplastic properties and lead to aggressive tumorigenesis. The simultaneous manifestation of cerebellar developmental defects as well as neoplastic changes as early as P5 in the SmoA2 mice makes this a powerful model to study the temporal progression of an embryonal tumor like medulloblastoma.

The SmoA2 mutation independently increases neuronal proliferation and affects neuronal migration in the cerebellum.

The Shh signaling pathway plays a crucial role in proliferation of GNPs by acting as a mitogen during postnatal cerebellar development (Wechsler-Reya and Scott, 1999). We therefore characterized the proliferative status of the SmoA2 cerebellum at different developmental stages. The first developmental stage we investigated was embryonic day (E)15.5 since the EGL consisting of proliferating GNPs is formed by this stage (Ben-Arie et al., 1997) and the ND2 promoter driving the SmoA2 transgene is activated at ~ E11 (Lin et al., 2004). Immunohistochemical (IHC) staining for proliferation marker, Ki67 shows an increased number of proliferating progenitors in the expanded EGL, compared to WT controls (Figure 2.3A, B). This feature is maintained at P5 with disorganized proliferating cells, which persist at P14 in SmoA2 mice (Figure 2.3F, G) as opposed to WT where proliferation is high at P5 but nearly complete by P14 (Figure 2.3C, D). In the P28 SmoA2 cerebellum, the Ki67 positive cells remain in the outer surface of the cerebellum in the same

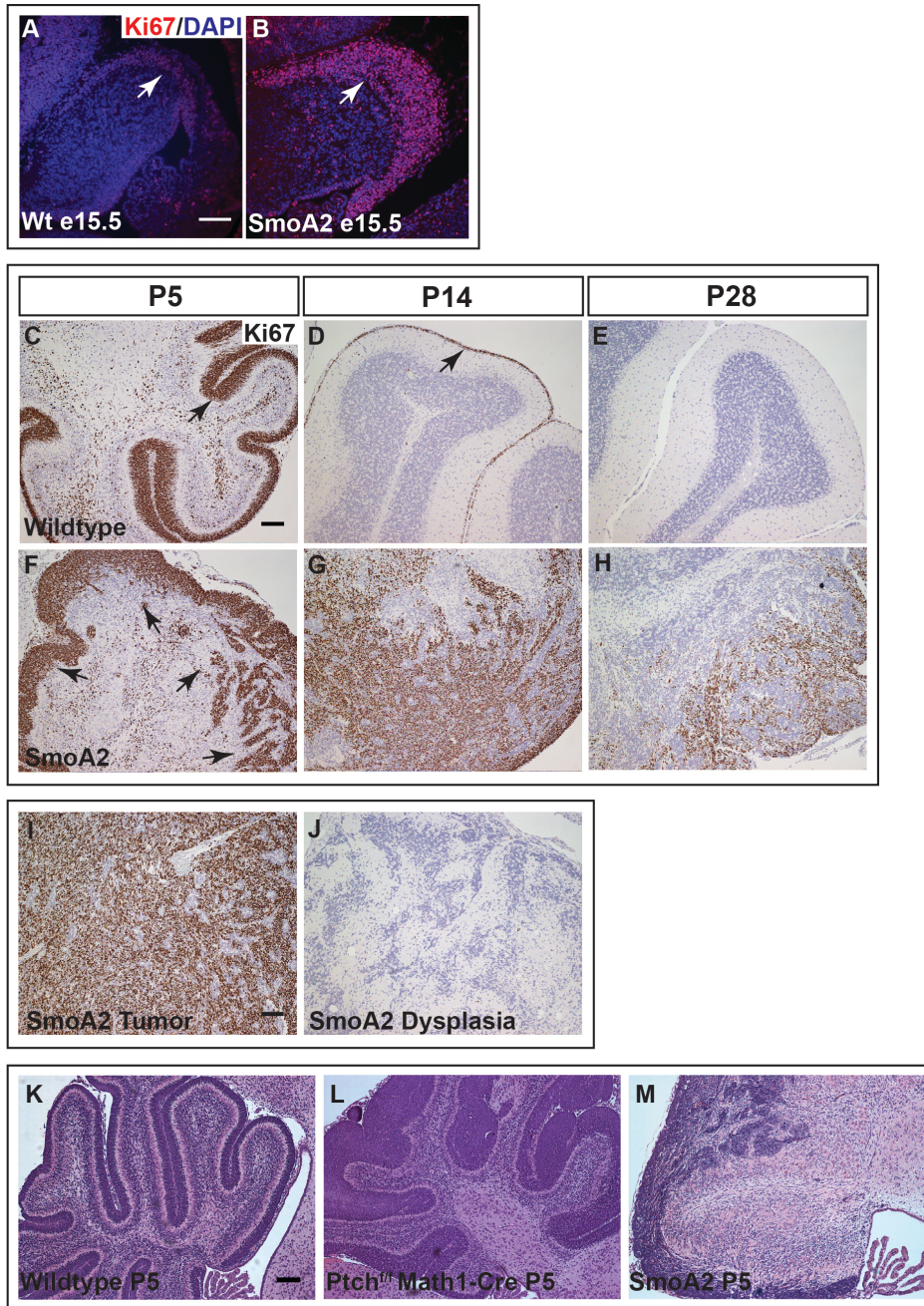


Figure 2.3

The SmoA2 mutation has independent effects on neuronal proliferation and neuronal and glial organization (A-B)

Ki67 immunohistochemistry (IHC) identifying proliferating GNPs marks the EGL (white arrow), which is expanded in SmoA2 mice compared to WT at embryonic day (E)15.5. IHC analysis for Ki67 in (C-E) WT cerebella at P5, P14 and P28 compared to that in (F-H) SmoA2 shows disorganized regions of proliferating GNPs (arrows) in SmoA2 at P5 compared to the defined EGL in WT. At P14, while a few proliferating cells remain in the outer EGL (arrow) in WT, there is an abundance of proliferating GNPs in SmoA2. At P28 proliferation is complete in WT whereas Ki67-positive cells are present along the superficial surface of the SmoA2 cerebellum. (I) SmoA2 tumors have an abundance of Ki67-positive cells, which are (J) undetectable in the dysplastic regions of the SmoA2 cerebella. (K-M) H&E staining of representative sagittal cerebellar sections show that while the EGL is expanded in both Ptch^{F/F}-Math1-Cre and SmoA2 models, mechanisms underlying foliation and neuronal migration to form the laminar cytoarchitecture are preserved in the former as opposed to the SmoA2 cerebellum. n=3 per group. Scale bar: (A-M) 100µm

region (Fig 2.3H) where the atypical cells are localized, as shown in Figure 2.1F. There are no Ki67-positive cells in the P28 WT cerebellum (Figure 2.3E). The SmoA2 tumors have extensive Ki67 staining compared to the dysplastic regions where Ki67 is undetectable (Figure 2.3 I, J).

Next we investigated whether the abnormal foliation and migration observed in the SmoA2 cerebellum is a consequence of excess GNPs generated from Shh hypersignaling that could potentially overwhelm and deregulate cell migration processes. To address this, we compared the P5 cerebella of the SmoA2 mice to an additional Shh-driven medulloblastoma model, the Patched conditional knock-out mice ($Ptch^{F/F}$ Math1-Cre) (Yang et al., 2008) (Figure 2.3K, L, M). At P5, the $Ptch^{F/F}$ Math1-Cre mice have a vastly increased number of GNPs. However, neuronal migration to form the laminar architecture and mechanisms underlying foliation appear to be preserved (Figure 2.3L). This shows that the neuronal disorganization in the SmoA2 cerebellum is not solely a consequence of uncontrolled GNP proliferation.

SmoA2 mutation causes aberrations in neuronal and glial organization

To investigate the cellular characteristics of the cerebellar dysplasias observed in the SmoA2 mice, we identified granule neurons and Purkinje cells as well as Bergmann glia that are critical in GNP migration using antibodies for NeuN, Calbindin and S100 respectively. By immunohistochemical techniques, we analyzed three distinct stages of cerebellar development namely P5, P14, and P28 as well as SmoA2 tumors and non-tumor cerebellar dysplasia in adult mice. All three markers showed massive disruptions in the organization of granule neurons, Purkinje cells and radial glia in the SmoA2 mice (Figure 2.4 D-F, J-L, P-R)

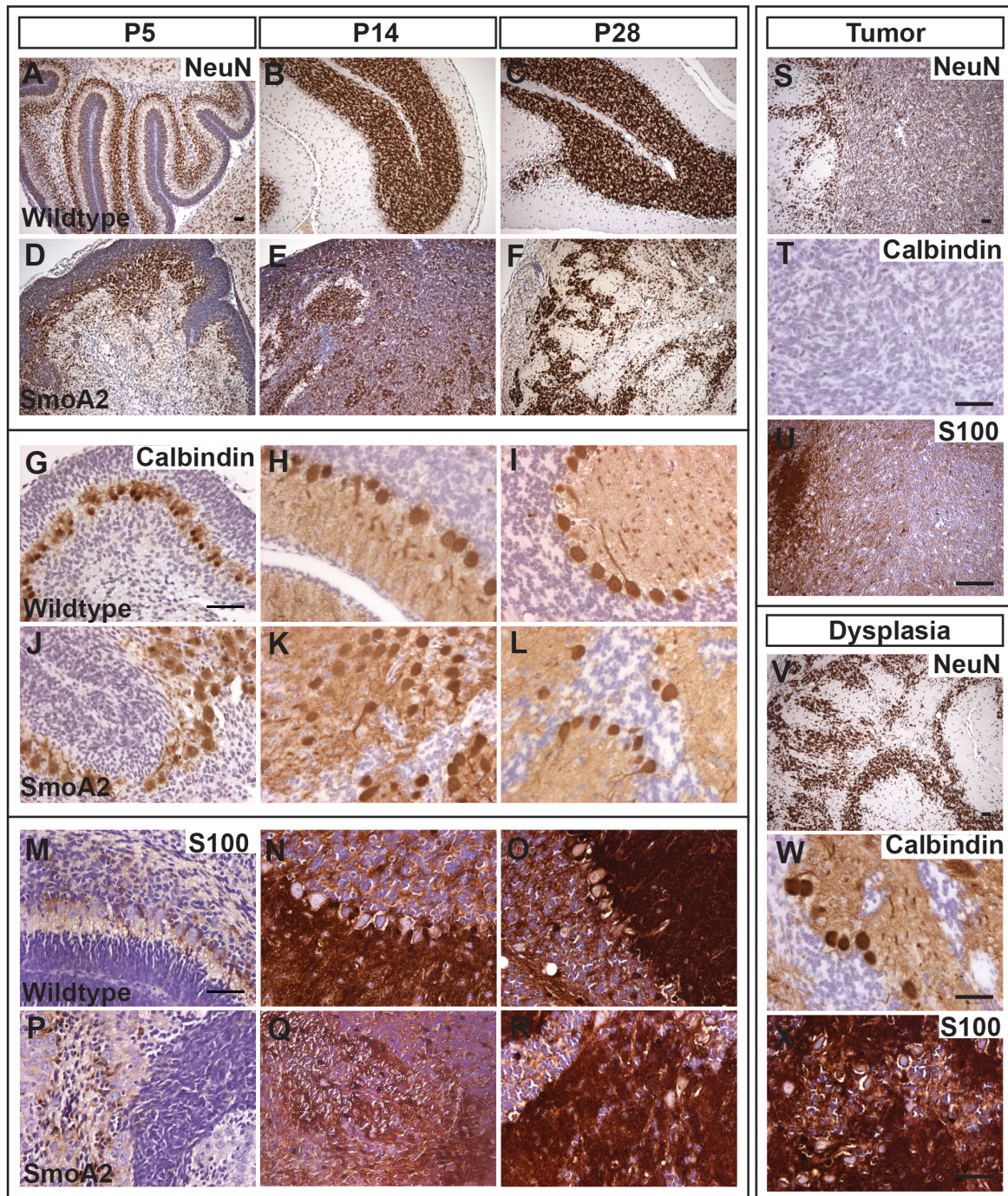


Figure 2.4

SmoA2-induced aberrations in neuronal and glial organization in the developing cerebellum

NeuN IHC analysis at P5, P14 and P28 developmental stages comparing (A-C) WT cerebella to (D-F) SmoA2 cerebella, show disorganized clusters of differentiated granule neurons (GN) amidst abundant NeuN negative cells at P5 and P14 in SmoA2. Calbindin IHC for Purkinje cells (PC) show, monolayer organization in (G-I) WT and (J-L) ectopic clusters in SmoA2 with disorganized dendritic arbors and axonal collaterals at P5, P14 and P28. (M-R) S100 IHC analysis for radial glia comparing (M-O) WT cerebella to (P-R) SmoA2, shows disorganized, entangled glial processes in the SmoA2 cerebellum at P5, P14 and P28. (S-U) SmoA2 tumors show heterogeneous NeuN staining, absence of PCs and heterogeneous S100 staining whereas (V-X) adjacent dysplasias are composed of mature but disorganized GNs, PCs and radial glia. n=3 per group. Scale Bar: (A-X) 100µm

compared to the WT littermate controls (Figure 2.4 A-C, G-I, M-O).

At P5, the SmoA2 cerebellum has an ill-defined outer region negative for NeuN and an inner region of NeuN positive mature neurons similar to the forming Internal granular layer (IGL) of the WT cerebellum (Figure 2.4A, D). At P14, in the SmoA2 cerebellum there are clusters of NeuN positive neurons marking islands of differentiated cells amidst a vast expanse of NeuN negative cells (Figure 2.4E) in stark contrast to the WT cerebellum where differentiated NeuN positive cells are located in the near complete IGL at this stage (Figure 2.4B). At P28, in SmoA2, majority of the neurons are NeuN positive representing a differentiated state with clusters of NeuN negative cells toward the outer surface of the cerebellum (Figure 2.4F), the same region where clusters of Ki67 positive proliferating cells are observed (Figure 2.3H).

Calbindin immunostaining shows that the Purkinje cells have severely disorganized dendritic arbors and axonal processes in the SmoA2 cerebella and the cell bodies fail to align in the characteristic monolayer array at all the developmental stages analyzed (Figure 2.4J-L) in comparison to WT controls (Figure 2.4 G-I). Compared to the WT controls (Figure 2.4 M-O), S100 staining of the radial glia show atypical glial tangles with entrapped granule neurons in ectopic locations in the SmoA2 mice (Figure 2.4P-R).

The SmoA2 tumors show a heterogeneous pattern of NeuN staining (Figure 2.4S); absence of Calbindin positive-Purkinje cells (Figure 2.4T) and sparse to absent S100-positive glia (Figure 2.4U). The SmoA2 adult dysplasias on the other hand consist of NeuN-positive neuronal cells (Figure 2.4V). The dysplastic regions also consist of disorganized Purkinje cells (Figure 2.4W) and disorganized glial fibrils (Figure 2.4X). These results demonstrate

that the GNP-specific expression of SmoA2 leads to widespread disruptions in migration and organization of other neuronal and glial cell types in the cerebellum.

Severe defects in cerebellar morphology do not cause overt anomalies in motor coordination in SmoA2 mice

The classic functions of the cerebellum which are regulation of balance and motor coordination are thought to be dependent on its organized laminar cytoarchitecture (Ghez, 1985). The granule neurons carry sensory inputs to the cerebellum while the Purkinje cells are the primary motor output from the cerebellum relaying motor information to higher brain centers. To assess potential abnormalities in motor coordination resulting from neuroanatomic defects of the SmoA2 cerebellum, we used a modified neurobehavioral assessment tool based on SHIRPA (Rogers et al., 1997) (see materials and methods for details). We investigated physical phenotype (weight, tremor, body position and tail position) and behavioral phenotype (grooming, locomotor activity, spontaneous motor activity). Additionally, we conducted the accelerated rotarod assay to test fore and hind limb coordination and balance) in both adult SmoA2 and age-matched WT control mice. No differences in physical phenotype were observed and except for a decrease in locomotor activity ($p < 0.01$), there were no significant differences in behavior phenotype measures between WT and SmoA2 mice (Table 2.1). Importantly, there was no difference in rotarod performance between SmoA2 and WT demonstrating that these mice were not deficient in motor coordination and balance. We also conducted a footprint analysis using stride length and stance width measures (Crawley, 1999) in both SmoA2 and WT mice which demonstrated no evidence of ataxic gait, a common consequence of cerebellar dysfunction

Table 2.1: Measures from Neurobehavioral Assessment

Test	Measure	WT			SmoA2		
		N	Mean	SEM	N	Mean	SEM
Rotarod	Latency to fall (secs)	8	222.4	1.04	12	189.8	0.59
Footprint Analysis	Stride length (cm)	3	63.2	3.84	4	60.4	2.13
	Stance width (cm)	3	22.5	0.64	4	23.3	1.03
*Locomotor activity * <i>p</i> value < 0.01	Number of times the mouse places at least one paw on the side of the cage during a 2-minute assessment	8	12.1	0.07	12	6.5	0.02

Table 2.1 Legend

Table 2.1 shows measures (mean) obtained from accelerated rotarod test, footprint analysis and locomotor activity as part of SHIRPA assessment to assess neurobehavior of SmoA2 mice with respect to age-matched WT control mice (age ≥ 2 months). N denotes the number of mice in each group. Except for a decrease in locomotor activity (*p* value < 0.01) in SmoA2 mice, there is no significant difference in any other measure between SmoA2 and WT mice.

(Table 2.1). Together, these data reveal no overt abnormalities in cerebellar function in SmoA2 mice despite massive disorganization in the cytoarchitecture.

SmoA2 and SmoA1 mutations lead to unique transcriptional profiles in the mouse cerebellum

To investigate whether the SmoA2 and SmoA1 mutations differentially activate the Shh pathway *in vivo*, we assessed mRNA levels of the canonical target genes by quantitative reverse transcription (qRT)-PCR in SmoA2 and SmoA1 P5 cerebella (Figure 2.5A). Except for total *Smo* expression (endogenous and transgene), which is 2.8 fold higher in SmoA2 compared to SmoA1, expressions of the remaining targets are not significantly different between SmoA2, SmoA1 and WT P5 mice. The extent of Shh pathway activation is similar because at P5, this pathway is highly active in both WT and the Smo mutants when the GNPs are in the maximal proliferative phase. At later stages, as expected, the levels of these targets are elevated in SmoA2 and SmoA1 cerebella (data not shown).

Next, to assess transcriptional changes downstream of SmoA2 and SmoA1, we evaluated global gene expression profiles of P5 SmoA2, SmoA1 and WT age-matched cerebella. We chose this specific developmental stage because (1) the phenotypes of SmoA2 and SmoA1 are robust and distinct at P5; (2) at P5 GNPs undergo proliferation, migration and differentiation and therefore expression profiling could capture key differences in multiple processes. Hierarchical cluster analysis shows that while the gene expression signature is unique for each group, at P5, transcriptionally the WT and SmoA1 cerebella resemble each other more closely than either resembles SmoA2 (Figure 2.5B), consistent with their phenotypes (Figure 2.1 A, D, G).

Compared to WT controls, we identified 106 transcripts in SmoA2 and 67 in SmoA1 that differed uniquely by an absolute fold change of greater than or equal to 2, $p < 0.001$ (Figure 2.5C). This highlights the complex transcriptional changes induced by the SmoA2 mutation that potentially underlie the intriguing phenotype.

To determine key biological processes that are different between SmoA2 and SmoA1, we used mRNAs over- and under-represented in SmoA2 compared to SmoA1 to conduct Gene Ontology (GO) gene set enrichment analyses (Ashburner et al., 2000). The ontological categories represented by the gene sets up- or down-regulated in SmoA2 compared to SmoA1 include *cell and neuronal fate specification and commitment, regulation of neuronal differentiation, neural crest cell migration, regulation of cell proliferation, neuron migration, neuronal projection, membrane anchorage, cell matrix adhesion, axonal and dendritic molecules, localization molecules, ligand gated ion channel activity, thyroid hormone metabolism* as well as various metabolic processes amongst others. In the cell fate commitment GO category, among other transcription factors, the expression of *MyoD*, a transcription factor that orchestrates muscle differentiation, was particularly intriguing since *MyoD* is neither known to be expressed nor have a function in the mammalian brain. qRT-PCR as well as Western blot analysis (data not shown) confirmed this ectopic expression pattern. We are currently exploring the significance of this unexpected finding. In summary, the biological processes reflected by the gene expression profiles are complex and ascertaining specific pathways remains a future direction. Our data demonstrate the fundamental differences between SmoA2 and SmoA1 at a molecular level that affect distinct biological processes.

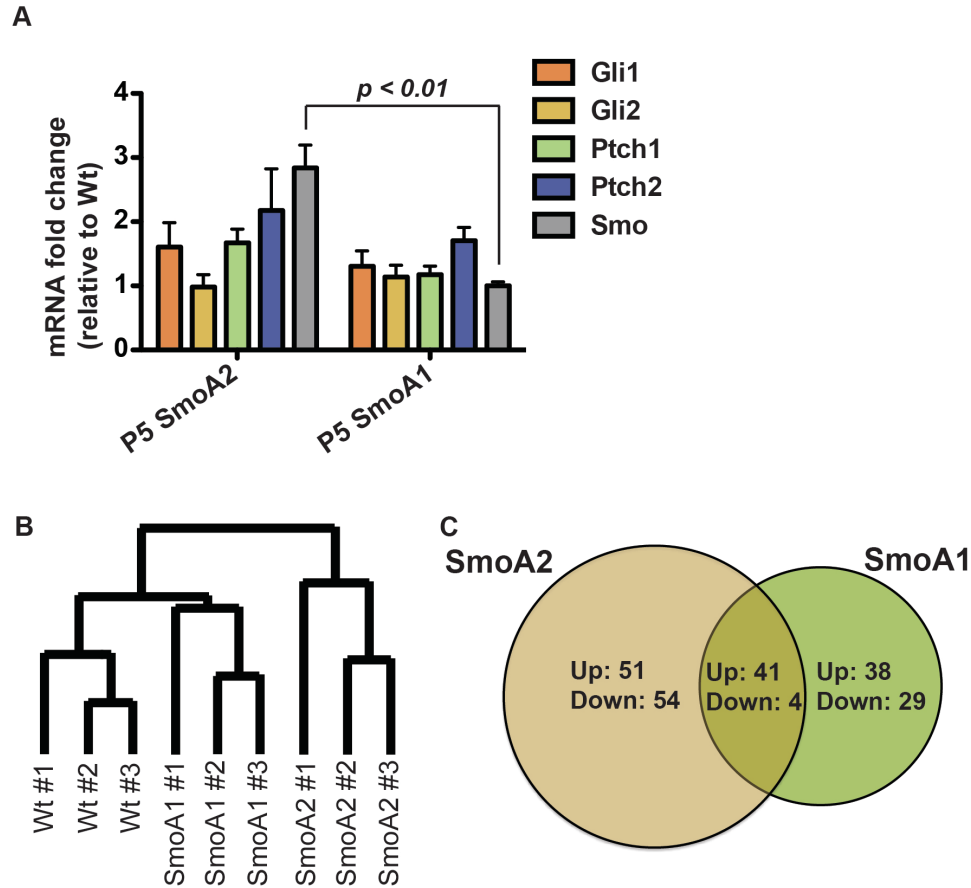


Figure 2.5

Transcriptional profiles of SmoA1 and SmoA2 P5 cerebella

(A) mRNA expression of canonical Shh target genes *Gli1*, *Gli2*, *Ptch1*, *Ptch2* and *Smo* (endogenous + transgene expression) as determined by qRT-PCR analysis using mRNA from WT, SmoA2 or SmoA1 P5 cerebella (n=3 per genotype). Columns represent average fold-change of each target in SmoA2 and SmoA1 relative to WT controls. *Gapdh* was used as the endogenous control. Each condition was run in triplicate. Total *Smo* expression, 2.8-fold higher in SmoA2 compared to SmoA1, is the only target whose difference was statistically significant (Student t-test; p value <0.01). Error bars represent \pm SEM (B) Hierarchical cluster analysis shows transcriptional similarity of WT and SmoA1 P5 cerebella in comparison to SmoA2 (n=3 per genotype) (C) Venn diagram shows unique and overlapping changes in transcript expression (≥ 2 absolute fold change, $p < 0.001$) between P5 SmoA2 and SmoA1 cerebella.

Table 2.2 Genes uniquely up-regulated in the postnatal day 5 SmoA2 cerebella compared to age-matched WT controls

Accession Number	Gene symbol	*Fold change
NM_145745	Adam34	5.5
NM_138944	Pou4f2	5.2
NM_026358	4930583H14Rik	4.7
NM_011143	Pou4f1	4.4
NM_011314	Saa2	4.3
NM_010866	MyoD	4
NM_021399	Bcl11b	3.8
NM_175631	Cbln4	3.7
AK047003	Herc1	3.5
ENSMUST00000067450	2700046A07Rik	3.4
AK141295	Sema3e	3.4
ENSMUST00000066060	Bcl11b	3
BB367552	Bcl11b	3
AK035897	Ranbp17	2.8
AK081638	None	2.7
NM_029530	6330527O06Rik	2.7
NM_181529	Syt15	2.6
AK050850	Igf2bp1	2.6
NM_001007584	OTTMUSG00000002038	2.5
NM_009951	Igf2bp1	2.5
NM_009144	Sfrp2	2.4
NM_009236	Sox18	2.4
ENSMUST00000066047	Bcl11b	2.3
NM_007662	Cdh15	2.3
NM_007606	Car3	2.2
ENSMUST00000035914	BC034090	2.2
AF017639	Cpxm2	2.2
NM_145497	BC016495	2.2
NM_007555	Bmp5	2.1
NM_023146	Ranbp17	2.1
AK030810	Cdk6	2.1
NM_172485	Thsd7b	2.1
NM_001045514	Akna	2
AK036025	None	2
NM_011923	Angptl2	2
AV290704	Angptl2	2
NM_009625	Adcyap1	2
NM_130858	Nxph3	2

Table 2.2 continued

Accession Number	Gene symbol	*Fold change
NM_145463	Shisa2	1.9
AK029182	None	1.9
AK020918	A930032L01Rik	1.9
NM_013820	Hk2	1.9
AK160412	Bmp5	1.9
CD562285	Car2	1.9
NM_008958	Ptch2	1.9
NM_139134	Chodl	1.9
ENSMUST00000074819	2410127L17Rik	1.9
NM_026929	Chac1	1.9
AK144315	Epb4.114b	1.9
AK027955	1110034N17Rik	1.9
NM_026929	Chac1	1.9

*Absolute Fold changes ≥ 2 are shown in this table.

Positive numbers mean increase in expression and negative numbers mean reduction in expression compared to age-matched WT controls (pooled)

All genes meet the $p < 0.01$ level of significance

Table 2.3 Genes uniquely down-regulated in the postnatal day 5 SmoA2 cerebella compared to age-matched WT controls

Accession Number	Gene symbol	*Fold change
NM_175647	Dmrta1	-4.3
CA323388	Sypl2	-3.3
NM_009022	Aldh1a2	-3
NM_146010	Tspan8	-2.9
NM_153565	Pcsk9	-2.9
DQ656357	D0Kist2	-2.8
BC030038	Sypl2	-2.7
NM_008766	Slc22a6	-2.7
BC069182	Trp73	-2.7
NM_173375	BC064033	-2.6
NM_018857	Msln	-2.6
NM_172709	Otop1	-2.5
ENSMUST00000039303	Npy1r	-2.4
NM_009864	Cdh1	-2.3
NM_011915	Wif1	-2.3
NM_010277	Gfap	-2.3
NM_181588	Cmb1	-2.2
NM_133661	Slc6a12	-2.2
NM_133229	Ripply3	-2.2
NM_013519	Foxc2	-2.2
AK039668	A730046J19Rik	-2.1
NM_148933	Slco4a1	-2.1
NM_144512	Slc6a13	-2.1
BC066851	Pcdhga12	-2.1
NM_007553	Bmp2	-2.1
NM_009714	Asgr1	-2.1
NM_007501	Neurod4	-2
NM_001010937	Gjb6	-2
NM_011153	None	-2
NM_008963	Ptgds	-2
NM_175012	Grp	-2
NM_007494	Ass1	-2
ENSMUST00000095183	Nrxn1	-2
NM_172870	Bnc2	-2
NM_021355	Fmod	-1.9
BC038653	Lyve1	-1.9
ENSMUST00000058077	E030011K20Rik	-1.9
NM_011324	Scnn1a	-1.9

Table 2.3 continued

Accession Number	Gene symbol	*Fold change
NM_172446	Lbxcor1	-1.9
AK032623	A930035E12Rik	-1.9
C78942	D1Ertd218e	-1.9
AK049102	A830029E22Rik	-1.9
NM_183183	Gprin3	-1.9
AK036173	None	-1.9
ENSMUST00000068175	Gm941	-1.9
AK047689	None	-1.9
NM_001024139	Adamts15	-1.9
AK081659	C130061O14Rik	-1.9
NM_146241	Trhde	-1.9
ENSMUST00000000031	None	-1.9
NM_172399	A930038C07Rik	-1.9
NM_008471	Krt19	-1.9
NM_010701	Lect1	-1.9
AK136780	Gm626	-1.9

* Absolute Fold changes (FC) ≥ 2 are shown in this table (p value < 0.001)

Fold changes expressed in negative numbers denote reduction in expression compared to age-matched WT controls (pooled)

Table 2.4 Genes uniquely up-regulated in the postnatal day 5 SmoA1 cerebella compared to age-matched WT controls

Accession Number	Gene symbol	*Fold change
NM_013496	Crabp1	11.5
NM_001013767	Capn11	4.9
AY540025	Mid1	4.1
ENSMUST00000011398	Thg1l	3.9
NM_139225	Defb10	3.4
XM_907202	Ccnblip1	3.3
NM_011436	Sorl1	3.3
NM_012011	Eif2s3y	3
NM_139219	Defb9	2.9
BC030050	621998	2.8
NM_207229	Plac9	2.7
NM_013823	Kl	2.6
BC085191	Diap3	2.6
AK049248	Slc4a5	2.3
NM_007739	Col8a1	2.3
NM_053181	Pdxdc1	2.3
NM_001080969	Thg1l	2.3
NM_026323	Wfdc2	2.2
NM_183389	Duxbl	2.2
ENSMUST00000054217	Wfikkn2	2.2
NM_021395	Hyou1	2.2
NM_025311	D14Ertd449e	2.2
CJ298892	AI317185	2.2
AK018742	Col8a1	2.1
NM_178446	Rbm47	2.1
NM_008312	Htr2c	2.1
ENSMUST00000034998	4930422I07Rik	2.1
AK018220	6330525I24Rik	2
AK160781	Plac9	2
AK133500	Comt1	2
AK152971	Rbm47	2
AK009210	2310007J06Rik	2
AK034789	5830458C19Rik	1.9
NM_199473	Col8a2	1.9
AK013119	Rcbtb2	1.9
AI987986	D14Ertd449e	1.9
AK083103	Mobp	1.9
NM_001009935	Txnip	1.9

Table 2.5 Genes uniquely down-regulated in the postnatal day 5 SmoA1 cerebella compared to age-matched WT controls

Accession Number	Gene symbol	*Fold change
NM_009209	Slc6a2	-7.4
NM_009431	Ctr9	-5.7
NM_008623	Mpz	-5.6
AK084170	D230004N17Rik	-4.8
AK159710	Wdfy1	-4.2
NM_175498	Pnma2	-4
NM_028121	Adpgk	-3.9
AK158527	None	-3.7
AK043426	A730094K22Rik	-3.4
AK034149	9330159M07Rik	-3.2
NM_001039533	Pdxdc1	-3.1
AK046789	B830008M09Rik	-3
AK042670	A730014G21Rik	-2.9
AK011224	Rbm3	-2.9
AK048966	C230086J09Rik	-2.9
AK050253	9430037G07Rik	-2.8
AK142900	None	-2.7
AK165554	Wdfy1	-2.6
AK142214	EG666451	-2.6
NM_016809	Rbm3	-2.6
DT932411	None	-2.3
BC058551	Il6st	-2.2
AK014787	4833428M15Rik	-2.1
NM_013603	Mt3	-2.1
XM_001006405	None	-2.1
NM_023831	1500035H01Rik	-2.1
NM_020279	Ccl28	-2
AK013947	Gmfb	-1.9
NM_001039198	Zfhx2	-1.9

* Absolute Fold changes (FC) ≥ 2 are shown in this table (p value < 0.001)

Fold changes expressed in negative numbers denote reduction in expression compared to age-matched WT controls (pooled)

Table 2.6 Genes up-regulated in both postnatal day 5 SmoA2 and SmoA1 cerebella compared to age-matched WT controls

Accession Number	Gene symbol	SmoA2 FC	SmoA1 FC
NM_021459	Isl1	8.5	2.4
NM_183173	Ankrd43	6.5	3
NM_010446	Foxa2	6.1	3
AK011210	2600014E21Rik	3.5	1.8
NM_001081171	Lama5	3.5	1.7
NM_001081127	Adamts14	3.3	1.6
AK021003	B230216N24Rik	3.2	1.5
NM_012008	Ddx3y	3.1	3.5
AK013627	2900040C04Rik	2.9	4
NM_016675	Cldn2	2.8	2.6
NM_139221	Defb11	2.7	3.5
NM_008034	Folr1	2.6	3.1
NM_016674	Cldn1	2.5	3.1
NM_011545	Tcf21	2.5	2.8
NM_172469	Clic6	2.4	3.2
NM_001035245	Trpm3	2.4	2.8
ENSMUST00000040002	1110059M19Rik	2.3	3.2
NM_134110	Kcne2	2.3	3.1
NM_001035246	Trpm3	2.3	2.4
NM_001017407	1700021K02Rik	2.3	1.6
NM_007472	Aqp1	2.2	3.3
AY134666	Sostdc1	2.2	2.8
NM_178768	Tmem72	2.2	2.6
ENSMUST00000099699	4631405J19Rik	2.2	1.5
NM_178406	Gpr153	2.2	1.3
NM_013697	Ttr	2.1	2.5
AK166311	Cdk6	2.1	1.3
NM_178396	Car12	2	2.5
NM_027399	Steap1	2	2.4
BC060172	Ccnd1	2	1.6
ENSMUST00000025631	Ostf1	2	1.5
NM_177152	Lrig3	2	1.3
AK013544	2900017F05Rik	1.9	2.2
NM_024283	1500015O10Rik	1.9	2
NM_007378	Abca4	1.9	1.9
AK164997	Ccnd1	1.9	1.5
AK076778	4930447K04Rik	1.9	1.4
BC057642	2010011I20Rik	1.9	1.4

Table 2.6 continued

Accession Number	Gene symbol	SmoA2 FC	SmoA1 FC
AK154197	Cdk6	1.9	1.3
NM_010664	Krt18	1.8	2.5
NM_138304	Calml4	1.6	2.5

* Absolute Fold changes (FC) ≥ 2 are shown in this table (p value < 0.001)

Fold changes expressed in negative numbers denote reduction in expression compared to age-matched WT controls (pooled)

Table 2.7 Genes down-regulated in both postnatal day 5 SmoA2 and SmoA1 cerebella compared to age-matched WT controls

Accession Number	Gene symbol	SmoA2 FC	SmoA1 FC
NM_010930	Nov	-2.8	-1.7
NM_026183	Slc47a1	-2.5	-1.8
ENSMUST00000040960	Slc6a20a	-2.2	-1.3
ENSMUST00000067444	Gfap	-2	-1.4

* Absolute Fold changes (FC) ≥ 2 are shown in this table (p value < 0.001)

Fold changes expressed in negative numbers denote reduction in expression compared to age-matched WT controls (pooled)

Discussion

In this study, we have established a mouse model of medulloblastoma that manifests severe defects in critical pathways of cerebellar development including neuronal proliferation, differentiation and migration stemming from an activating mutation, SmoA2. Our comparative analysis reveals vastly different phenotypic effects of the SmoA2 and SmoA1 mutations and thereby demonstrates the complexity of the downstream molecular pathways regulated by a single molecule. The lack of a significant difference in the level of activation of the Shh pathway at P5 suggests that the phenotypic differences are not exclusively due to extent of pathway activation. The similarity in global transcriptional profiles between the WT and SmoA1 mice in early development is in concurrence with phenotype of SmoA1 being indistinguishable from WT at that stage whereas the SmoA2 phenotype and transcriptional profile stand unique. We have demonstrated how two activating mutations in an identical domain of a single protein can cause unique changes. Identifying molecular pathways uniquely employed by SmoA2 and SmoA1 variants with cues from the GO classification remains an important future direction that may provide further insights into the mechanics of the Shh pathway both in normal development and tumorigenesis.

The cell of origin of the Shh-driven subtype of medulloblastomas has been shown to belong to the granule neuron lineage (Goodrich et al., 1997; Hallahan et al., 2004; Oliver et al., 2005; Gilbertson and Ellison, 2008; Hatton et al., 2008; Schuller et al., 2008; Yang et al., 2008). However, why the niche of the superficial surface of the cerebellum is conducive to tumorigenesis as seen in several mouse models (Oliver et al., 2005; Hatton et al., 2008; Yang et al., 2008) including SmoA2, is yet to be understood. In the Patched heterozygous model (Oliver et al., 2005), ectopic rests of pre-neoplastic cells that have failed to undergo proper

migration reside in the niche of the EGL whereas the vast majority of GNPs mature and organize correctly. Intriguingly, in the SmoA2 developing cerebellum the vast majority of GNPs undergo abnormal migration and manifest neoplastic features early in development. However, the frank tumors remain confined to the superficial surface of the cerebellum. By design of the transgene, each GNP should express the SmoA2 oncogenic mutation, yet dysplasias adjacent to the tumors consist of normally differentiated granule neurons. This suggests that potential cell-extrinsic factors in the pial surface might act on a subset of SmoA2 cells arrested in migration leading to tumor initiation. The cells that have migrated away from the EGL differentiate or regress. Alternatively, cell-extrinsic factors could attract neoplastic cells to the pial surface by providing a favorable environment for tumor growth. The leptomeningeal membrane known to secrete chemokines and other trophic factors (Stylianopoulou et al., 1988; Klein et al., 2001), is one potential source of such extrinsic signals. Future experiments to further characterize the environmental niche and the residing precursors will provide further insights into the development of this subtype of medulloblastoma.

An interesting phenomenon observed in the SmoA2 developing cerebellum is the apparent regression of the hypercellularity observed throughout the developing cerebellum. Progenitor cells in the developing cerebellum appear to have neoplastic characteristics morphologically as well as functionally as shown by transplantation experiments. Yet, in a mature SmoA2 cerebellum, the dysplasias histologically seem to have fewer cells and consist of mature neurons. The early neoplastic lesions are confined to the superficial surface of the cerebellum while the rest of the cerebellum remains dysplastic. Spontaneous regression has been documented in certain cancers such as the highly malignant Stage IV-S neuroblastoma

(D'Angio et al., 1971; Nickerson et al., 2000) the molecular basis of which is poorly understood. There is conflicting data regarding the role of apoptosis in spontaneous regression in neuroblastoma (Yu et al., 2011). We have been unable to detect any significant apoptotic cell death by immunohistochemistry for activated caspase 3 (data not shown). Whether the processes underlying the apparent regression observed in the SmoA2 cerebellum include delayed neuronal differentiation programs, caspase dependent and possible caspase independent programmed cell death like autophagic degeneration as implicated in neuroblastoma (Kitanaka et al., 2002), are yet to be determined.

Shh signaling acting through the Smo-Gli axis has been shown to regulate foliation with the extent of foliation proportional to the level of signaling (Corrales et al., 2004; Corrales et al., 2006). However, increased cell-autonomous Shh signaling in the SmoA2 model leads to disruptions distinct from phenotypes reported in previous studies (Corrales et al., 2004; Hallahan et al., 2004; Corrales et al., 2006; Hatton et al., 2008; Yang et al., 2008). We have demonstrated that the disorganized cytoarchitecture of the SmoA2 cerebellum cannot be attributed to exclusively increased proliferation of GNPs as defects in foliation and migration are not observed in the Ptch conditional knock-out mice (Yang et al., 2008). The effects of cell-autonomous Shh signaling on neuronal migration are yet to be understood. Further investigation of the SmoA2 gene expression profile will potentially provide further insights into the role of Shh signaling on neuronal migration in cerebellar development.

The stereotyped neuronal circuitry of the cerebellum, critical for its function as a motor coordination center, depends on the stereotypic arrangement and distinct morphologies of Purkinje cells, granule neurons and the deep cerebellar neurons (Chizhikov and Millen, 2003). In addition to the reiterative circuitry, it has been shown that topological gene

expression patterns in Purkinje cells define longitudinal domains that are essential for proper targeting of incoming cerebellar afferents (Wassef et al., 1992; Sotelo and Chedotal, 1997; Nishida et al., 2002). Our data reporting the dysplastic phenotype of the SmoA2 cerebellum and the lack of any overt neurobehavioral deficiencies question the indispensability of this highly stereotypic arrangement for proper functioning of the cerebellum. Both the morphology and organization of Purkinje cells and granule neurons are severely disrupted in the SmoA2 cerebellum. Yet the lack of detectable behavioral anomalies in the SmoA2 mice suggests that the transmissions of afferent and efferent signals seem to be largely maintained. Mutant mice such as *reeler* and *staggerer* have neuroanatomic defects most pronounced in the cerebellum (Goldowitz et al., 1997; Goldowitz and Hamre, 1998; Rice and Curran, 1999) with ectopic Purkinje cells, lack of foliation and a reduction in the number of granule neurons. These mice display ataxia and uncoordinated movement characteristic of cerebellar malfunctions. Yet, intriguingly SmoA2 mutants with some phenotypic similarities in terms of disruptions in the laminar architecture with more severe morphological abnormalities in multiple cell types, maintain grossly normal motor behavior.

In summary, through the characterization of the unique phenotype of the SmoA2 model, we address key aspects of cerebellar development and function as well as of medulloblastoma biology that are yet to be understood. The SmoA2 model is therefore a valuable addition to the existing mouse models of medulloblastoma. Medulloblastoma is known to be a cancer resulting from deregulated developmental signals. The developmental phenotype of the SmoA2 model will therefore allow investigation of cerebellar developmental pathways and aberrations thereof that potentially lead to medulloblastoma formation.

Materials and Methods

Generation of the ND2:SmoA1 and ND2:SmoA2 Transgenic Lines

The ND2:SmoA1 and ND2:SmoA2 transgenic mouse lines were previously described (Hallahan et al., 2004; Hatton et al., 2008). All mice were maintained in accordance with the NIH Guide for the Care and Use of Experimental Animals with approval from the Fred Hutchinson Cancer Research Center Institutional Animal Care and Use Committee (IR#1457).

Mouse pathology and Immunohistochemistry

Mice were anesthetized using CO₂ inhalation, the cerebellum removed, and tissue snap-frozen for RNA studies, GNP isolation or fixed in 10% paraformaldehyde for pathological examination. Tissue blocks were paraffin-embedded, cut into 4- μ m sections, and stained with Hematoxyline and Eosin using standard methods. For immunohistochemical analysis, mouse NeuN (Millipore), rabbit Calbindin (Millipore,1:500), rat Ki67 (DAKO), S100 (DAKO), antibody was used; secondary antibodies were applied according to Vectastain Elite avidin-biotin complex method instructions (Vector Laboratories), and detection was carried out with 3,3'-diaminobenzidine reagent (Vector Laboratories). Sections were visualized with a Nikon E800 microscope, and images were captured using the CoolSnap cf color camera (FHCRC Scientific Imaging Core).

RNA isolation and Gene expression analysis

Total RNA was isolated from trizol lysates of each cerebella from P5 WT, Smo/Smo and SmoA2 cerebella (n=3 animals per genotype) using the Promega SV-96 RNA isolation

kit. Microarray analysis was performed by use of custom designed Affymetrix arrays. Extracted RNA was quantified by use of RiboGreen RNA Quantitation Reagent (Invitrogen) and its quality assessed by use of the Agilent RNA 6000 Pico Kit (Agilent, Santa Clara, CA) in an Agilent 2100 Bioanalyzer (Agilent). Samples were amplified and labeled by use of the Ovation WB protocol (NuGEN Technologies, San Carlos, CA), according to the manufacturer's instructions. The resulting amplified cDNAs were hybridized to Affymetrix gene expression chips (Mouse Rosetta Custom Affymetrix 1.0, Affymetrix, Santa Clara, CA). Images were analyzed by use of Affymetrix GeneChip Operating Software (GCOS) and processed further to derive sequence-based intensities by use of the RMA algorithm. Rosetta Resolver system (Rosetta Biosoftware, Seattle, WA) was used to calculate fold changes and ratio *p*-values for the differential expression of genes in each of three replicates of SmoA1 or SmoA2 versus a virtual pool of age-matched WT controls (n=3). *p*-values were calculated using the Rosetta intensity based Affymetric error model. Genes that were present in at least two of the three replicates for SmoA1 and SmoA2 with a *p*-value of <0.01 and absolute average fold change of ≥ 2 were considered significantly differentially expressed genes. For clustering analysis we first filtered the data to remove data from probe sets whose expression levels did not significantly vary across the samples (defined as top 50% least variable). The filtered data was then clustered using traditional hierarchical clustering. The GO enrichment analysis was carried out using a hypergeometric test for each unique category. We selected significantly enriched categories as any with $FDR < 10\%$. Microarray data have been deposited in the NCBI Gene Expression Omnibus and are accessible through GEO series accession number GSE34593.

Quantitative Reverse Transcription PCR

For quantitative reverse transcription PCR (qRT-PCR), RNA was isolated using RNeasy Kit (Invitrogen), DNase (Qiagen) treated and converted to cDNA using the ABI Taqman Reverse Transcription kit (Applied Biosystems, Foster City, CA). Reactions were set up using Taqman Master Mix and run on an ABI 7000 Sequence Detection System. Taqman Gene Expression Assays (Applied Biosystems) were used for mouse *Gli1*, *Gli2*, *Ptch1*, *Ptch2*, *Smo*. Data were analyzed using ABI GeneAmp SDS software. All of the conditions were run in triplicate and normalized to mouse *Gapdh* control.

Behavioral Tests

Rotarod Test was conducted using RotaRod (Model 7650; Ugo Basile Comerio, Italy) accelerating from 3 to 30 rpm over a 5-min period. The mice were given a trial run prior to the timed run where the latency to fall was recorded.

Footprint assay: The bottom of each foot was coated with non-toxic paint. The mouse was allowed to walk through a small tunnel on white paper. Stride length (distance between two hind paw prints) and stance width (distance between opposite hind paw prints perpendicular to the walking trajectory) were calculated. Each mouse was given a trial run before the final run.

Modified SHIRPA

SHIRPA stands for SmithKline Beecham Pharmaceuticals; Harwell, MRC Mouse Genome Centre and Mammalian Genetics Unit; Imperial College School of Medicine at St Mary's; Royal London Hospital, St Bartholomew's and the Royal London School of Medicine; Phenotype Assessment. Our lab developed an abbreviated behavioral test based on the above

that we called the Modified SHIRPA. A single observer evaluated mice for weight, physical phenotype – *tremor*: 1=none/mild 2=marked; *body position*: 1=elongated 2=hunched/rounded; *tail position*: 1=horizontally extended 2=dragging/straub; behavior phenotype – *grooming*: 1=slow/casual 2=none/excessive; *spontaneous activity*: 1=moderate mouse covers all quadrants of cage 2=slow 1-3 quadrants, 3=none/darting/circling; *locomotor activity*: the number of times the mouse places atleast one of its paws on the side of the cage over a 2-minute period).

Statistical tests

Student t-test was used to determine if differences observed between measurements obtained from two groups being compared were statistically significant. The level of significance was set at $p < 0.01$.

Chapter 3

A novel role of MyoD, a muscle differentiation factor, as a tumor suppressor in mouse models of medulloblastoma

Abstract

Medulloblastoma, an embryonal tumor of the cerebellum, is the most common pediatric brain malignancy. For decades, it has been known that a small subset of medulloblastomas present with myogenic differentiation. However, the mechanistic basis and significance of this biological anomaly remain to be determined. We have identified previously unknown expression of muscle differentiation factor, MyoD in cerebellar tumors from mouse models of medulloblastoma as well as in a subset of human medulloblastomas. At a cellular level, MyoD is expressed in mitotically active cells and intriguingly, in mouse tumors does not activate the muscle differentiation program. To understand the functional consequence of this finding in medulloblastoma genesis, we have conducted genetic studies to assess tumor formation in the SmoA1 and SmoA2 medulloblastoma models, on a MyoD-deficient background. We demonstrate that MyoD acts as a haploinsufficient tumor suppressor as the MyoD^{wt/-}; SmoA1 and MyoD^{wt/-}; SmoA2 mice have an accelerated onset of tumors compared to MyoD^{wt/wt}; SmoA1 or MyoD^{wt/wt}; SmoA2 mice respectively. Our findings suggest that the expression of MyoD might be an oncogene-induced compensatory response in the cerebellum to suppress tumor growth by restoring balance between proliferation and differentiation, similar to the role of some other bHLH transcription factors. Harnessing this latent tumor suppressor network to induce differentiation or cell cycle arrest holds promise for future therapeutic interventions.

Introduction

Medulloblastoma is the most common pediatric brain cancer that continues to be the leading cause of cancer-related deaths in children below 9 years of age (Oliver et al., 2005). Medulloblastomas are classified into various histological categories, which are often associated with the underlying molecular basis of tumorigenesis (Gibson et al., 2010; Sengupta et al., 2011). Medullomyoblastoma is a rare histological variant of medulloblastoma which presents with myogenic differentiation (Banerjee and Kak, 1973; Smith and Davidson, 1984; Rao et al., 1990; Holl et al., 1991; Schiffer et al., 1992; Mahapatra et al., 1998). The molecular basis or significance of this pathological anomaly has never been investigated.

MyoD, a basic-helix-loop (bHLH) transcription factor is a critical regulator of the muscle differentiation program (Tapscott, 2005). MyoD together with myogenic transcription factors Myf5, MRF4 and Myogenin hetero dimerize with members of the E-protein subfamily to drive muscle specification, expression of skeletal muscle genes and muscle differentiation (Cao et al., 2010). Studies have demonstrated that forced expression of MyoD is able to convert various non-muscle cells such as fibroblasts, chondroblasts, retinal pigmented epithelial cells amongst others into the skeletal muscle lineage (Choi et al., 1990; Weintraub et al., 1991). Gerber and Tapscott showed that forced expression of MyoD in neural tumor lines *in vitro* largely failed to induce myogenesis (Gerber and Tapscott, 1996). There is no experimental evidence of MyoD expression or function in the brain.

Studies have demonstrated that the expression of MyoD in certain cell types may be actively suppressed (Woloshin et al., 1995; Lee et al., 2004). It has been speculated that aberrant cell division leading to crisis situations such as neoplastic changes, may result in

release of suppression of differentiation factors like MyoD as a way to limit proliferation (Tapscott, 2005). Although historically recognized as a master regulator of the skeletal muscle differentiation program, over the years, MyoD has been shown to be associated with various kinds of cancers, the functional significance of which is yet to be explored.

DNA methylation of promoter associated CpG islands is a known mechanism for silencing tumor suppressor genes. *MYOD* was shown to have age related methylation in normal colon and hypermethylation in colon cancers (Ahuja et al., 1998). The MyoD CpG island shows a progressive increase in methylation during oncogenic transformation of the 10T1/2 cell line suggesting that the expression of MyoD is unfavorable for oncogenesis (Rideout et al., 1994). A recent study shows direct regulation of BRCA1 transcription by MyoD suggesting that MyoD may be part of a signaling complex that induces transcription of tumor suppressor gene BRCA1, which is reduced in sporadic breast and ovarian cancers (Jin et al., 2011). Therefore, the aforementioned findings suggest that the correlation of MyoD with cancer is not a mere association but likely an indication of important underlying functional consequences.

The pathophysiology of medullomyoblastoma and the possible function of MyoD in tumorigenesis led us to investigate a potential involvement of MyoD in medulloblastoma. We demonstrate ectopic expression of MyoD in three mouse models of medulloblastoma in proliferative tumor cells. During early cerebellar development, MyoD expression is detected in the granule neuron progenitors when they are in the peak of proliferation. The association of MyoD with the proliferative phase in normal cerebellar development as well as in tumors led us to investigate the functional consequence of MyoD expression. We demonstrate using

mouse genetics that MyoD functions as a potential haploinsufficient tumor suppressor in mouse medulloblastoma, a novel function for MyoD in the brain.

Results

MyoD is expressed in a subset of human medulloblastomas

To investigate whether MyoD is expressed in human medulloblastomas, we performed quantitative reverse transcription PCR (qRT-PCR) analysis using mRNA from primary tumor specimens. Eight out of 29 specimens investigated had *MYOD* mRNA expression 10-fold over normal controls (Table 3.1). Since we normalized the data to normal cerebellar controls in which *MYOD* mRNA expression was undetectable, the analysis results in exaggerated fold changes. We therefore show the range of Ct values obtained in *MYOD* expressing versus non-expressing tumors. We have not been able to confirm MYOD protein expression in human medulloblastoma clinical specimens using immunohistochemistry due to technical challenges associated with immunodetection methods. It remains possible that similar to *Myf5* in the brain, MYOD is transcribed but not translated in human medulloblastoma cells.

MyoD is expressed in mouse models of medulloblastoma

Next, to understand the biological significance of MyoD expression, we sought to establish an appropriate animal model and investigated MyoD expression in mouse medulloblastoma. qRT-PCR analysis shows elevated *MyoD* mRNA in tumors from the ND2:SmoA2 mice (manuscript in preparation, Chapter 2) relative to WT age-matched adult mice (Figure 3.1A). Interestingly, *MyoD* mRNA is not expressed in SmoA2 cerebella that fail to develop into tumors. Next we investigated MyoD protein expression in tumors from SmoA2 mice and two additional mouse models of medulloblastoma - ND2:SmoA1 homozygous (Hallahan et al., 2004; Hatton et al., 2008) and Patched conditional knock out

Table 3.1**Assessment of *MyoD* mRNA in a subset of human medulloblastomas**

Tissue type	No. Of samples	MYOD Ct value	PPIA Ct average value (endogenous control)
Normal cerebellum	3	Ct = 40	20.3
Non-MYOD expressing medulloblastoma	21	Ct \geq 35	19.7
MYOD-expressing medulloblastoma	8	26.1 \leq Ct \leq 34	19.7

TABLE LEGEND

qRT-PCR analysis using primary human medulloblastoma specimens show ≥ 10 -fold expression of *MYOD* mRNA in 8 out of 29 specimens compared to normal cerebellar controls. *CYCLOPHILIN A (PPIA)* was used as the endogenous control for data normalization, Ct values of which are comparable across the three groups.

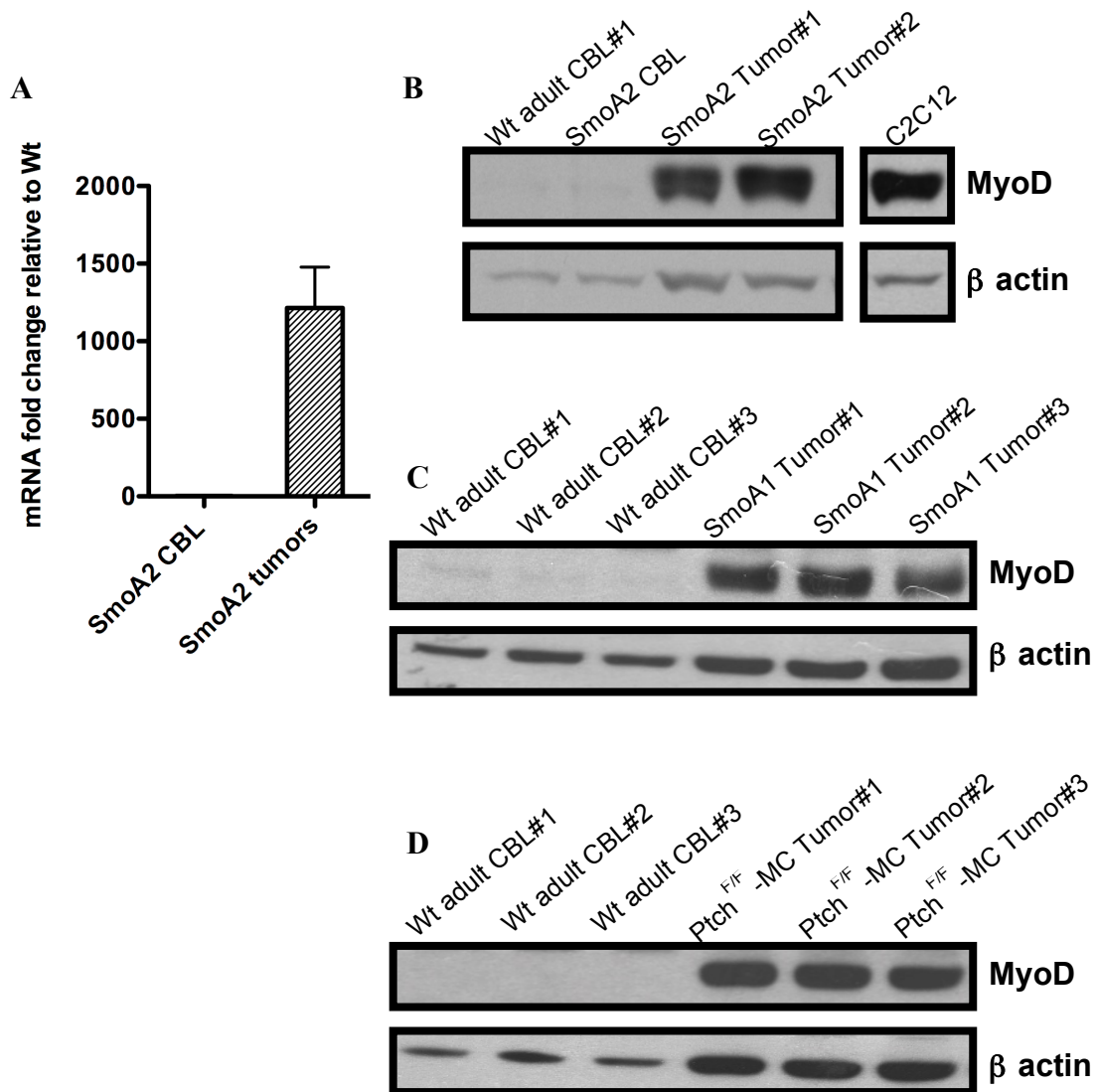


Figure 3.1

MyoD is expressed in cerebellar tumors in mouse models of medulloblastoma.

A. qRT-PCR analysis using mRNA isolated from tumors from SmoA2 mouse model of medulloblastoma and SmoA2 cerebella (CBL) without tumors show high expression of *MyoD* mRNA in tumors compared to WT adult CBL as well as SmoA2 CBL which have not developed tumors. β 2 microglobulin was used as the endogenous control for data normalization. **B, C, D.** Western blot analyses using protein lysates from WT and SmoA2, SmoA1 and *Ptch*^{F/F} Math-Cre (MC) tumors show strong expression of MyoD in all three tumor types comparable to levels observed in differentiated C2C12 muscle progenitor cells used as a positive control in the same experiment (B). MyoD protein is not detectable in adult WT CBL or in SmoA2 CBL that do not develop tumors. The analysis was repeated with three different antibodies in multiple replicates. Representative blots are shown in this figure. β actin was used as the loading control.

mice (Ptch^{F/F} Math1-Cre) (Yang et al., 2008). Western blot analyses reveal strong MyoD expression at the protein level in tumors from all three medulloblastoma models with no detectable expression in WT adult cerebella (Figure 3.1B). MyoD protein expression, similar to mRNA, is undetectable in SmoA2 cerebella that have not developed into tumors. This demonstrates a correlation between MyoD and tumor status of the mouse cerebellum independent of the driving oncogenic mutation.

MyoD is associated with the proliferative status of tumor cells

The ectopic expression of MyoD, a muscle differentiation factor in cerebellar tumors led us identify the cell type and elucidate the proliferative status of the cells it is expressed in. Immunofluorescence analyses demonstrate that MyoD is almost exclusively expressed in actively proliferating cells that express Ki67 and remains undetectable in the Ki67-negative cell population. MyoD and Ki67 expression are also undetectable in the WT adult cerebellum (Figure 3.2).

MyoD is expressed during early cerebellar development in wildtype and medulloblastoma mouse models

Medulloblastoma is an example of how aberrations in developmental pathways lead to tumorigenesis and many genes deregulated in cancer are known to be involved in normal developmental processes (Marino, 2005; Gilbertson and Ellison, 2008). Therefore, we investigated if MyoD mRNA and protein are expressed during cerebellar development at postnatal day (P) 5 because it is a stage when the cerebellum is undergoing critical developmental changes with the granule neuron progenitors (GNPs) in the phase of maximal

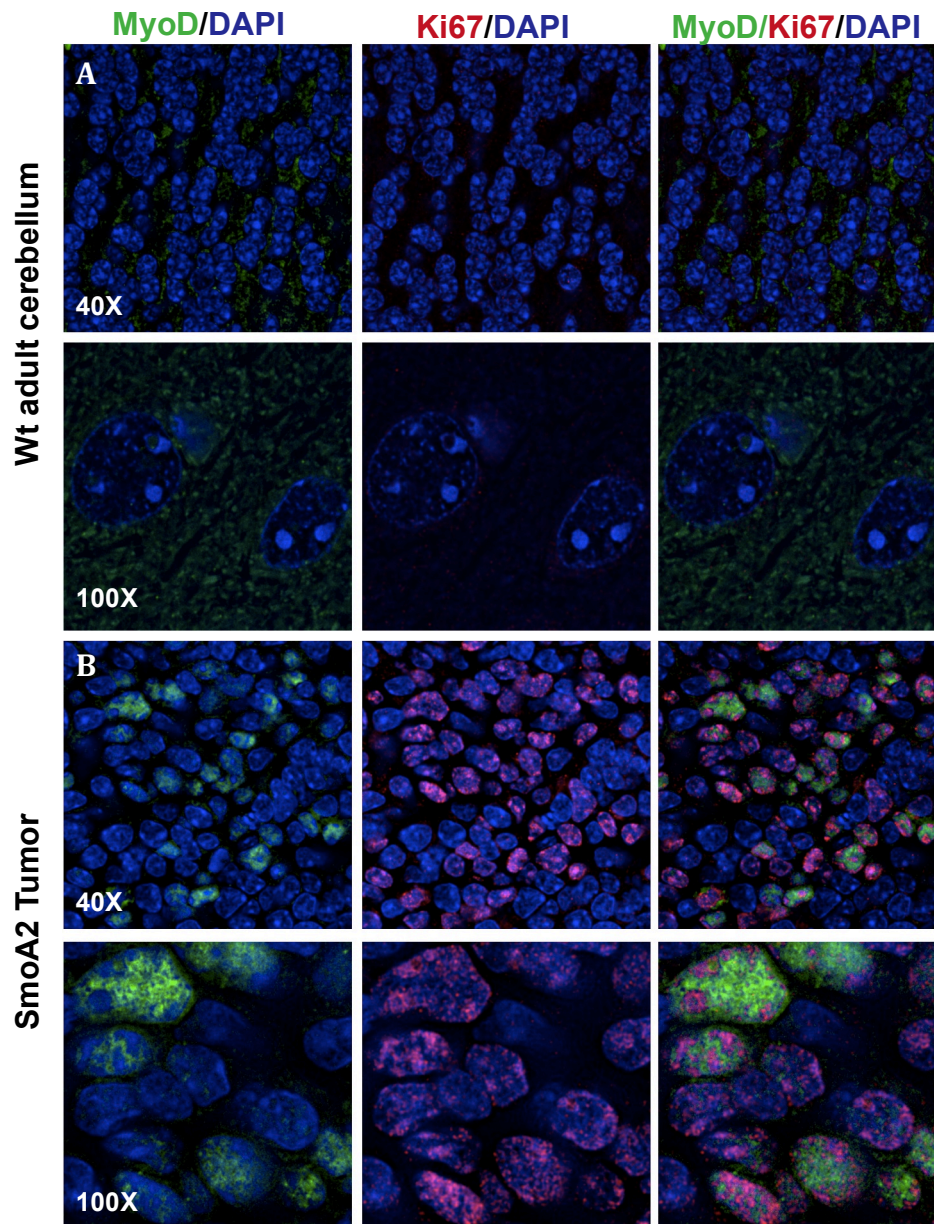


Figure 3.2

Cerebellar tumor cells undergoing proliferation express MyoD.

Immunofluorescence analyses for MyoD and proliferation marker, Ki67 show co-expression of both proteins in proliferating tumor cells. MyoD expression is undetectable in non-proliferating Ki67-negative cells in the tumor and the WT adult cerebellum which consists of postmitotic mature granule neurons. DAPI was used as the counterstain. 40X and 100X magnification were used for imaging.

proliferation. Intriguingly, compared to WT adult cerebellum, we observe elevated *MyoD* mRNA expression in WT P5 cerebellum (Figure 3.3A). The WT adult cerebellum consists of post-mitotic differentiated granule neurons whereas the WT P5 cerebellum consists of actively dividing GNPs. *MyoD* transcription is further increased in the *Ptch*^{F/F} *Math1*-Cre mice at P5 (Figure 3.3A) as well as in *SmoA1* and *SmoA2* (data not shown). Consistent with mRNA expression, we detect low levels of *MyoD* protein in WT P5 and *SmoA1* P5 cerebellum, which are phenotypically indistinguishable at this stage (Figure 3.3B). *MyoD* protein expression is elevated in *SmoA2* P5 mice, which is similar to the *Ptch*^{F/F} *Math1*-Cre cerebellum, undergoes hyper-proliferation at P5. This finding suggests that *MyoD* expression in early development occurs when GNPs are undergoing proliferation.

Proliferating granule neuron progenitors express *MyoD* in development

We conducted immunohistochemical analysis to identify the cell type in the developing cerebellum that expresses *MyoD*. We observe *MyoD* expression in a small subset of cells in the WT P5 mice primarily in the proliferative outer EGL that are also positive for Ki67 (Figure 3.4). The expression pattern is similar in *SmoA1* mice, which are phenotypically indistinguishable from WT at the P5 stage. *MyoD* is highly expressed in *SmoA2* and *Ptch*^{F/F} *Math1*-Cre cerebella both of which undergo massive GNP hyperproliferation leading to an expanded EGL at P5.

***MyoD* acts as a haploinsufficient tumor suppressor mouse medulloblastoma**

To investigate the biological significance of *MyoD* expression in cerebellar tumors, we investigated the effect of loss of *MyoD* on tumorigenesis. We crossed ND2:*SmoA1* and

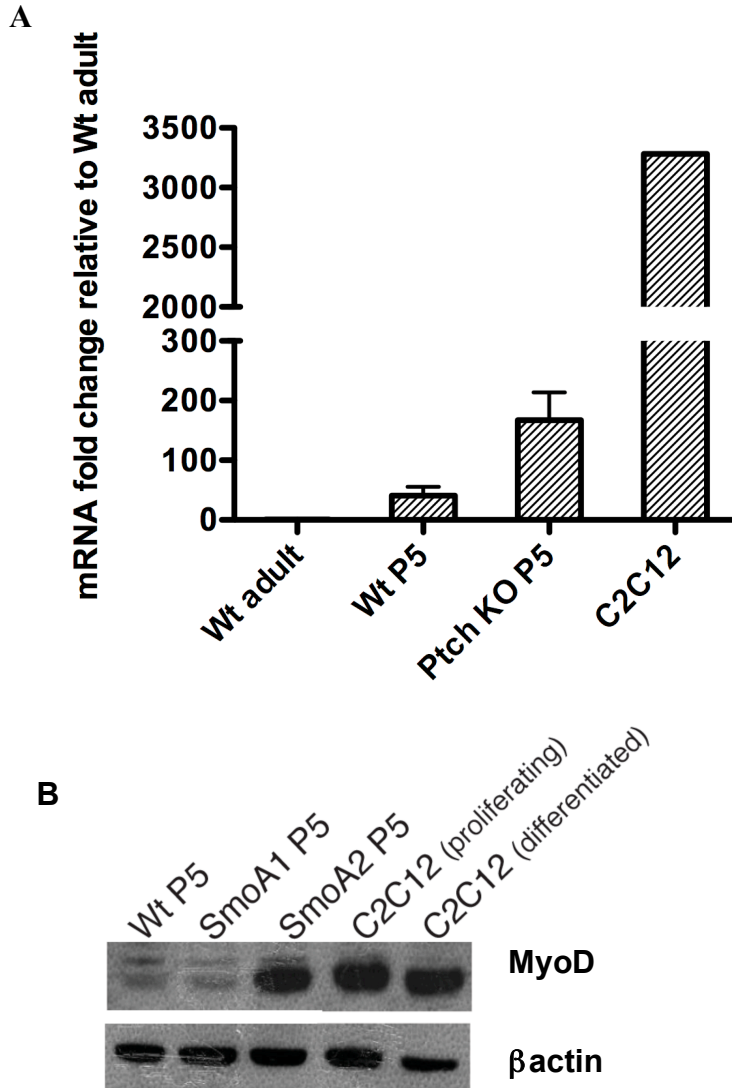


Figure 3.3

MyoD is expressed in the proliferative phase of early cerebellar development in mice.

A. qRT-PCR analysis using postnatal day (P) 5 GNP-enriched cell lysates of cerebella isolated from P5 WT and *Ptch*^{F/F} Math-Cre mice, show, in comparison to WT adult cerebella, elevated expression of *MyoD* mRNA in WT P5 cerebella which is further increased in P5 *Ptch*^{F/F} Math-Cre (*Ptch* KO) cerebella. mRNA from C2C12 differentiated muscle progenitor cells was used as the positive control for *MyoD* expression. β2 microglobulin was used as the endogenous control for data normalization. **B.** Western blot analyses using protein lysates of P5 cerebella show low levels of MyoD protein expression in P5 WT and SmoA1 cerebella, which are phenotypically indistinguishable at this stage. The level of expression is increased in SmoA2 P5 cerebella and is comparable to endogenous MyoD levels in muscle progenitor C2C12 cells in proliferating (PM) and differentiation (DM) states. β actin was used as the loading control.

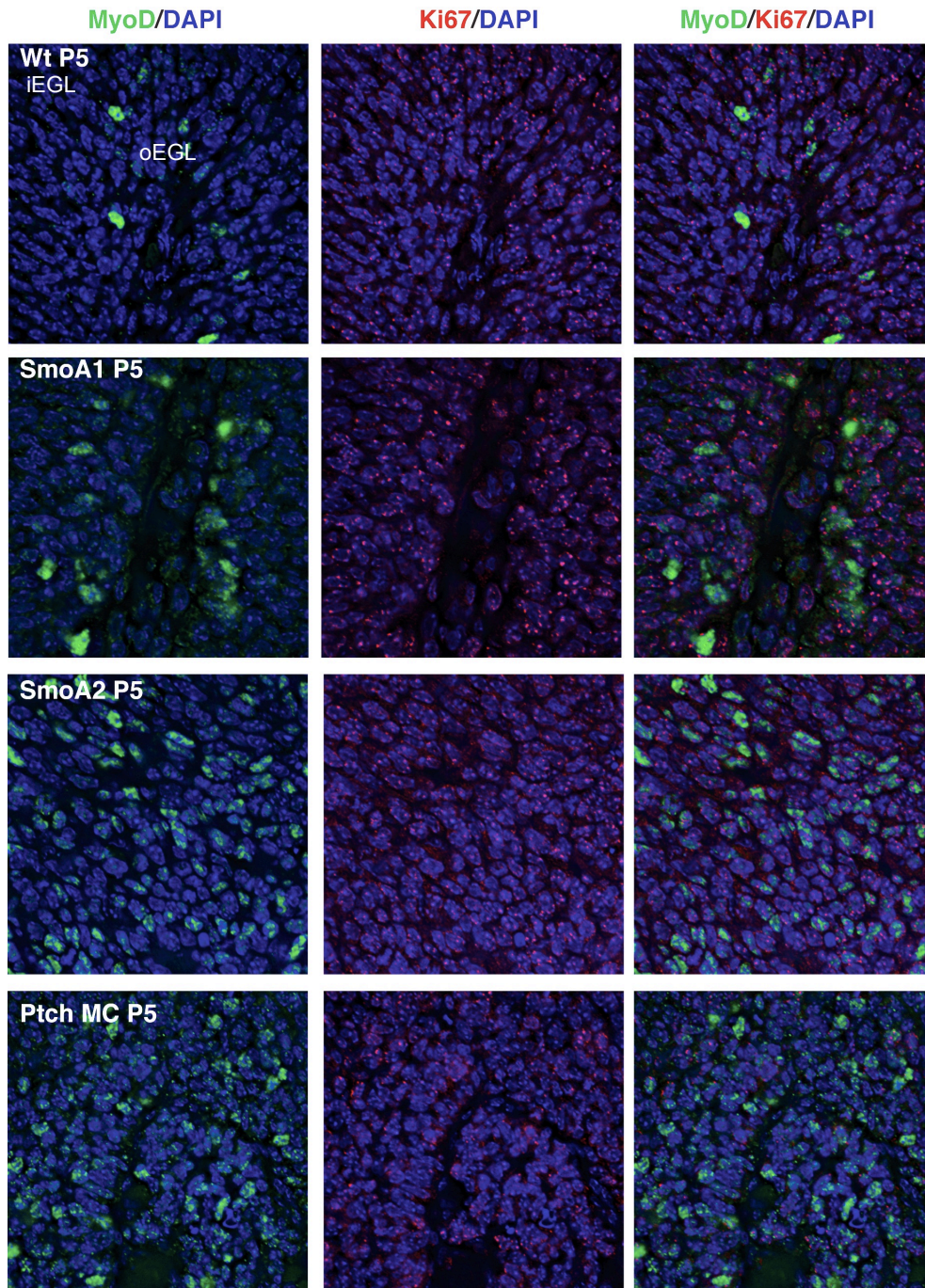


Figure 3.4

MyoD is expressed in proliferating granule neuron progenitors during cerebellar development.

Immunofluorescence analyses for MyoD and proliferation marker, Ki67 shows co-expression of both antigens in proliferating GNPs in WT, SmoA1, SmoA2 and Ptch^{F/F} Math1-Cre (MC) P5 cerebella. In WT and SmoA1 P5 cerebella, which are phenotypically identical at this stage, MyoD-positive cells appear to be restricted to the outer external granular layer (oEGL). In SmoA2 and Ptch^{F/F} Math1-Cre P5 cerebella, the EGL is expanded with hyper-proliferating GNPs, a large fraction of which are MyoD-positive. 40X magnification was used for imaging.

ND2:SmoA2 mice to MyoD^{-/-} mice (Rudnicki et al., 1992) to obtain MyoD^{-/-}; SmoA1 and MyoD^{-/-}; SmoA2 mice using a 2-step breeding strategy. Kaplan Meier survival analyses reveals that the MyoD^{-/-};SmoA1 (n=102) and MyoD^{-/-};SmoA1(n=83) mice have an accelerated onset of tumors compared to MyoD^{wt/wt};SmoA1 (n=108) and MyoD^{wt/wt};SmoA2 (n=99) mice respectively ($p < 0.001$) (Figure 3.5). Due to the compromised health resulting from the loss of both alleles of MyoD and paucity of MyoD^{-/-}; SmoA2 genotype from our genetic cross, we have been unable to recover a sufficient number of MyoD^{-/-}; SmoA2 mice required to study the effect of loss of both alleles of MyoD on tumorigenesis. Based on histopathological analyses, the MyoD-expressing cells in the mouse tumors do not show morphological features of skeletal muscle differentiation (Figure 3.5). Through genetic analyses we demonstrate that MyoD acts as a haploinsufficient tumor suppressor in cerebellar tumorigenesis in mice.

Regulation of muscle differentiation program genes by MyoD in cerebellar tumors

To identify the molecules regulated by MyoD consequent to its expression in the tumor cells, we investigated by qRT-PCR the mRNA levels of genes known to be regulated by MyoD in the muscle differentiation program, namely *Myf5*, *Myog*, *Desmin*, *Cdh15* and *Inhibitors of differentiation (Id)* genes *Id2* and *Id3*. Since the biochemical functions of Id proteins are similar, and Id1 and Id3 have overlapping expression patterns (Lyden et al., 1999), we chose to assess Id3 and Id2.

MyoD expression, as expected, is reduced in the MyoD^{-/-}; SmoA2 mice compared to MyoD^{wt/wt}; SmoA2 ($p < 0.05$). (Figure 3.6A). Both *Myf5* and *Myog* are up regulated in

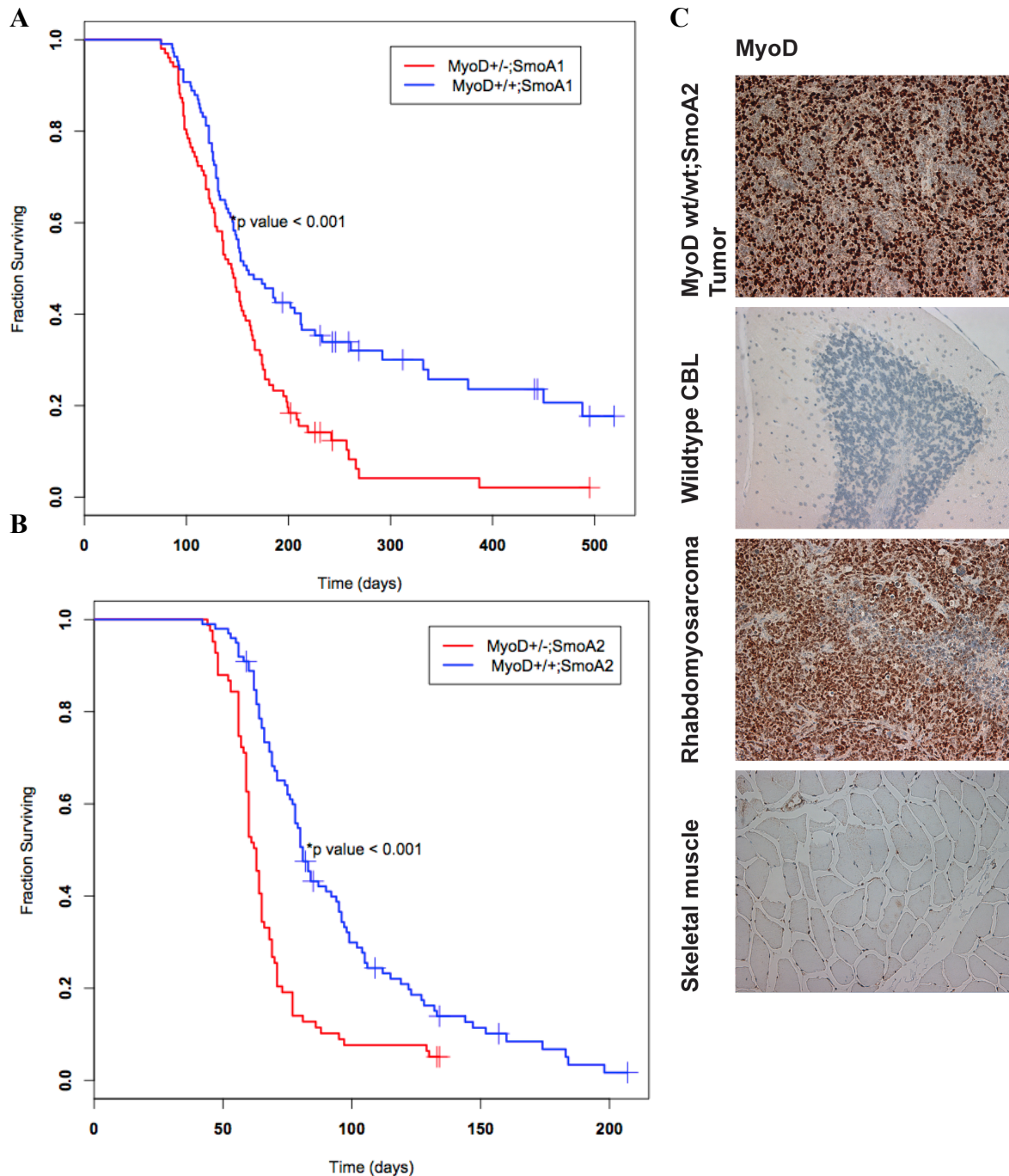


Figure 3.5

Loss of MyoD accelerates tumor onset in SmoA1 and SmoA2 models

Kaplan Meier survival analysis using (A) MyoD wt/wt;SmoA1 (n=108), MyoD wt/-;SmoA1 (n=102) and (B) MyoD wt/wt;SmoA2 (n=99), MyoD wt/-;SmoA2 (n=83) show earlier onset of tumors in SmoA1 and SmoA2 mice lacking one copy of MyoD. The difference in survival is statistically significant ($p \leq 0.001$) (C) MyoD IHC in representative MyoD wt/wt;SmoA2 tumor, WT mouse cerebellum (CBL), human rhabdomyosarcoma (RD) and human skeletal muscle show the lack of myogenic features in SmoA2 tumors similar to RD also known to overexpress MyoD that fails to cause differentiation.

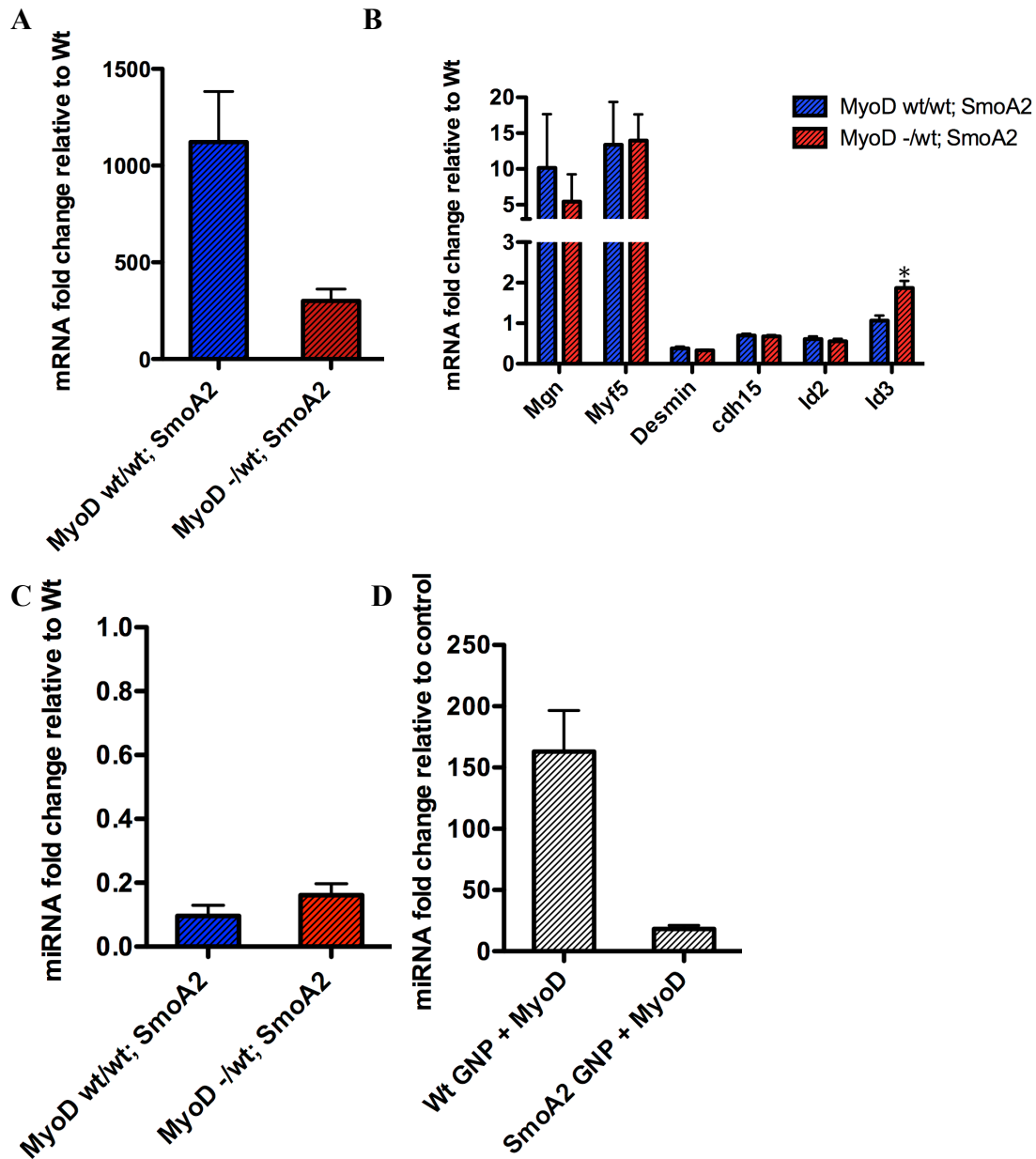


Figure 3.6

MyoD mediated regulation of muscle differentiation program genes in the cerebellar tumors

A. qRT-PCR analysis using total RNA from MyoD wt/wt; SmoA2 (n=5) and MyoD -/wt; SmoA2 (n=5) tumors show a decrease in *MyoD* transcription in the latter group with the loss of an allele of MyoD. **B.** qPCR analysis of known targets of MyoD. Compared to WT cerebella, mRNA levels of *Myogenin*, *Myf5* are increased in tumors from both groups of mice with no significant inter-group difference. Loss of an allele of MyoD causes *Id3* levels to increase about 2-fold in MyoD -/wt; SmoA2 compared to MyoD wt/wt; SmoA2 tumors (* $p < 0.01$). *Cdh15*, *Desmin* and *Cxcr4* are not significantly altered. $\beta 2$ microglobulin was used as the endogenous control for data normalization for A and B. **C** qRT-PCR analyses of miR-206 show reduced expression in both MyoD wt/wt; SmoA2 (n=6) and MyoD -/wt; SmoA2 (n=6) tumors compared to Wt cerebella with no significant inter-group difference. Sno 202 was used as the endogenous control for data normalization. **D.** Wt and SmoA2 GNPs were harvested from P5 cerebella and transduced *in vitro* with GFP (control) and MyoD expressing lentiviral constructs. MyoD causes a higher induction of miR-206 in WT GNPs compared to SmoA2 as measured by miR assay, Error bars represent standard error of the mean.

tumors from both groups but the inter-group difference is not statistically significant (Figure 3.6B). Consistent with the well-established inverse biological relationship between MyoD and Id3, *Id3* levels increase by about 2-fold in the MyoD -/wt; SmoA2 mice compared to MyoD wt/wt; SmoA2 ($p < 0.05$) (Figure 3.6B).

We also investigated expression of miR-206, a microRNA induced by MyoD during myogenic differentiation (Rosenberg et al., 2006) and known to have tumor suppressor properties in several cancers (Adams et al., 2007; Kondo et al., 2008; Song et al., 2009; Taulli et al., 2009; Wang et al., 2011; Chen et al., 2012). Although originally thought to be a muscle-specific microRNA, miR-206 has been shown to be enriched in the cerebellum the functional implications of which are yet unknown (Olsen et al., 2009).

Contrary to what we expected, miR-206 levels are reduced in the MyoD expressing tumors compared to WT controls, with no discernible difference between MyoD -/wt; SmoA2 and MyoD wt/wt; SmoA2 mice (Figure 3.6C). To elucidate this further, we overexpressed MyoD in WT and SmoA2 P5 GNP *in vitro* using a MyoD-expressing lentiviral vector and measured miR-206 levels. Although MyoD induces miR-206 in both WT GNP and SmoA2 GNP, the expression of miR 206 in WT GNP is significantly higher compared to SmoA2 (Figure 3.6D). This suggests that the oncogenic SmoA2 mutation might impair the ability of MyoD to induce miR-206 expression, which together with the deficiencies in other muscle differentiation genes may explain the lack of myogenesis in these tumors.

MyoD inhibits Id3 transcription

To confirm if the transcriptional up-regulation of *Id3* associated with down-regulation

of *MyoD* in the *MyoD* $-/-$ wt; SmoA2 tumors (Figure 3.6B) is caused by reduced *MyoD*, we carried out shRNA-mediated silencing of *MyoD* using two different constructs in GNP isolated from P5 ND2:SmoA2 mice and measured both *Id3* and *MyoD* levels. Pro-proliferative *Id* genes are known inhibitors of *MyoD*-mediated differentiation in myogenesis (Jen et al., 1992) and expressed in the cerebellum (Andres-Barquin et al., 2000). qRT-PCR analysis reveals that the loss of *MyoD* causes a transcriptional increase in *Id3* levels in *MyoD*-shRNA transduced SmoA2 GNPs compared to untransduced controls *in vitro*. This suggests that *MyoD* may function to suppress transcription of pro-proliferative *Id3* (Figure 3.7).

Next, we mined the metaGEO database which consists of expression profiles from more than 5,000 distinct gene expression studies across 3 different species (human, mouse, rat) to identify to studies in which *MyoD* expression was significantly variable. We identified published study GSE24628 by Gibson et al. as one of the top studies where *MyoD* expression showed the most variability. Interestingly, the study involved gene expression profiling of Wnt and Shh driven mouse medulloblastomas, postnatal GNPs and embryonic dorsal brainstem cells (Gibson et al., 2010). Consistent with our findings, we find increased expression of *MyoD* in the Shh-driven medulloblastomas followed by P7 GNPs compared to the other conditions (Figure 3.8). In addition, in this dataset we find an inverse correlation between *MyoD* and *Id3* consistent with our findings - the Shh-driven medulloblastomas have high *MyoD* expression and low *Id3* levels whereas the Wnt-driven medulloblastomas have low *MyoD* and high *Id3*. These findings combined suggest that *MyoD* has an inhibitory effect on *Id3* transcription in medulloblastoma.

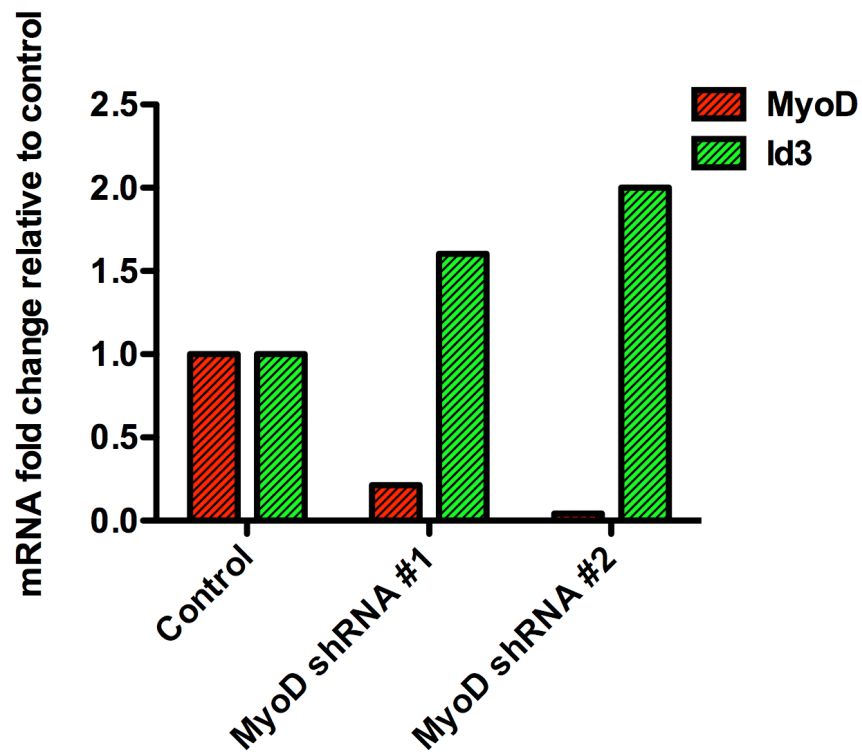


Figure 3.7

Loss of MyoD leads to increased *Id3* transcription

SmoA2 P5 GNP were harvested and transduced *in vitro* with two different MyoD-shRNA expressing lentiviral vectors. Compared to untransduced controls, shRNA-mediated silencing of MyoD results in increased *Id3* transcription as revealed by qPCR analysis. $\beta 2$ microglobulin was used as the endogenous control for data normalization.

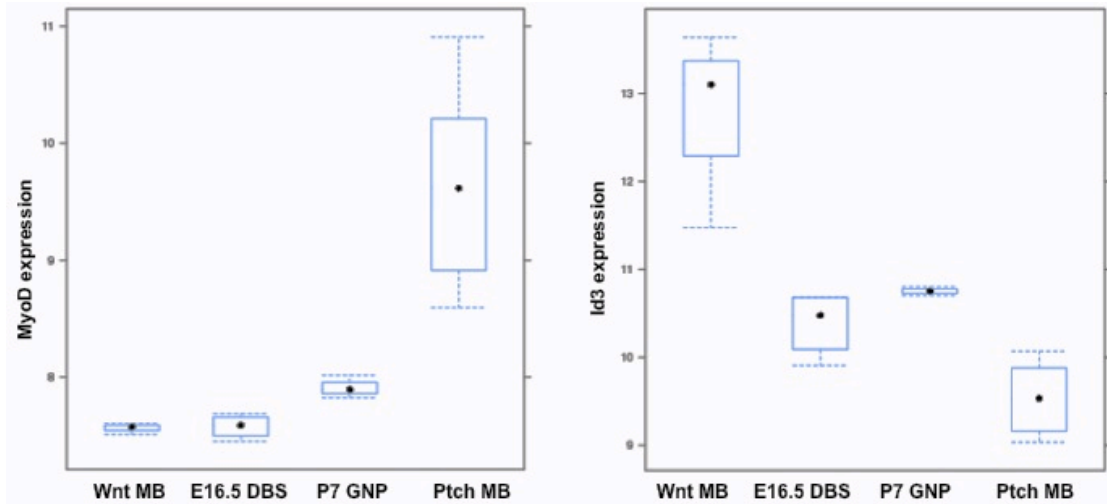


Figure 3.8

Inverse Correlation between MyoD and Id3

Exploration of the metaGEO database to find studies in which MyoD expression is significantly variable, led to the identification of study GSE24628 involving gene expression profiling of Wnt-driven mouse medulloblastomas (Wnt MB), Shh-driven mouse medulloblastomas (Ptch-MB), postnatal day (P)7 GNPs and embryonic day (E) 16.5 dorsal brain stem cells. Box-plots show MyoD and Id3 gene expression to be inversely correlated in this study.

MyoD induces muscle differentiation in primary human medulloblastoma cells

The tumor suppressor role of MyoD in mouse models of medulloblastoma led us to investigate the functional significance of MyoD expression in human medulloblastoma. For *in vitro* studies, we chose to generate a patient-derived primary medulloblastoma line instead of using established cell lines since the former represents the molecular profile of the original tumor more appropriately. We expressed MyoD using a lentiviral vector in a patient-derived primary medulloblastoma cell line that lacks endogenous MYOD expression as verified by qRT-PCR analysis. Consequent to MyoD expression, the cells assumed a filamentous/fibrillar morphology suggesting possible neuronal or myogenic differentiation. Immunocytochemical staining for neuronal differentiation marker beta tubulin (Tuj1) and muscle differentiation marker Myosin heavy chain (MHC) confirmed that the tumor cells had differentiated into MHC positive myofibrils (Figure 3.9).

Our finding showing myogenesis in human medulloblastoma primary cells following forced expression of MyoD *in vitro* is different from our observation in mouse medulloblastoma where MyoD does not induce myogenesis *in vivo* but acts as a tumor suppressor. Therefore, while these differences could stem from differences in MyoD dosage *in vivo* versus *in vitro*, it is also possible that the function of MyoD as a tumor suppressor in mice is through a pathway independent of myogenesis. Whether the terminal differentiation observed in human cells contributes to tumor suppression in human tumors is yet to be determined.

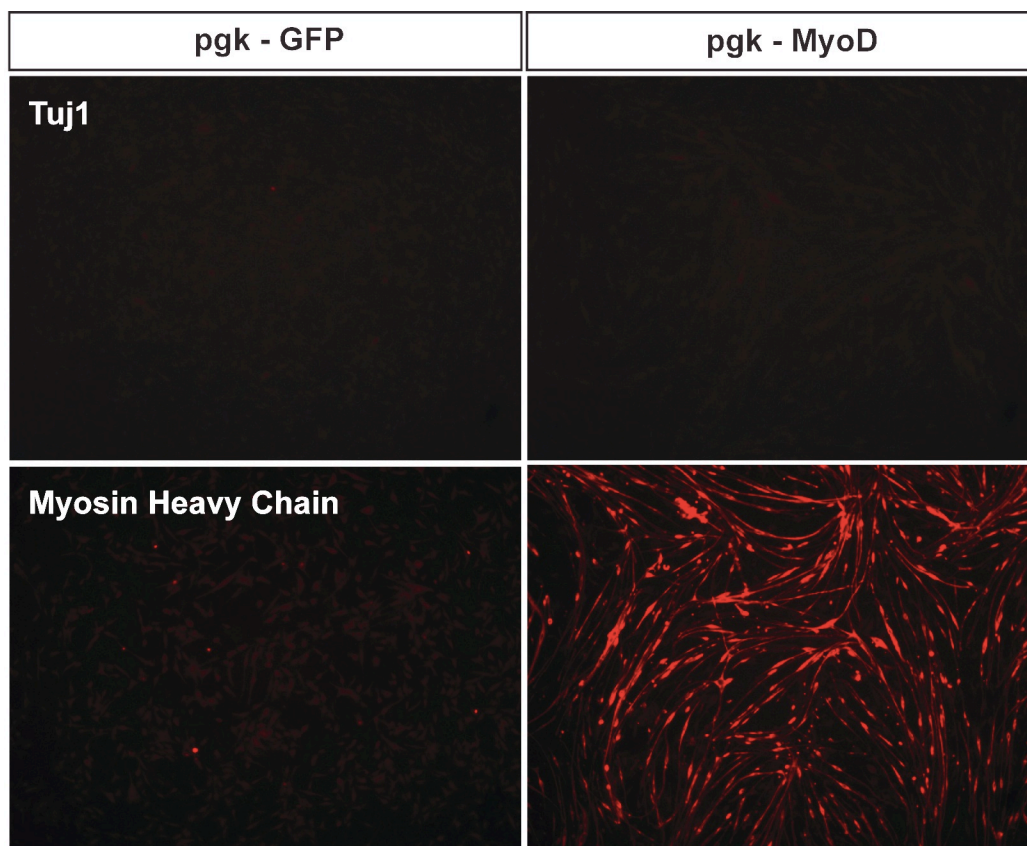


Figure 3.9

Expression of MyoD induces myogenic differentiation in human medulloblastoma primary cell line

MyoD was expressed in a patient-derived medulloblastoma primary cell line using a lentiviral vector. Immunofluorescence analyses were carried out using antibodies for neuronal differentiation marker, beta tubulin (Tuj1) and muscle differentiation marker, Myosin heavy chain (MHC). Following MyoD expression, the tumor cells assumed fibrillar morphology that stain positive for MHC.

Discussion

In this study, we have discovered a novel tumor suppressor function of muscle differentiation factor, MyoD in mouse medulloblastoma. We show that MyoD is ectopically expressed both at the transcript and protein level in cerebellar tumors from three different mouse models of medulloblastoma namely ND2:SmoA1, ND2:SmoA2 and Patched conditional knock-out mice (Hallahan et al., 2004; Hatton et al., 2008; Yang et al., 2008). These models have been genetically engineered such that they have constitutive Shh signaling in the cerebellum, which leads to tumorigenesis. Through mouse genetic studies, we show that the SmoA1 and SmoA2 mice on a MyoD deficient background have an accelerated onset of tumors. The consequence of loss of only a single allele of MyoD is profound and intriguing. This finding is supported by similar dosage effects observed for other bHLH family transcription factors (Erickson and Cline, 1991; Bain et al., 1994; Zhuang et al., 1994; Lyden et al., 1999).

Molecular characterization of human medulloblastomas categorizes the disease into four subtypes – SHH-driven, WNT-driven, MYC amplified and a subtype with yet unknown genetic determinants (Taylor et al., 2011). The vast majority of the existing mouse models represent Shh-driven medulloblastoma (Hatten and Roussel, 2011). Due to the lack of mouse models that recapitulate other subtypes of medulloblastoma except for a recent Wnt-driven model (Gibson et al., 2010), our findings are specific to the Shh-driven mouse medulloblastomas. It is possible that these results are specific for the Shh-driven mouse models since MyoD is known to be influenced by Shh signaling (Tapscott, 2005; Barakat et al., 2010).

MyoD has not been previously known to be expressed or have a functional role in the brain. A study by Kablar et al. suggested that the promoter of *MyoD1* is permissive to expression in the brain but different regulatory elements within the promoter (eg. negative *cis* regulatory element) prevents *MyoD1* from being expressed in the brain (Kablar, 2002). Therefore, it is possible that the effect of the negative regulatory elements is overcome as a consequence of the oncogenic mutation leading to the expression of MyoD, a transcription factor that has the capacity to drive differentiation. The study showing expression of *Myf5* as an axonal marker in the brain at the transcript level (Tajbakhsh and Buckingham, 1995; Daubas et al., 2000) sets a precedent for the discovery of other myogenic regulators in the brain with functions potentially different from those known in the skeletal muscle lineage.

We demonstrate *MYOD* expression at a transcriptional level in a small subset of human medulloblastomas. Although molecular characterization of these medulloblastomas was beyond the scope of our study, we assessed *GLI1* levels to identify the SHH-driven subtype and did not find a correlation between *MYOD* and *GLI1* expression (data not shown). This suggests that MYOD expression in human medulloblastoma may not be subtype-specific. Our inability to detect MYOD protein in human medulloblastoma cells could be due to technical difficulties associated with immunodetection or a true absence of *MYOD* translation in human tumors. We show that forced expression of MyoD in a human medulloblastoma primary line lacking endogenous *MYOD* mRNA, causes the tumor cells to differentiate and express myosin heavy chain protein, a structural protein of the skeletal muscle lineage. It has been shown that forced expression of MyoD largely fails to induce myogenesis in neural tumor cell lines except for a medulloblastoma and a glioblastoma line, due to the deficiency of factor/s needed for myogenesis (Gerber and Tapscott, 1996). It is

possible that the potential myogenesis following forced expression of MyoD in the one primary medulloblastoma line we tested, is yet another rare exception. Alternatively, the myogenic factors downstream of MyoD are lost in cell lines but preserved in primary lines that more closely represent the original tumors. The rare occurrence of human medullomyoblastoma makes it challenging to determine if expression of MYOD is the underlying molecular basis of this particular histological variant. Aberrations in cell cycle control and terminal differentiation are key features of cancer cells (Gerber and Tapscott, 1996). Whether the induction of terminal differentiation by MyoD in human medulloblastoma cells is a way of limiting tumor growth is a question yet to be answered. We are unable to detect myogenic differentiation in mouse medulloblastomas that express high MyoD. Therefore, based on our findings, it remains possible that the role of MyoD in driving myogenesis may be independent of its role as a tumor suppressor in mice.

MyoD has not been shown to have a role in oncogenesis but several studies associate MyoD with different kinds of cancers, which indicates a possible functional significance. DNA methylation of promoter-associated CpG islands of MyoD has been found in colon and prostate cancer (Ahuja et al., 1998; Mishra et al., 2010) and chemically-induced oncogenic transformation of 10T1/2 cells *in vitro* shows a progressive increase in MyoD promoter methylation (Jones et al., 1990; Rideout et al., 1994), a mechanism well known to silence tumor suppressor genes in cancer (Hatada et al., 2006). A recent study shows a direct correlation between MYOD and BRCA1 expression in sporadic human breast cancer a large percentage of which have reduced normal BRCA1 as well as MYOD (Jin et al., 2011). MyoD directly induces BRCA1 transcription with c-myc and is thought to play a role in

breast cancer susceptibility (Jin et al., 2011). These studies point at a potential tumor suppressor role of MyoD in cancer.

Malignant transformation involves complex genetic changes that commonly lead to activation of oncogenes and loss of tumor suppressor genes that provide a proliferative growth advantage. However, mammalian systems also have inherent defense mechanisms against oncogenic stimuli that cause cells to undergo apoptosis, senescence (Leonart et al., 2009; Romagosa et al., 2011) or differentiation (Watt et al., 2008) as fail-safe mechanisms to prevent uncontrolled proliferation and consequent tumorigenesis. Networks that drive proliferation often harbor intrinsic growth-suppressive properties that are reflected in the phenomena of oncogene-induced apoptosis (eg. p53 induction by oncogenes Myc, E2F) or oncogene-induced senescence (Ras-induced activation of chromatin modifying factors that produce a repressive state *in vitro*)(Lowe et al., 2004).

Although counterintuitive, a number of tumor suppressor genes are overexpressed in cancer to possibly inhibit uncontrolled proliferation. Examples include p16^{INK4a} (Romagosa et al., 2011); TP73 of the p53 family associated with improved survival outcomes in medulloblastoma patients (Castellino et al., 2007); pRb2/p130 in hepatocellular carcinoma (Huynh, 2004), Cdx2 in colorectal adenocarcinoma (Witek et al., 2005); S100A11 in pancreatic carcinogenesis (Ohuchida et al., 2006) and that of wildtype p53 in a subset of gliomas which also express antiapoptotic protein Bcl-2 to potentially subvert p53 mediated apoptosis (Alderson et al., 1995). In light of the above examples, the expression of MyoD in tumors possibly represents a novel latent fail-safe mechanism in the cerebellum induced in response to an oncogenic signal. Interestingly, in this case, MyoD is not normally expressed in the normal adult cerebellum but is activated in response to the oncogenic stimuli. Its

activation in an ectopic environment may explain why even though MyoD is able to prolong survival as demonstrated by our genetic studies, it acts as only a partial brake on tumorigenesis due to the timing of when it is activated and/or suboptimal activation of downstream targets.

Our study shows that MyoD expression correlates with the proliferative status of cells be it during normal GNP proliferation in development or in tumors. MyoD is undetectable in WT or SmoA2 cerebella that do not develop into tumors even though they are genetically identical to those that do. This suggests MyoD is expressed in response to uncontrolled proliferation in tumors or a high degree of normal proliferation during postnatal GNP expansion development. Our finding showing MyoD expression exclusively in Ki67-positive proliferating cells supports this hypothesis. The prolonged proliferative phase in normal cerebellar development makes the cerebellum vulnerable to neoplastic changes (Wang and Zoghbi, 2001). Thus it remains possible that MyoD expression in WT GNPs during normal development is a preemptive protective mechanism to prevent potential transformational events common in highly proliferative tissues

Mouse medulloblastomas that express MyoD, also express *Myf5* and *Myogenin* amongst the MyoD-regulated genes that were assessed in this study. However, the lack of expression of other targets as well as the absence of features of skeletal muscle differentiation in the tumors suggest that the tumor suppressor function of MyoD is not exerted through its known targets in the muscle differentiation program. Additionally, *Myf5* and *Myogenin* levels are not significantly different between the early onset MyoD *-/-*wt; SmoA2 and late onset MyoD wt/wt; SmoA2 tumor groups, which further suggests the

presence of alternative downstream players in the MyoD-regulated tumor suppressor pathway.

Id proteins antagonize MyoD-mediated differentiation by sequestering E proteins, the heterodimeric partner of MyoD during skeletal muscle development (Jen et al., 1992). The pro-proliferative Id proteins function in tumorigenesis (Zebedee and Hara, 2001; Ruzinova and Benezra, 2003; Sikder et al., 2003), are expressed in the nervous system (Andres-Barquin et al., 2000) and inhibit neural differentiation (Lyden et al., 1999). We observe a difference in *Id3* transcript levels between tumors from MyoD wt/wt; SmoA2 versus MyoD -/wt; SmoA2, with the loss of MyoD in the latter associated with an increase in *Id3*. A partial reduction in Id dosage has been shown to inhibit tumor growth and decrease tumor angiogenesis (Lyden et al., 1999). An inverse correlation between *MyoD* and *Id3* is also observed in the gene expression study by Gibson et al (Gibson et al., 2010) comparing different medulloblastoma subtypes and GNPs. Therefore it is possible that MyoD-mediated *Id3* suppression in the MyoD wt/wt; SmoA2 mice contributes to the improved survival in this group and the loss of this suppression results in accelerated tumor onset in MyoD -/wt; SmoA2 mice. The regulation of *Id3* by MyoD in the tumors is further supported by our *in vitro* data showing an increase in *Id3* transcription following shRNA-mediated MyoD silencing in P5 GNPs that have high levels of endogenous MyoD.

miR-206 although originally recognized as a muscle-specific microRNA (Kim et al., 2006) and a target of MyoD in the muscle differentiation program (Rosenberg et al., 2006), has been recently shown to be enriched in the cerebellum (Olsen et al., 2009). miR-206 has tumor suppressor functions in various cancers namely metastatic lung cancer, endometrial cancer and breast cancer (Adams et al., 2007; Kondo et al., 2008; Song et al., 2009; Taulli et

al., 2009; Wang et al., 2011; Chen et al., 2012). Although yet to be studied in the context of medulloblastoma, microRNA profiling shows miR-206 to be one of 24 miRNAs down-regulated in proliferating mouse GNP and medulloblastomas when compared to mature mouse cerebellum (Uziel et al., 2009). Here we validate that miR-206 is down-regulated in medulloblastoma. However, since miR-206 is induced by MyoD during muscle differentiation, the down regulation of miR-206 in MyoD-expressing tumors is counterintuitive. This conundrum is explained by our *in vitro* data, which shows that forced expression of MyoD induces miR-206 but compared to WT GNPs, miR-206 induction is reduced in the SmoA2 GNPs. This indicates a disrupted MyoD-mediated miR-206 regulation in the oncogenic context both *in vitro* and *in vivo*. The dysregulation of the downstream effector miR-206 may partly explain why MyoD is unable to induce myogenesis or acts as a partial brake on tumorigenesis in mouse medulloblastoma.

Tumor cells possess the potential for self destruction – the very oncogenic mutations required for uncontrolled proliferation can unbridle tumor suppressor programs still intact in the cells but not active since the molecular networks connecting proliferation and tumor suppression become uncoupled in cancer (Lowe et al., 2004). Therapeutic interventions directed at harnessing one's own latent tumor suppressor networks that are originally coupled to proliferative pathways but uncoupled in cancer, hold promise for treatment of cancer (Lowe et al., 2004). Chen et al showed that a synthetic peptide fragment of MyoD with high affinity for Id1 reduced proliferation and induced apoptosis in breast and colon cancer cells *in vitro* (Chen et al., 2010). Although the association of MYOD and medulloblastoma is yet unknown, its tumor suppressor function in mice and possible expression in a subset of

human medulloblastomas makes the MyoD-mediated latent tumor suppressor network of therapeutic interest.

In summary, our study unveils an ectopic expression pattern of MyoD in medulloblastoma and cerebellar development in mice and demonstrates a novel tumor suppressor function of MyoD, hitherto recognized as exclusively a muscle differentiation factor. This study demonstrates how a protective biological network can be activated to counter oncogenic effects thereby paving the path for developing therapies that would allow activation of such an inherent fail-safe mechanism to block tumorigenesis.

Materials and Methods

ND2:Smo Transgenic and MyoD wt/- Mouse Lines

The ND2:SmoA1, ND2:SmoA2 transgenic mouse lines, Patched conditional knock out mice and MyoD +/- mice and genotyping protocols have been previously described (Rudnicki et al., 1992; Hallahan et al., 2004; Hatton et al., 2008; Yang et al., 2008). All mice were maintained in accordance with the NIH Guide for the Care and Use of Experimental Animals with approval from the Fred Hutchinson Cancer Research Center Institutional Animal Care and Use Committee (IR#1457).

Mouse pathology and Immunohistochemistry

Mice were anesthetized using CO₂ inhalation, the cerebellum removed, and tissue snap-frozen for RNA studies, GNP isolation or fixed in 4% paraformaldehyde for histological examination. Fixed tissue were paraffin-embedded, cut into 4-μm sections. For immunofluorescence analyses, MyoD (mouse 5.8A, BD Biosciences 1:200), rabbit Ki67 (Novocastra, 1:100) followed by anti-mouse Fab-fragment ME-kit, secondary CSA-SA Alexa 350 polymer (Molecular probes, Invitrogen) and Alexa 647 for Ki-67. For Immunohistochemical analyses, antibodies used were MyoD1 (mouse 5.8A, BD Biosciences 1:1000), followed by anti-mouse Fab frag-ME kit/CSA detection kit. Data was confirmed using additional MyoD antibodies (rat Active motif 1:50) and (rabbit Santa cruz M-318). Sections were visualized with Nikon 800 or DeltaVision Deconvolution microscope (FHCRC Scientific Imaging Core).

Quantitative Reverse Transcription PCR

For quantitative reverse transcription PCR (qRT-PCR), RNA was isolated using miRNAeasy Kit (Invitrogen), DNase (Qiagen) treated and converted to cDNA using the ABI High Capacity Reverse Transcription kit (Applied Biosystems, Foster City, CA). Reactions were set up using ABI SYBR green or Taqman Master Mix and run on an ABI 7000 Sequence Detection System. Taqman Gene Expression Assays (Applied Biosystems) were used for *Ms MyoD*, *Hs MYOD*, *Hs PPIA*, *Ms b2m*, *Hs GLII*, and ABI Taqman miR assays for mir206 and sno202. Primer sequences designed using Primer3 software (Rozen and Skaletsky, 2000) for the SYBR assay are as follows: *Cpha* endogenous control Forward 5'-gagctgtttgcagacaaagttc-3', Reverse 5'-ccctggcacatgaatcctgg-3' (kind gift from the lab of Dr. Sunil Hingorani); *MyoD1* Forward 5'-cccgcgctccaactgctctg-3', Reverse 5'-ggctcgacacagccgcactc-3'; *Desmin* Forward 5'-ataccgacaccagatccagtccta-3', Reverse 5'-tgctcatcagggagtcgtt-3' ; *Myogenin* Forward 5'-gtcccaaccaggagatcatt-3', Reverse 5'-gacgtaagggagtgagattgtg-3'; *Cadherin15* Forward 5'-catgctgtcactcagtcaggag-3', Reverse 5'-gggcgatctgagtgacagca-3'; *Myf5* Forward 5'-gcatgcctgaatgtaacagc-3', Reverse 5'-gctcggatggctctgtagac-3'; *Id2* Forward 5'-ccagagacctggacagaacc-3'; Reverse 5'-attcagatgcctgcaaggac-3'; *Id3* Forward 5'-gaggagcttttgcactgac-3'; Reverse 5'-gagagagggtcccagagtcc-3', (kind gift from the lab of Dr. Stephen Tapscott), *CXCR4* Forward 5'-acggctgtagagcgagtggt-3, Reverse 5'-ggtgggcaggaagatcctat-3'. Data were analyzed using ABI GeneAmp SDS software. All conditions were run in triplicate and normalized to mouse *b2m* or *Cpha* and human *PPIA* endogenous control.

Western Blot Analysis

Protein lysates were prepared using (0.5% TritonX, 0.25% sodium deoxycholate, 1mM

PMSF, 10mM NaF, 1mM Na-orthovanadate, Roche protease inhibitor cocktail) lysis buffer. Equal amounts of proteins from each sample (25 µg) were subject to SDS-PAGE using NuPAGE Novex Bis-Tris gels (Invitrogen), X-Cell SureLock Mini cell (Invitrogen), transferred to nitrocellulose membranes, and probed with three different antibodies MyoD (C-20, Santa Cruz Biotechnology, 1:200), (BD Biosciences, 1:150) and rabbit 6975b (kind gift Dr. Stephen Tapscott), loading control β -actin (Abcam, 1:5000). Horseradish peroxidase conjugated secondary antibodies were obtained from Jackson ImmunoResearch and used at 1:8000 dilutions. Proteins were detected by incubating membranes in chemiluminiscent substrate (ECL kit, Pierce) followed by exposure to X-OMAT Kodak Scientific Imaging Film.

Lentiviral constructs

MyoD-expressing lentiviral vector was designed by cloning mouse MyoD into pRRLSIN.cPPT.PGK-GFP.WPRE lentiviral vector backbone (Addgene plasmid 12252) using BamH1 and Sal1 sites replacing GFP cassette (gift from Tapscott lab). The original vector was used as the GFP expressing control. Mouse GIPZ lentiviral MyoD shRNAmir set (Open Biosystems, Thermo Fisher Scientific) was used for MyoD knockdown. Recombinant replication incompetent lentivirus was produced as previously described (Munoz et al., 2011)

Preparation of granule neuron precursor (GNP) cultures, primary medulloblastoma culture, lentiviral transduction and immunocytochemistry

GMPs were harvested from P5-P7 mice and primary cultures were established as previously described (Lee et al., 2009). Primary medulloblastoma lines were established as described

previously(Pollard et al., 2009). Lentiviral transductions were carried out with multiplicity of infection 2 for GNP and 10 for primary medulloblastoma line and all assays were carried out 72 hours post transduction. Antibodies used for immunocytochemistry were Myosin Heavy Chain (mouse MF 20, DSHB) and Tuj1 (mouse, Sigma), secondary Texas Red

Survival Analysis

Survival curves were plotted using Kaplan-Meier method and compared using two-sided log-rank test. All statistical analyses were performed in R statistical systems (<http://www.r-project.org>). These estimates were made using two-sided log-rank test at $p < 0.001$ significance level. Survival analyses used animal death times as events and mice that were still alive at the time of analysis as censored data.

Chapter 4

Role of extrinsic Sonic Hedgehog signaling in the tumor microenvironment for the growth and maintenance of non-Sonic hedgehog driven medulloblastomas

Introduction

It is well accepted that mutations causing aberrations in the intrinsic Shh signaling pathway, lead to proliferation of tumorigenic cells in numerous types of cancers (Ruiz i Altaba, 2008) including medulloblastoma (Gilbertson and Ellison, 2008). A study by Yauch *et al.* sheds light on the *extrinsic* role of Shh by which it can activate the pathway in non-malignant stromal cells that are part of the tumor microenvironment and can support tumor growth through mechanisms not yet known (Ruiz i Altaba, 2008; Yauch et al., 2008). This study reinforces the critical role of the stromal microenvironment on epithelial tumor growth.

It is known that 25-30% of medulloblastoma cases are caused by activating gene mutations in the SHH pathway, as shown by molecular profiling studies which categorize medulloblastomas into five subtypes based on their molecular signatures (Thompson et al., 2006). Given the role of Shh in extrinsic signaling in the tumor micro-environment in other types of cancer (Yauch et al., 2008), Shh could play an additional role even in the other four Non-Shh medulloblastoma subtypes, by creating a tumor microenvironment favorable for tumor proliferation and maintenance. This is important because in addition to therapies targeted against medulloblastoma tumor cells, targeting tumor microenvironment may be necessary for successful treatment. Furthermore, survival of medulloblastoma cells has been shown to be dependent on their microenvironment in primary culture experiments (Rutka et

al., 1987). Therefore, if medulloblastomas lacking activating Shh mutations respond to Shh inhibition in pre-clinical mouse studies, it will be reasonable to include Shh antagonists as part of a multi-agent therapy for all recurrent medulloblastoma patients. This would potentially benefit many more children affected by this cancer. On the other hand, if medulloblastomas that lack activating Shh mutations do not respond to Shh inhibition in pre-clinical studies, it will be important to focus human clinical trials on patients only with Shh pathway mutations.

Cyclopamine, a Smo-antagonist (Taipale et al., 2000) effectively kills mouse and human medulloblastoma cells (Berman et al., 2002) and a pre-clinical study conducted in our lab has shown that IPI-926, a derivative of cyclopamine targeting Smo, causes dramatic regression of medulloblastomas in Patched conditional knock-out mice (Yang et al., 2008) that develop Shh-driven aggressive medulloblastomas by postnatal day 21. Understanding the role of extrinsic Shh signaling in the microenvironment and effect on non-Shh driven medulloblastomas will be crucial for making therapy decisions and patient care. In this study we determined if IPI-926 induces remission in mouse models with xenografts from human medulloblastomas that are not caused by mutations in the SHH pathway.

Results

Determination of IPI-926 Dosage Regimen

We generated a mouse allograft tumor line by orthotopically transplanting tumor cells from the genetically engineered mouse model (GEMM) of medulloblastoma - Ptch1 conditional knock out model (Ptch1^{flox/flox}; Math1-Cre) (Yang et al., 2008). Our previous studies demonstrated complete tumor regression in the GEMM Ptch1^{flox/flox}; Math1-Cre mice following IPI-926 treatment (data not shown). The allograft line carrying the same tumors was therefore used to determine the best tolerated dose for athymic mice as well as served as a positive control in the preclinical trial. The doses tested were 20mg/kg administered daily, 40mg/kg administered daily, 40mg/kg administered thrice weekly (in this case there was an interval of 72 hours between the last dose of the week given on Friday and first dose the following week given on Monday) or 40mg/kg administered every 48 hours. Using quantitative RT-PCR, we measured mRNA levels of the Shh pathway effector *Gli1* as an endpoint (Figure 4.1) with respect to untreated controls. Based on the data, we determined that 40mg/kg of IPI-926, every 48 hours to be the best tolerated dose that led to the most effective inhibition of the Shh pathway (Figure 4.1). We also observed dramatic regression of tumors in these mice.

Effect of IPI-926 on human xenograft medulloblastomas

Tumors from Ptch1^{flox/flox}; Math1-Cre mice, human xenograft lines L2123 and L984, both Non-SHH driven, were transplanted orthotopically into cerebella of athymic recipient mice. Based on natural history study of tumor onset in each of these lines, we enrolled mice in the drug trial prior to manifestation of clinical symptoms of tumor. IPI-926

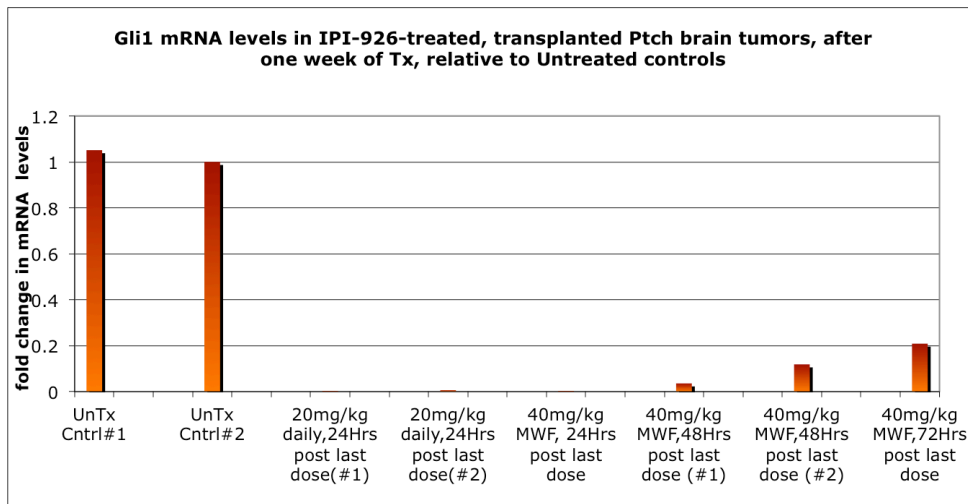


Figure 4.1

Determination of best-tolerated dose of IPI-926 by assessment of Shh target *Gli1* in Shh-driven mouse medulloblastomas

Athymic mice with *Ptch*^{fl^{ox}/fl^{ox}}-*Math1*-Cre allograft tumors were administered by daily gavage IPI-926 20mg/kg daily (n=2), 40mg/kg daily (n=1), 40mg/kg every 48 hours (n=2) or 40mg/kg thrice weekly (n=1) (in which case was an interval of 72 hours between the last dose of the week given on Friday and first dose the following week given on Monday). mRNA was harvested from the tumors to measure *Gli1* levels by qPCR relative to untreated controls (UnTx Cntrl). β 2-microglobulin was used for data normalization. 40mg/kg every 48 hours was determined to be the best tolerated dose that caused effective inhibition of *Gli1* levels.

and vehicle were administered by oral gavage for 6 weeks, 40mg/kg every 48 hours. Kaplan-Meier survival curves in Figure 4.2 and 4.3 summarize our results.

After 6 weeks of IPI-926 treatment, athymic mice with *Ptch*^{flox/flox}; *Math1-Cre* allograft tumors survived where as all mice in the vehicle arm succumbed to tumors (Figure 4.2). Even though the mice were asymptomatic at enrollment, as we had expected based on our natural history study, the mice had histological tumors at enrollment.

Hematoxylin-Eosin staining shows histology of the cerebella of mice A, B, C (marked with boxes in Kaplan Meier curve) at pre-enrollment, in the IPI-926 drug arm at 6 weeks and after 6 weeks of treatment when the tumors grew back.

With the same dosing regimen, we did not observe an effect of IPI-926 treatment on tumors from either the L2123 (Figure 3) or L984 (Figure 4) human medulloblastoma lines. These mice were also asymptomatic at enrollment.

Conclusions

Our preclinical studies demonstrate that IPI-926 did not lead to improvement in survival for mice that carried Non-SHH driven human medulloblastomas. The positive control consisting of mice carrying allograft tumors from Patched conditional knock out mice (Shh-driven) worked well and a clear survival advantage was observed. This finding is important in making recommendations that human clinical trials using IPI-926 should include only patients with SHH-driven medulloblastomas. For others, advantages of SHH inhibition may be further tested by including SHH antagonists as part of a multi-agent therapy and/or in metronomic trials.

Study Design

- Ptc f/f; Math-Cre tumors from mouse GEMM transplanted into cerebellum of Nu/Nu recipients
- Treatment: 40 mg/kg oral every 48 hours
- Trial start date: 22 days post transplant
- Majority were symptomatic
- 6 weeks of treatment
- n= 5 IPI-926
- n= 5 Vehicle

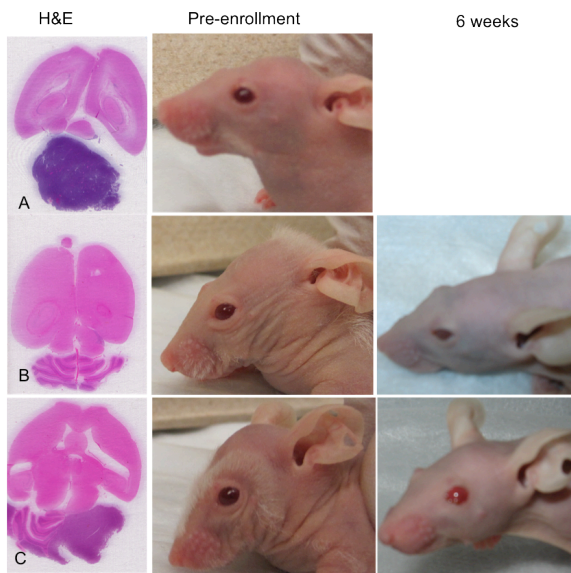
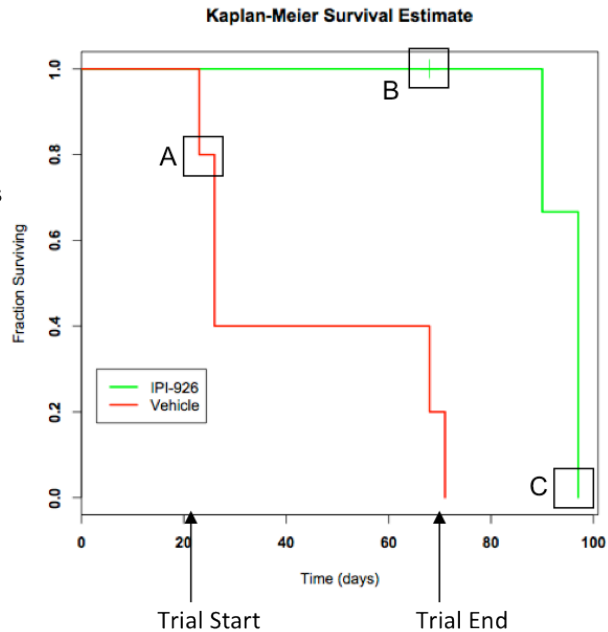


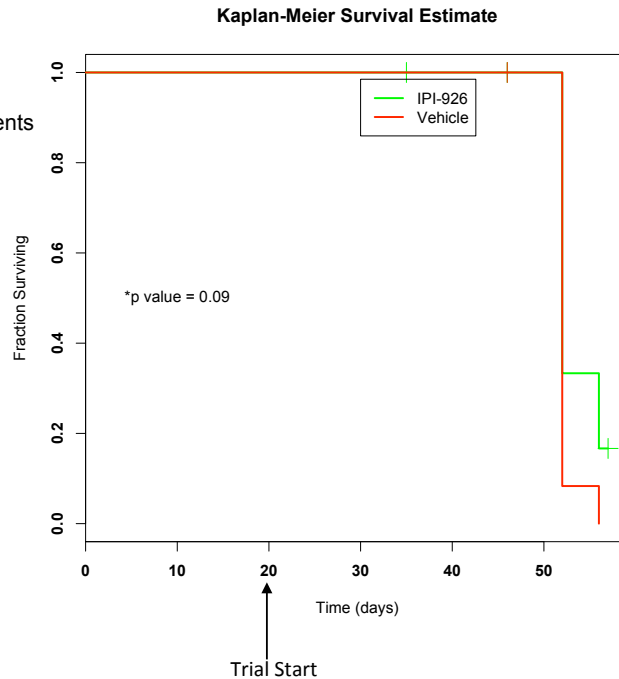
Figure 4.2

Response of $Ptch^{flox/flox}$ -Math1-Cre allograft tumors to IPI-926 treatment

$Ptch^{flox/flox}$ -Math1-Cre allograft tumors were harvested from GEMM tumors and transplanted orthotopically into cerebella of athymic (Nu/Nu) recipients. Mice were randomized into the IPI-926 (n=5) or vehicle (n=5) arms and enrolled into the preclinical trial 22 days post transplant when most mice were symptomatic. 40mg/kg IPI-926 was administered by oral gavage every 48 hours for 6 weeks. Kaplan Meier survival curves show that at 6 weeks all mice in the drug arm survived while those in the vehicle arm succumbed to tumors. However, after withdrawal of IPI-926, the tumors grew back and mice eventually succumbed to tumors. A represents a mouse in the vehicle arm that succumbed to tumor, B represents a mouse in the IPI-926 arm whose tumor regressed in response to the drug and C represents a mouse in the IPI-926 arm that succumbed to tumor after treatment was stopped. Hematoxylin Eosin staining of representative brain sections from A, B and C are shown with tumors consisting of hematoxylin stained mass of blue cells.

Study Design

- L984 human medulloblastoma transplanted in the cerebella of athymic recipients
- Treatment: 40 mg/kg oral every 48 hours
- Trial start: 20 days post transplant
 - all animals were asymptomatic
- n= 14 IPI-926
- n= 13 Vehicle



Study Design

- L2123 Non-SHH human medulloblastoma transplanted in cerebella of athymic recipients
- Treatment: 40 mg/kg oral every 48 hours
- Trial start: 33 days post transplant
 - all mice were asymptomatic
- n= 9 IPI-926
- n= 9 Vehicle

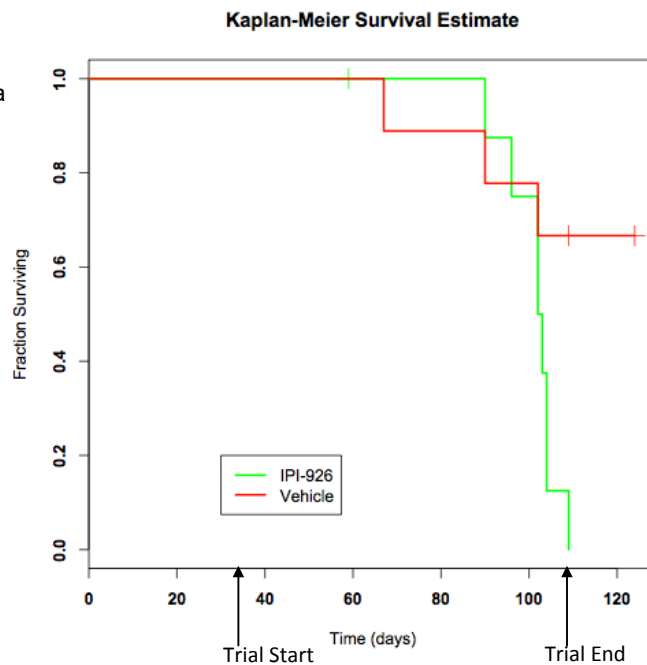


Figure 4.3

Response of human medulloblastoma xenograft tumors to IPI-926 treatment

Tumors from human medulloblastomas xenograft lines L984 (indeterminate mutation) and Non-SHH driven L2123 were transplanted orthotopically into cerebella of athymic (Nu/Nu) recipients. Mice were randomized into the IPI-926 or vehicle arms and enrolled in the preclinical trial 20-33 days post transplant. All mice were asymptomatic at this stage. 40mg/kg IPI-926 was administered by oral gavage every 48 hours till all mice in either arm succumbed to tumors. Kaplan Meier survival curves show that IPI-926 has no effect in the human tumor lines tested since all mice in both drug and vehicle arm succumb to tumors.

Chapter 5

Conclusions and Future Directions

SmoA2 studies

Through my studies as described in Chapter 2, I have demonstrated the fundamental differences between two activating point mutations, SmoA1 and SmoA2, in the same domain of a single gene. Both mutations lead to constitutively active Shh signaling that result in medulloblastoma genesis but have completely disparate effects of cerebellar development. While the SmoA1 mutation does not lead to any apparent developmental defects, the SmoA2 mutation leads to massive disruptions starting early in development. SmoA1 and SmoA2 lead to different global transcriptional profiles in the early postnatal cerebellum. One of the important next steps is to understand the cell-autonomous effects of the SmoA2 mutation with cues from the gene ontology categories represented by the gene expression data. First, in light of the extensive neuronal migration defects observed in the cerebellum, it will be interesting to investigate how the SmoA2 mutation affects GNP migration patterns in controlled *in vitro* experiments using advanced time lapse imaging techniques. Second, the SmoA1 and SmoA2 mutations potentially harness different downstream effectors, identification of which would further our understanding of the mechanics of the Shh pathway. Immunoprecipitation assay followed by mass spectrometry based proteomic identification of molecules that directly interact with SmoA1 and SmoA2 would help in characterization of novel molecules in the Shh pathway involved in signal transduction from the membrane to the nucleus. Third, in both SmoA1 and SmoA2 models, we observe tumors initiating from the pial surface. Characterization of this niche will be an important step in furthering our knowledge about medulloblastoma biology. One possibility is that

chemoattractants or trophic factors secreted from the leptomeningeal membranes (pia and arachnoid mater) contribute to making a niche conducive for neoplastic cells to survive and proliferate. Surgical implantation of beads soaked with the known secreted factors like Sdf1- α , TGF β amongst others, into brains of WT and mutant brains may allow us to study the effect of these factors on attracting or favoring the persistence of neoplastic cells in this niche. It is also possible that additional cell intrinsic effects in the SmoA1 or SmoA2 expressing cells cause a sub-population of cells to reside along the nutrient rich pial surface whereas others that migrate inwards regress or differentiate into normal granule neurons. By design of the transgenes, every GNP is expected to express the SmoA1 or SmoA2 oncogene, yet majority of the GNPs seem to mature into normal neurons while atypical cells remain along the pial surface. Using laser capture technology, isolation of the atypical cells along the pial surface and the normal mature neurons to compare gene expression profiles will allow us to uncover additional cell intrinsic “second hits” that allow a subpopulation to initiate tumors. Fourth, perhaps the most intriguing aspect of the SmoA2 phenotype is the normal neurobehavior of the mice despite the completely disrupted cerebellar cytoarchitecture. Injection of transsynaptic viral tracers into the SmoA2 brains (Boldogkoi et al., 2009) followed by two-photon/confocal microscopy will allow mapping of the cortico-cerebellar circuitry to help understand how cerebellar functionality is maintained.

MyoD Studies

Through my studies described in chapter 3, I have discovered a hitherto unknown expression pattern of MyoD in the cerebellum and demonstrated a novel tumor suppressor function of MyoD in mouse medulloblastoma with potential clinical significance. The next steps are

first, to investigate if MyoD can impair tumorigenic potential of human medulloblastoma cells and to determine the underlying mechanisms. This question can be addressed by forced expression of MyoD in additional medulloblastoma cell lines followed by transplantation into recipient mice to monitor tumor initiation and growth and characterize resulting tumors in experimental and control groups with markers of proliferation and differentiation. For this experiment, I am currently cloning a MyoD lentiviral vector with a fluorescent marker that will allow sorting of positively transduced cells prior to transplantation. Second, it remains to be determined if endogenous MYOD is expressed at a protein level in a subset of human medulloblastomas. Immunohistochemical detection of MYOD on human medulloblastoma tissue has not yielded definitive results due to technical issues. I will carry out Western blot analyses as an alternative approach. Third, to identify molecules besides Id3 that are involved in the MyoD mediated tumor suppressor network, gene expression profiling from the late onset MyoD wt/wt SmoA2 and early onset MyoD -/wt; SmoA2 tumors will be a pertinent approach. Third, to determine if MyoD exerts its tumor suppressor effect through Id3, the effect of overexpressing and silencing Id3, on tumorigenesis will be studied. Fourth, experimental approaches to assess the functional significance of MyoD expression in early postnatal development will need to be determined. MyoD possibly does not regulate GNP proliferation since histological analyses of cerebellar sections from MyoD -/- , MyoD -/wt and MyoD wt/wt does not reveal any apparent differences in GNP number.

Bibliography

- Adams BD, Furneaux H, White BA (2007) The micro-ribonucleic acid (miRNA) miR-206 targets the human estrogen receptor-alpha (ERalpha) and represses ERalpha messenger RNA and protein expression in breast cancer cell lines. *Mol Endocrinol* 21:1132-1147.
- Ahuja N, Li Q, Mohan AL, Baylin SB, Issa JP (1998) Aging and DNA methylation in colorectal mucosa and cancer. *Cancer research* 58:5489-5494.
- Alder J, Lee KJ, Jessell TM, Hatten ME (1999) Generation of cerebellar granule neurons in vivo by transplantation of BMP-treated neural progenitor cells. *Nat Neurosci* 2:535-540.
- Alderson LM, Castleberg RL, Harsh GRt, Louis DN, Henson JW (1995) Human gliomas with wild-type p53 express bcl-2. *Cancer research* 55:999-1001.
- Andres-Barquin PJ, Hernandez MC, Israel MA (2000) Id genes in nervous system development. *Histol Histopathol* 15:603-618.
- Ashburner M, Ball CA, Blake JA, Botstein D, Butler H, Cherry JM, Davis AP, Dolinski K, Dwight SS, Eppig JT, Harris MA, Hill DP, Issel-Tarver L, Kasarskis A, Lewis S, Matese JC, Richardson JE, Ringwald M, Rubin GM, Sherlock G (2000) Gene ontology: tool for the unification of biology. The Gene Ontology Consortium. *Nat Genet* 25:25-29.
- Ayrault O, Zhao H, Zindy F, Qu C, Sherr CJ, Roussel MF (2010) Atoh1 inhibits neuronal differentiation and collaborates with Gli1 to generate medulloblastoma-initiating cells. *Cancer research* 70:5618-5627.
- Bain G, Maandag EC, Izon DJ, Amsen D, Kruisbeek AM, Weintraub BC, Krop I, Schlissel MS, Feeney AJ, van Roon M, et al. (1994) E2A proteins are required for proper B cell development and initiation of immunoglobulin gene rearrangements. *Cell* 79:885-892.
- Banerjee AK, Kak VK (1973) Teratoid tumour of the cerebellum. *J Pathol* 111:285-287.

- Baptista CA, Hatten ME, Blazeski R, Mason CA (1994) Cell-cell interactions influence survival and differentiation of purified Purkinje cells in vitro. *Neuron* 12:243-260.
- Barakat MT, Humke EW, Scott MP (2010) Learning from Jekyll to control Hyde: Hedgehog signaling in development and cancer. *Trends in molecular medicine* 16:337-348.
- Ben-Arie N, Bellen HJ, Armstrong DL, McCall AE, Gordadze PR, Guo Q, Matzuk MM, Zoghbi HY (1997) Math1 is essential for genesis of cerebellar granule neurons. *Nature* 390:169-172.
- Berman DM, Karhadkar SS, Hallahan AR, Pritchard JI, Eberhart CG, Watkins DN, Chen JK, Cooper MK, Taipale J, Olson JM, Beachy PA (2002) Medulloblastoma growth inhibition by hedgehog pathway blockade. *Science* 297:1559-1561.
- Boldogkoi Z, Balint K, Awatramani GB, Balya D, Busskamp V, Viney TJ, Lagali PS, Duebel J, Pasti E, Tombacz D, Toth JS, Takacs IF, Scherf BG, Roska B (2009) Genetically timed, activity-sensor and rainbow transsynaptic viral tools. *Nature methods* 6:127-130.
- Briggs KJ, Corcoran-Schwartz IM, Zhang W, Harcke T, Devereux WL, Baylin SB, Eberhart CG, Watkins DN (2008) Cooperation between the Hic1 and Ptch1 tumor suppressors in medulloblastoma. *Genes & development* 22:770-785.
- Calin GA, Croce CM (2006) MicroRNA signatures in human cancers. *Nat Rev Cancer* 6:857-866.
- Cao Y, Yao Z, Sarkar D, Lawrence M, Sanchez GJ, Parker MH, MacQuarrie KL, Davison J, Morgan MT, Ruzzo WL, Gentleman RC, Tapscott SJ (2010) Genome-wide MyoD binding in skeletal muscle cells: a potential for broad cellular reprogramming. *Dev Cell* 18:662-674.
- Castellino RC, De Bortoli M, Lin LL, Skapura DG, Rajan JA, Adesina AM, Perlaky L, Irwin MS, Kim JY (2007) Overexpressed TP73 induces apoptosis in medulloblastoma. *BMC Cancer* 7:127.

- Chen CH, Kuo SC, Huang LJ, Hsu MH, Lung FD (2010) Affinity of synthetic peptide fragments of MyoD for Id1 protein and their biological effects in several cancer cells. *J Pept Sci* 16:231-241.
- Chen JK, Taipale J, Cooper MK, Beachy PA (2002) Inhibition of Hedgehog signaling by direct binding of cyclopamine to Smoothened. *Genes & development* 16:2743-2748.
- Chen X, Yan Q, Li S, Zhou L, Yang H, Yang Y, Liu X, Wan X (2012) Expression of the tumor suppressor miR-206 is associated with cellular proliferative inhibition and impairs invasion in ERalpha-positive endometrioid adenocarcinoma. *Cancer Lett* 314:41-53.
- Chizhikov V, Millen KJ (2003) Development and malformations of the cerebellum in mice. *Mol Genet Metab* 80:54-65.
- Cho YJ, Tsherniak A, Tamayo P, Santagata S, Ligon A, Greulich H, Berhoukim R, Amani V, Goumnerova L, Eberhart CG, Lau CC, Olson JM, Gilbertson RJ, Gajjar A, Delattre O, Kool M, Ligon K, Meyerson M, Mesirov JP, Pomeroy SL (2011) Integrative genomic analysis of medulloblastoma identifies a molecular subgroup that drives poor clinical outcome. *Journal of clinical oncology : official journal of the American Society of Clinical Oncology* 29:1424-1430.
- Choi J, Costa ML, Mermelstein CS, Chagas C, Holtzer S, Holtzer H (1990) MyoD converts primary dermal fibroblasts, chondroblasts, smooth muscle, and retinal pigmented epithelial cells into striated mononucleated myoblasts and multinucleated myotubes. *Proceedings of the National Academy of Sciences of the United States of America* 87:7988-7992.
- Cohen MM, Jr. (2010) Hedgehog signaling update. *Am J Med Genet A* 152A:1875-1914.
- Corbit KC, Aanstad P, Singla V, Norman AR, Stainier DY, Reiter JF (2005) Vertebrate Smoothened functions at the primary cilium. *Nature* 437:1018-1021.
- Corrales JD, Blaess S, Mahoney EM, Joyner AL (2006) The level of sonic hedgehog signaling regulates the complexity of cerebellar foliation. *Development* 133:1811-1821.

- Corrales JD, Rocco GL, Blaess S, Guo Q, Joyner AL (2004) Spatial pattern of sonic hedgehog signaling through Gli genes during cerebellum development. *Development* 131:5581-5590.
- Crawford JR, MacDonald TJ, Packer RJ (2007) Medulloblastoma in childhood: new biological advances. *Lancet Neurol* 6:1073-1085.
- Crawley JN (1999) Behavioral phenotyping of transgenic and knockout mice: experimental design and evaluation of general health, sensory functions, motor abilities, and specific behavioral tests. *Brain Research* 835:18-26.
- D'Angio GJ, Evans AE, Koop CE (1971) Special pattern of widespread neuroblastoma with a favourable prognosis. *Lancet* 1:1046-1049.
- Daubas P, Tajbakhsh S, Hadchouel J, Primig M, Buckingham M (2000) Myf5 is a novel early axonal marker in the mouse brain and is subjected to post-transcriptional regulation in neurons. *Development* 127:319-331.
- Denef N, Neubuser D, Perez L, Cohen SM (2000) Hedgehog induces opposite changes in turnover and subcellular localization of patched and smoothened. *Cell* 102:521-531.
- Duplan SM, Theoret Y, Kenigsberg RL (2002) Antitumor activity of fibroblast growth factors (FGFs) for medulloblastoma may correlate with FGF receptor expression and tumor variant. *Clin Cancer Res* 8:246-257.
- Er U, Yigitkanli K, Kazanci B, Ozturk E, Sorar M, Bavbek M (2008) Medullomyoblastoma: teratoid nature of a quite rare neoplasm. *Surg Neurol* 69:403-406.
- Erickson JW, Cline TW (1991) Molecular nature of the Drosophila sex determination signal and its link to neurogenesis. *Science* 251:1071-1074.
- Fernandez LA, Northcott PA, Dalton J, Fraga C, Ellison D, Angers S, Taylor MD, Kenney AM (2009) YAP1 is amplified and up-regulated in hedgehog-associated medulloblastomas and mediates Sonic hedgehog-driven neural precursor proliferation. *Genes & development* 23:2729-2741.

- Ferretti E, De Smaele E, Di Marcotullio L, Screpanti I, Gulino A (2005) Hedgehog checkpoints in medulloblastoma: the chromosome 17p deletion paradigm. *Trends in molecular medicine* 11:537-545.
- Ferretti E, De Smaele E, Miele E, Laneve P, Po A, Pelloni M, Paganelli A, Di Marcotullio L, Caffarelli E, Screpanti I, Bozzoni I, Gulino A (2008) Concerted microRNA control of Hedgehog signalling in cerebellar neuronal progenitor and tumour cells. *Embo J* 27:2616-2627.
- Fogarty MP, Emmenegger BA, Gräsfeder LL, Oliver TG, Wechsler-Reya RJ (2007) Fibroblast growth factor blocks Sonic hedgehog signaling in neuronal precursors and tumor cells. *Proceedings of the National Academy of Sciences of the United States of America* 104:2973-2978.
- Fujita S (1967) Quantitative analysis of cell proliferation and differentiation in the cortex of the postnatal mouse cerebellum. *J Cell Biol* 32:277-287.
- Gajjar A et al. (2006) Risk-adapted craniospinal radiotherapy followed by high-dose chemotherapy and stem-cell rescue in children with newly diagnosed medulloblastoma (St Jude Medulloblastoma-96): long-term results from a prospective, multicentre trial. *Lancet Oncol* 7:813-820.
- Gerber AN, Tapscott SJ (1996) Tumor cell complementation groups based on myogenic potential: evidence for inactivation of loci required for basic helix-loop-helix protein activity. *Molecular and cellular biology* 16:3901-3908.
- Ghez C, Fahn, S. (1985) The Cerebellum, in *Principles of Neural Science*, 2nd Edition. New York: Elsevier.
- Gibson P et al. (2010) Subtypes of medulloblastoma have distinct developmental origins. *Nature* 468:1095-1099.
- Gilbertson RJ, Ellison DW (2008) The origins of medulloblastoma subtypes. *Annu Rev Pathol* 3:341-365.
- Goldowitz D, Hamre K (1998) The cells and molecules that make a cerebellum. *Trends Neurosci* 21:375-382.

- Goldowitz D, Cushing RC, Laywell E, D'Arcangelo G, Sheldon M, Sweet HO, Davisson M, Steindler D, Curran T (1997) Cerebellar disorganization characteristic of reeler in scrambler mutant mice despite presence of reelin. *The Journal of neuroscience : the official journal of the Society for Neuroscience* 17:8767-8777.
- Gong S, Zheng C, Doughty ML, Losos K, Didkovsky N, Schambra UB, Nowak NJ, Joyner A, Leblanc G, Hatten ME, Heintz N (2003) A gene expression atlas of the central nervous system based on bacterial artificial chromosomes. *Nature* 425:917-925.
- Goodrich LV, Milenkovic L, Higgins KM, Scott MP (1997) Altered neural cell fates and medulloblastoma in mouse patched mutants. *Science* 277:1109-1113.
- Hahn H, Wojnowski L, Specht K, Kappler R, Calzada-Wack J, Potter D, Zimmer A, Muller U, Samson E, Quintanilla-Martinez L (2000) Patched target Igf2 is indispensable for the formation of medulloblastoma and rhabdomyosarcoma. *J Biol Chem* 275:28341-28344.
- Hallahan AR, Pritchard JI, Chandraratna RA, Ellenbogen RG, Geyer JR, Overland RP, Strand AD, Tapscott SJ, Olson JM (2003) BMP-2 mediates retinoid-induced apoptosis in medulloblastoma cells through a paracrine effect. *Nature medicine* 9:1033-1038.
- Hallahan AR, Pritchard JI, Hansen S, Benson M, Stoeck J, Hatton BA, Russell TL, Ellenbogen RG, Bernstein ID, Beachy PA, Olson JM (2004) The SmoA1 mouse model reveals that notch signaling is critical for the growth and survival of sonic hedgehog-induced medulloblastomas. *Cancer Res* 64:7794-7800.
- Hansen T, Olsen L, Lindow M, Jakobsen KD, Ullum H, Jonsson E, Andreassen OA, Djurovic S, Melle I, Agartz I, Hall H, Timm S, Wang AG, Werge T (2007) Brain expressed microRNAs implicated in schizophrenia etiology. *PLoS One* 2:e873.
- Hartmann W, Koch A, Brune H, Waha A, Schuller U, Dani I, Denkhaus D, Langmann W, Bode U, Wiestler OD, Schilling K, Pietsch T (2005) Insulin-like growth factor II is involved in the proliferation control of medulloblastoma and its cerebellar precursor cells. *Am J Pathol* 166:1153-1162.
- Hatada I, Fukasawa M, Kimura M, Morita S, Yamada K, Yoshikawa T, Yamanaka S, Endo C, Sakurada A, Sato M, Kondo T, Horii A, Ushijima T, Sasaki H (2006) Genome-wide profiling of promoter methylation in human. *Oncogene* 25:3059-3064.

Hatten ME (2002) New directions in neuronal migration. *Science* 297:1660-1663.

Hatten ME, Roussel MF (2011) Development and cancer of the cerebellum. *Trends Neurosci* 34:134-142.

Hatton BA, Knoepfler PS, Kenney AM, Rowitch DH, de Alboran IM, Olson JM, Eisenman RN (2006) N-myc is an essential downstream effector of Shh signaling during both normal and neoplastic cerebellar growth. *Cancer Res* 66:8655-8661.

Hatton BA, Villavicencio EH, Tsuchiya KD, Pritchard JL, Ditzler S, Pullar B, Hansen S, Knoblaugh SE, Lee D, Eberhart CG, Hallahan AR, Olson JM (2008) The Smo/Smo model: hedgehog-induced medulloblastoma with 90% incidence and leptomeningeal spread. *Cancer Res* 68:1768-1776.

Holl T, Kleihues P, Yasargil MG, Wiestler OD (1991) Cerebellar medulloblastoma with advanced neuronal differentiation and hamartomatous component. *Acta Neuropathol* 82:408-413.

Huangfu D, Anderson KV (2006) Signaling from Smo to Ci/Gli: conservation and divergence of Hedgehog pathways from *Drosophila* to vertebrates. *Development* 133:3-14.

Hui CC, Angers S (2011) Gli proteins in development and disease. *Annu Rev Cell Dev Biol* 27:513-537.

Huynh H (2004) Overexpression of tumour suppressor retinoblastoma 2 protein (pRb2/p130) in hepatocellular carcinoma. *Carcinogenesis* 25:1485-1494.

Jen Y, Weintraub H, Benezra R (1992) Overexpression of Id protein inhibits the muscle differentiation program: in vivo association of Id with E2A proteins. *Genes & development* 6:1466-1479.

Jensen P, Zoghbi HY, Goldowitz D (2002) Dissection of the cellular and molecular events that position cerebellar Purkinje cells: a study of the *math1* null-mutant mouse. *The Journal of neuroscience : the official journal of the Society for Neuroscience* 22:8110-8116.

- Jin W, Liu Y, Chen L, Zhu H, Di GH, Ling H, Wu J, Shao ZM (2011) Involvement of MyoD and c-myc in regulation of basal and estrogen-induced transcription activity of the BRCA1 gene. *Breast Cancer Res Treat* 125:699-713.
- Jones PA, Wolkowicz MJ, Rideout WM, 3rd, Gonzales FA, Marziasz CM, Coetzee GA, Tapscott SJ (1990) De novo methylation of the MyoD1 CpG island during the establishment of immortal cell lines. *Proceedings of the National Academy of Sciences of the United States of America* 87:6117-6121.
- Kablar B (2002) Different regulatory elements within the MyoD promoter control its expression in the brain and inhibit its functional consequences in neurogenesis. *Tissue Cell* 34:164-169.
- Kim HK, Lee YS, Sivaprasad U, Malhotra A, Dutta A (2006) Muscle-specific microRNA miR-206 promotes muscle differentiation. *J Cell Biol* 174:677-687.
- Kim J, Inoue K, Ishii J, Vanti WB, Voronov SV, Murchison E, Hannon G, Abeliovich A (2007) A MicroRNA feedback circuit in midbrain dopamine neurons. *Science* 317:1220-1224.
- Kitanaka C, Kato K, Ijiri R, Sakurada K, Tomiyama A, Noguchi K, Nagashima Y, Nakagawara A, Momoi T, Toyoda Y, Kigasawa H, Nishi T, Shirouzu M, Yokoyama S, Tanaka Y, Kuchino Y (2002) Increased Ras expression and caspase-independent neuroblastoma cell death: possible mechanism of spontaneous neuroblastoma regression. *J Natl Cancer Inst* 94:358-368.
- Klein RS, Rubin JB, Gibson HD, DeHaan EN, Alvarez-Hernandez X, Segal RA, Luster AD (2001) SDF-1 alpha induces chemotaxis and enhances Sonic hedgehog-induced proliferation of cerebellar granule cells. *Development* 128:1971-1981.
- Klisch TJ, Xi Y, Flora A, Wang L, Li W, Zoghbi HY (2011) In vivo Atoh1 targetome reveals how a proneural transcription factor regulates cerebellar development. *Proceedings of the National Academy of Sciences of the United States of America* 108:3288-3293.
- Komuro H, Yacubova E, Rakic P (2001) Mode and tempo of tangential cell migration in the cerebellar external granular layer. *The Journal of neuroscience : the official journal of the Society for Neuroscience* 21:527-540.

- Kondo N, Toyama T, Sugiura H, Fujii Y, Yamashita H (2008) miR-206 Expression is down-regulated in estrogen receptor alpha-positive human breast cancer. *Cancer research* 68:5004-5008.
- Kool M, Koster J, Bunt J, Hasselt NE, Lakeman A, van Sluis P, Troost D, Meeteren NS, Caron HN, Cloos J, Masic A, Ylstra B, Grajkowska W, Hartmann W, Pietsch T, Ellison D, Clifford SC, Versteeg R (2008) Integrated genomics identifies five medulloblastoma subtypes with distinct genetic profiles, pathway signatures and clinicopathological features. *PLoS One* 3:e3088.
- Lee H, Habas R, Abate-Shen C (2004) MSX1 cooperates with histone H1b for inhibition of transcription and myogenesis. *Science* 304:1675-1678.
- Lee HY, Greene LA, Mason CA, Manzini MC (2009) Isolation and culture of post-natal mouse cerebellar granule neuron progenitor cells and neurons. *J Vis Exp*.
- Lin CH, Stoeck J, Ravanpay AC, Guillemot F, Tapscott SJ, Olson JM (2004) Regulation of neuroD2 expression in mouse brain. *Developmental biology* 265:234-245.
- Lleonart ME, Artero-Castro A, Kondoh H (2009) Senescence induction; a possible cancer therapy. *Mol Cancer* 8:3.
- Lowe SW, Cepero E, Evan G (2004) Intrinsic tumour suppression. *Nature* 432:307-315.
- Lum L, Beachy PA (2004) The Hedgehog response network: sensors, switches, and routers. *Science* 304:1755-1759.
- Lyden D, Young AZ, Zagzag D, Yan W, Gerald W, O'Reilly R, Bader BL, Hynes RO, Zhuang Y, Manova K, Benezra R (1999) Id1 and Id3 are required for neurogenesis, angiogenesis and vascularization of tumour xenografts. *Nature* 401:670-677.
- Mahapatra AK, Sinha AK, Sharma MC (1998) Medulloblastoma. A rare cerebellar tumour in children. *Childs Nerv Syst* 14:312-316.
- Marino S (2005) Medulloblastoma: developmental mechanisms out of control. *Trends Mol Med* 11:17-22.

- Markant SL, Wechsler-Reya RJ (2011) Personalized Mice: Modeling the Molecular Heterogeneity of Medulloblastoma. *Neuropathol Appl Neurobiol*.
- Mehler MF, Mattick JS (2006) Non-coding RNAs in the nervous system. *J Physiol* 575:333-341.
- Mishra DK, Chen Z, Wu Y, Sarkissyan M, Koeffler HP, Vadgama JV (2010) Global methylation pattern of genes in androgen-sensitive and androgen-independent prostate cancer cells. *Mol Cancer Ther* 9:33-45.
- Munoz NM, Beard BC, Ryu BY, Luche RM, Trobridge GD, Rawlings DJ, Scharenberg AM, Kiem HP (2011) Novel reporter systems for facile evaluation of I-SceI-mediated genome editing. *Nucleic Acids Res*.
- Nickerson HJ, Matthay KK, Seeger RC, Brodeur GM, Shimada H, Perez C, Atkinson JB, Selch M, Gerbing RB, Stram DO, Lukens J (2000) Favorable biology and outcome of stage IV-S neuroblastoma with supportive care or minimal therapy: a Children's Cancer Group study. *Journal of clinical oncology : official journal of the American Society of Clinical Oncology* 18:477-486.
- Nishida K, Flanagan JG, Nakamoto M (2002) Domain-specific olivocerebellar projection regulated by the EphA-ephrin-A interaction. *Development* 129:5647-5658.
- Northcott PA, Fernandez LA, Hagan JP, Ellison DW, Grajkowska W, Gillespie Y, Grundy R, Van Meter T, Rutka JT, Croce CM, Kenney AM, Taylor MD (2009) The miR-17/92 polycistron is up-regulated in sonic hedgehog-driven medulloblastomas and induced by N-myc in sonic hedgehog-treated cerebellar neural precursors. *Cancer research* 69:3249-3255.
- Northcott PA, Korshunov A, Witt H, Hielscher T, Eberhart CG, Mack S, Bouffet E, Clifford SC, Hawkins CE, French P, Rutka JT, Pfister S, Taylor MD (2011a) Medulloblastoma comprises four distinct molecular variants. *Journal of clinical oncology : official journal of the American Society of Clinical Oncology* 29:1408-1414.
- Northcott PA, Hielscher T, Dubuc A, Mack S, Shih D, Remke M, Al-Halabi H, Albrecht S, Jabado N, Eberhart CG, Grajkowska W, Weiss WA, Clifford SC, Bouffet E, Rutka JT, Korshunov A, Pfister S, Taylor MD (2011b) Pediatric and adult sonic hedgehog medulloblastomas are clinically and molecularly distinct. *Acta Neuropathol* 122:231-240.

Ohuchida K, Mizumoto K, Ohhashi S, Yamaguchi H, Konomi H, Nagai E, Yamaguchi K, Tsuneyoshi M, Tanaka M (2006) S100A11, a putative tumor suppressor gene, is overexpressed in pancreatic carcinogenesis. *Clin Cancer Res* 12:5417-5422.

Oliver TG, Read TA, Kessler JD, Mehmeti A, Wells JF, Huynh TT, Lin SM, Wechsler-Reya RJ (2005) Loss of patched and disruption of granule cell development in a pre-neoplastic stage of medulloblastoma. *Development* 132:2425-2439.

Olsen L, Klausen M, Helboe L, Nielsen FC, Werge T (2009) MicroRNAs show mutually exclusive expression patterns in the brain of adult male rats. *PLoS One* 4:e7225.

Pietsch T, Waha A, Koch A, Kraus J, Albrecht S, Tonn J, Sorensen N, Berthold F, Henk B, Schmandt N, Wolf HK, von Deimling A, Wainwright B, Chenevix-Trench G, Wiestler OD, Wicking C (1997) Medulloblastomas of the desmoplastic variant carry mutations of the human homologue of *Drosophila* patched. *Cancer research* 57:2085-2088.

Pollard SM, Yoshikawa K, Clarke ID, Danovi D, Stricker S, Russell R, Bayani J, Head R, Lee M, Bernstein M, Squire JA, Smith A, Dirks P (2009) Glioma stem cell lines expanded in adherent culture have tumor-specific phenotypes and are suitable for chemical and genetic screens. *Cell Stem Cell* 4:568-580.

Pomeroy SL et al. (2002) Prediction of central nervous system embryonal tumour outcome based on gene expression. *Nature* 415:436-442.

Rakic P, Sidman RL (1973) Organization of cerebellar cortex secondary to deficit of granule cells in weaver mutant mice. *J Comp Neurol* 152:133-161.

Rao C, Friedlander ME, Klein E, Anzil AP, Sher JH (1990) Medullomyoblastoma in an adult. *Cancer* 65:157-163.

Rao G, Pedone CA, Del Valle L, Reiss K, Holland EC, Fults DW (2004) Sonic hedgehog and insulin-like growth factor signaling synergize to induce medulloblastoma formation from nestin-expressing neural progenitors in mice. *Oncogene* 23:6156-6162.

Reifenberger J, Wolter M, Weber RG, Megahed M, Ruzicka T, Lichter P, Reifenberger G (1998) Missense mutations in SMOH in sporadic basal cell carcinomas of the skin

- and primitive neuroectodermal tumors of the central nervous system. *Cancer Res* 58:1798-1803.
- Rice DS, Curran T (1999) Mutant mice with scrambled brains: understanding the signaling pathways that control cell positioning in the CNS. *Genes & development* 13:2758-2773.
- Rideout WM, 3rd, Eversole-Cire P, Spruck CH, 3rd, Hustad CM, Coetzee GA, Gonzales FA, Jones PA (1994) Progressive increases in the methylation status and heterochromatinization of the myoD CpG island during oncogenic transformation. *Mol Cell Biol* 14:6143-6152.
- Rogers DC, Fisher EM, Brown SD, Peters J, Hunter AJ, Martin JE (1997) Behavioral and functional analysis of mouse phenotype: SHIRPA, a proposed protocol for comprehensive phenotype assessment. *Mamm Genome* 8:711-713.
- Rohatgi R, Milenkovic L, Scott MP (2007) Patched1 regulates hedgehog signaling at the primary cilium. *Science* 317:372-376.
- Romagosa C, Simonetti S, Lopez-Vicente L, Mazo A, Lleonart ME, Castellvi J, Ramon y Cajal S (2011) p16(Ink4a) overexpression in cancer: a tumor suppressor gene associated with senescence and high-grade tumors. *Oncogene* 30:2087-2097.
- Rosenberg MI, Georges SA, Asawachaicharn A, Analau E, Tapscott SJ (2006) MyoD inhibits Fstl1 and Utrn expression by inducing transcription of miR-206. *J Cell Biol* 175:77-85.
- Rozen S, Skaletsky H (2000) Primer3 on the WWW for general users and for biologist programmers. *Methods Mol Biol* 132:365-386.
- Rubin JB, Choi Y, Segal RA (2002) Cerebellar proteoglycans regulate sonic hedgehog responses during development. *Development* 129:2223-2232.
- Rubin LL, de Sauvage FJ (2006) Targeting the Hedgehog pathway in cancer. *Nature reviews Drug discovery* 5:1026-1033.
- Rudnicki MA, Braun T, Hinuma S, Jaenisch R (1992) Inactivation of MyoD in mice leads to up-regulation of the myogenic HLH gene Myf-5 and results in apparently normal muscle development. *Cell* 71:383-390.

- Ruiz i Altaba A (2008) Therapeutic inhibition of Hedgehog-Gli signaling in cancer: epithelial, stromal, or stem cell targets? *Cancer Cell* 14:281-283.
- Ruiz i Altaba A, Palma V, Dahmane N (2002) Hedgehog-Gli signalling and the growth of the brain. *Nature reviews Neuroscience* 3:24-33.
- Rutka JT, Dougherty DV, Giblin JR, Edwards MS, McCulloch JR, Rosenblum ML (1987) Growth of a medulloblastoma on normal leptomeningeal cells in culture: interaction of tumor cells and normal cells. *Neurosurgery* 21:872-878.
- Ruzinova MB, Benezra R (2003) Id proteins in development, cell cycle and cancer. *Trends Cell Biol* 13:410-418.
- Saury JM, Emanuelson I (2011) Cognitive consequences of the treatment of medulloblastoma among children. *Pediatr Neurol* 44:21-30.
- Schiffer D, Giordana MT, Pezzotta S, Pezzulo T, Vigliani MC (1992) Medullomyoblastoma: report of two cases. *Childs Nerv Syst* 8:268-272.
- Schuller U, Heine VM, Mao J, Kho AT, Dillon AK, Han YG, Huillard E, Sun T, Ligon AH, Qian Y, Ma Q, Alvarez-Buylla A, McMahon AP, Rowitch DH, Ligon KL (2008) Acquisition of granule neuron precursor identity is a critical determinant of progenitor cell competence to form Shh-induced medulloblastoma. *Cancer Cell* 14:123-134.
- Selvadurai HJ, Mason JO (2011) Wnt/beta-catenin signalling is active in a highly dynamic pattern during development of the mouse cerebellum. *PLoS One* 6:e23012.
- Sengupta R, Dubuc A, Ward S, Yang L, Northcott P, Woerner BM, Kroll K, Luo J, Taylor MD, Wechsler-Reya RJ, Rubin JB (2011) CXCR4 activation defines a new subgroup of Sonic Hedgehog driven Medulloblastoma. *Cancer research*.
- Sikder HA, Devlin MK, Dunlap S, Ryu B, Alani RM (2003) Id proteins in cell growth and tumorigenesis. *Cancer Cell* 3:525-530.
- Sillitoe RV, Joyner AL (2007) Morphology, molecular codes, and circuitry produce the three-dimensional complexity of the cerebellum. *Annu Rev Cell Dev Biol* 23:549-577.

- Smeyne RJ, Chu T, Lewin A, Bian F, Sanlioglu S, Kunsch C, Lira SA, Oberdick J (1995) Local control of granule cell generation by cerebellar Purkinje cells. *Molecular and cellular neurosciences* 6:230-251.
- Smith TW, Davidson RI (1984) Medullomyoblastoma. A histologic, immunohistochemical, and ultrastructural study. *Cancer* 54:323-332.
- Song G, Zhang Y, Wang L (2009) MicroRNA-206 targets notch3, activates apoptosis, and inhibits tumor cell migration and focus formation. *J Biol Chem* 284:31921-31927.
- Sotelo C, Chedotal A (1997) Development of the olivocerebellar projection. *Perspect Dev Neurobiol* 5:57-67.
- Spassky N, Han YG, Aguilar A, Strehl L, Besse L, Laclef C, Romaguera Ros M, Garcia-Verdugo JM, Alvarez-Buylla A (2008) Primary cilia are required for cerebellar development and Shh-dependent expansion of progenitor pool. *Dev Biol*.
- Stylianopoulou F, Herbert J, Soares MB, Efstratiadis A (1988) Expression of the insulin-like growth factor II gene in the choroid plexus and the leptomeninges of the adult rat central nervous system. *Proceedings of the National Academy of Sciences of the United States of America* 85:141-145.
- Sudarov A, Joyner AL (2007) Cerebellum morphogenesis: the foliation pattern is orchestrated by multi-cellular anchoring centers. *Neural Dev* 2:26.
- Swartling FJ et al. (2010) Pleiotropic role for MYCN in medulloblastoma. *Genes & development* 24:1059-1072.
- Taipale J, Chen JK, Cooper MK, Wang B, Mann RK, Milenkovic L, Scott MP, Beachy PA (2000) Effects of oncogenic mutations in Smoothened and Patched can be reversed by cyclopamine. *Nature* 406:1005-1009.
- Tajbakhsh S, Buckingham ME (1995) Lineage restriction of the myogenic conversion factor myf-5 in the brain. *Development* 121:4077-4083.
- Tapscott SJ (2005) The circuitry of a master switch: MyoD and the regulation of skeletal muscle gene transcription. *Development* 132:2685-2695.

- Taulli R, Bersani F, Foglizzo V, Linari A, Vigna E, Ladanyi M, Tuschl T, Ponzetto C (2009) The muscle-specific microRNA miR-206 blocks human rhabdomyosarcoma growth in xenotransplanted mice by promoting myogenic differentiation. *J Clin Invest* 119:2366-2378.
- Taylor MD, Northcott PA, Korshunov A, Remke M, Cho YJ, Clifford SC, Eberhart CG, Parsons DW, Rutkowski S, Gajjar A, Ellison DW, Lichter P, Gilbertson RJ, Pomeroy SL, Kool M, Pfister SM (2011) Molecular subgroups of medulloblastoma: the current consensus. *Acta Neuropathol*.
- Thompson MC, Fuller C, Hogg TL, Dalton J, Finkelstein D, Lau CC, Chintagumpala M, Adesina A, Ashley DM, Kellie SJ, Taylor MD, Curran T, Gajjar A, Gilbertson RJ (2006) Genomics identifies medulloblastoma subgroups that are enriched for specific genetic alterations. *J Clin Oncol* 24:1924-1931.
- Uziel T, Karginov FV, Xie S, Parker JS, Wang YD, Gajjar A, He L, Ellison D, Gilbertson RJ, Hannon G, Roussel MF (2009) The miR-17~92 cluster collaborates with the Sonic Hedgehog pathway in medulloblastoma. *Proc Natl Acad Sci U S A* 106:2812-2817.
- Vachon P, Girard C, Theoret Y (2004) Effects of basic fibroblastic growth factor on the growth of human medulloblastoma xenografts. *J Neurooncol* 67:139-146.
- Vaillant C, Monard D (2009) SHH pathway and cerebellar development. *Cerebellum* 8:291-301.
- Wang VY, Zoghbi HY (2001) Genetic regulation of cerebellar development. *Nat Rev Neurosci* 2:484-491.
- Wang X, Ling C, Bai Y, Zhao J (2011) MicroRNA-206 is associated with invasion and metastasis of lung cancer. *Anat Rec (Hoboken)* 294:88-92.
- Wassef M, Cholley B, Heizmann CW, Sotelo C (1992) Development of the olivocerebellar projection in the rat: II. Matching of the developmental compartmentations of the cerebellum and inferior olive through the projection map. *J Comp Neurol* 323:537-550.
- Watt FM, Frye M, Benitah SA (2008) MYC in mammalian epidermis: how can an oncogene stimulate differentiation? *Nat Rev Cancer* 8:234-242.

- Wechsler-Reya RJ, Scott MP (1999) Control of neuronal precursor proliferation in the cerebellum by Sonic Hedgehog. *Neuron* 22:103-114.
- Weintraub H, Davis R, Tapscott S, Thayer M, Krause M, Benezra R, Blackwell TK, Turner D, Rupp R, Hollenberg S, et al. (1991) The myoD gene family: nodal point during specification of the muscle cell lineage. *Science* 251:761-766.
- Wen X, Lai CK, Evangelista M, Hongo JA, de Sauvage FJ, Scales SJ (2010) Kinetics of hedgehog-dependent full-length Gli3 accumulation in primary cilia and subsequent degradation. *Molecular and cellular biology* 30:1910-1922.
- Witek ME, Nielsen K, Walters R, Hyslop T, Palazzo J, Schulz S, Waldman SA (2005) The putative tumor suppressor Cdx2 is overexpressed by human colorectal adenocarcinomas. *Clin Cancer Res* 11:8549-8556.
- Wolfe-Christensen C, Mullins LL, Scott JG, McNall-Knapp RY (2007) Persistent psychosocial problems in children who develop posterior fossa syndrome after medulloblastoma resection. *Pediatr Blood Cancer* 49:723-726.
- Woloshin P, Song K, Degnin C, Killary AM, Goldhamer DJ, Sassoon D, Thayer MJ (1995) MSX1 inhibits myoD expression in fibroblast x 10T1/2 cell hybrids. *Cell* 82:611-620.
- Xie J, Murone M, Luoh SM, Ryan A, Gu Q, Zhang C, Bonifas JM, Lam CW, Hynes M, Goddard A, Rosenthal A, Epstein EH, Jr., de Sauvage FJ (1998) Activating Smoothed mutations in sporadic basal-cell carcinoma. *Nature* 391:90-92.
- Yang ZJ, Ellis T, Markant SL, Read TA, Kessler JD, Bourbonoulas M, Schuller U, Machold R, Fishell G, Rowitch DH, Wainwright BJ, Wechsler-Reya RJ (2008) Medulloblastoma can be initiated by deletion of Patched in lineage-restricted progenitors or stem cells. *Cancer Cell* 14:135-145.
- Yauch RL, Gould SE, Scales SJ, Tang T, Tian H, Ahn CP, Marshall D, Fu L, Januario T, Kallop D, Nannini-Pepe M, Kotkow K, Marsters JC, Rubin LL, de Sauvage FJ (2008) A paracrine requirement for hedgehog signalling in cancer. *Nature* 455:406-410.

- Yu F, Zhu X, Feng C, Wang T, Hong Q, Liu Z, Tang S (2011) Proteomics-based identification of spontaneous regression-associated proteins in neuroblastoma. *J Pediatr Surg* 46:1948-1955.
- Zebedee Z, Hara E (2001) Id proteins in cell cycle control and cellular senescence. *Oncogene* 20:8317-8325.
- Zhuang Y, Soriano P, Weintraub H (1994) The helix-loop-helix gene E2A is required for B cell formation. *Cell* 79:875-884.
- Zindy F, Knoepfler PS, Xie S, Sherr CJ, Eisenman RN, Roussel MF (2006) N-Myc and the cyclin-dependent kinase inhibitors p18Ink4c and p27Kip1 coordinately regulate cerebellar development. *Proceedings of the National Academy of Sciences of the United States of America* 103:11579-11583.

CURRICULUM VITAE

Educational Background:

- 08/2006 – 01/2012 **Doctor of Philosophy in Molecular and Cellular Biology**
University of Washington and Fred Hutchinson Cancer
Research Center, Seattle, Washington
Dissertation Title: Understanding the role of the Sonic hedgehog
signal transduction pathway in cerebellar development and
medulloblastoma
Advisor: Dr. James M. Olson
- 08/2004 – 05/2006 **Masters in Public Health (MPH) in Epidemiology**
Emory University, Atlanta, Georgia
Major: Epidemiology, GPA 3.96
Thesis: Racial disparities in receipt of hormonal therapy for breast
cancer
Advisor: Dr. MaryJo Lund
- 08/2002 - 10/2003 **Doctoral program** - changed in 2nd year to MPH
Baylor College of Medicine, Houston, Texas
Molecular and Cellular Biology, GPA 3.7
- 09/1998 - 08/2001 **Bachelors of Science**, First Class with Physiology Honors
Presidency College, University of Calcutta, India

Research Experience:

- 03/2012 – present **Postdoctoral Associate** - Fred Hutchinson Cancer Research
Center, Seattle, Washington
Advisor: Dr. James M. Olson
- 2006 – 2012 **Graduate Research Assistant** - Fred Hutchinson Cancer Research
Center and University of Washington, Seattle, WA
Advisor: Dr. James M. Olson

Project Overview:

- Designed and executed scientific experiments that led to identification of muscle differentiation factor, MyoD as a molecule that interacts with the Sonic hedgehog pathway (Shh) in the process of medulloblastoma genesis.
 - Identified a novel tumor suppressor function of MyoD expressed ectopically in the neoplastic cerebellum in mouse models of medulloblastoma.
 - Characterized a new genetic mouse model of medulloblastoma with a unique mutation in Smoothed (SmoA2) driving hyperactive Shh signaling.
 - Demonstrated the differences between two apparently similar mutations in Smoothed, SmoA1 and SmoA2, on cerebellar development, tumorigenesis and global transcriptional profiles.
- As member of a research team, actively contributed toward:
- Development of a platform consisting of patient-derived orthotopic xenograft mouse models for personalized medicine endeavors.
 - Planning, coordination and execution of a preclinical drug trial, related assays and data analysis.

Graduate Rotation Project Topics:

- Role of N-Myc and NeuroD2 in neuronal proliferation & differentiation
Advisor: Dr. James M. Olson
- Effects of Environmental Agents on Parkinson's Disease
Advisor: Dr. Leo Pallanck
- Deciphering the functions of the different domains of Dystrophin
Advisor: Dr. Jeffrey Chamberlain

10/2004 – 05/2006

Research Assistant**Centers for Disease Control and Prevention (CDC), Atlanta**

Multi Drug Resistant Tuberculosis Research Group

Supervisor: Dr. Peter Cegielski

Designed database using *Epi Info* software and conducted data analysis using SAS statistical software for a multinational prospective epidemiological study of multidrug resistant tuberculosis treatment through second-line drugs.

05/2005 – 08/2005

Summer Intern**Wyeth Pharmaceuticals, Collegeville, Pennsylvania**

Global Health Outcomes Assessment (Research and Development)

Supervisors: Dr. Amitabh Singh and Dr. Rezaul Khandker

- Analyzed and reported Phase II Clinical Trial Health Outcomes data of Idiopathic Pulmonary Fibrosis patient study population
- Authored and presented internal research report on '*Comorbidity of Depression in Rheumatoid Arthritis patients and Possible Pharmacological Interventions*' to Rheumatology Global Brand Team

08/2002 - 10/2003

Graduate Research Assistant**Baylor College of Medicine, Houston, Texas**

Executed scientific experiments, analyzed, interpreted and presented data for research projects in areas of nuclear receptor biology, alternative mRNA-splicing regulation and Transforming growth factor-beta signaling pathway.

05/2002 - 08/2002

Project Intern**Baylor College of Medicine, Houston, Texas**

Supervisor: Dr. Nancy Weigel

Investigated the role of co-repressors in regulation of agonist dependent transcriptional activity of androgen and progesterone receptors.

Technical support provided in study by AgoulNIK *et al.* (2003) JBC 278.

11/2000 - 12/2000

Group Leader - Undergraduate Field Research Project**Presidency College, University of Calcutta, Calcutta, India**

Supervisor: Dr. Amrita Banerjee Maitra

Conducted an observational epidemiological study on employees of Rajasthan Atomic Power Station and a cohort of local inhabitants from adjoining rural areas to examine possible physiological effects due to long-term exposure to nuclear radiation, along with dietary survey and evaluation of existing health amenities.

Research related Skills:

- Grant and manuscript writing, scientific presentations and reports, manuscript peer-review

- Tissue culture techniques including establishment of primary cell lines, Transfection, Lentivirus production, Transduction.
- Use of mouse models for *in vivo* studies including surgical techniques to develop patient-derived orthotopic xenograft mouse models, Colony management, Histopathological analysis, Participation in preclinical trials
- DNA and RNA assays including Nuclei acid extraction, Cloning, Site-directed mutagenesis, Quantitative RT-PCR, miRNA assays
- Protein assays including Immunoprecipitation, Western blot analysis, Immunocytochemistry, Immunohistochemistry
- Imaging and Microscopy
- Computer skills include proficiency in Microsoft Word, Excel, Powerpoint, Adobe Photoshop, Adobe Illustrator, ImageJ, Prism Graphpad

Fellowships:

Pre-doctoral Training Grant in Developmental Biology,
National Institutes of Health (07/2009-03/2012)

Special Honors & Awards:

Member of Delta Omega Honorary Society in Public Health	2006
Govt. of India National Merit Scholarship for B.Sc. Examination	2001
Best Student Award for highest academic grade - B.Sc.1 st .Year	1999
Govt. of India National Merit Award for Secondary Examination	1996

Teaching Experience:

Graduate Teaching Assistant, - University of Washington, Seattle, WA
Courses:
Advanced Cell Biology
Instructor: Dr. Charles Laird
Biochemistry 441
Instructor: Dr. Ted Young and Dr. William Parson

Meetings and Lectures:

- American Association for Cancer Research Annual Meeting, Chicago, IL.
Presentation (Poster): A novel tumor-suppressor role of MyoD, a muscle differentiation factor, in mouse models of medulloblastoma
- Society for Developmental Biology Northwest Meeting, Friday Harbor, WA
Presentation (Talk): Role of MyoD in Medulloblastoma
- Society for Neuroscience Conference, San Diego, CA
Presentation (Poster): A mouse model of medulloblastoma reveals a novel tumor suppressive function of muscle differentiation factor, MyoD in the cerebellum.
- Bear Necessities Pediatric Cancer Foundation Research Symposium, Chicago, IL
Presentation (Talk, invited): Investigating two oncogenic mutations in Smoothed with vastly different effects on cerebellar development in mice

Publications:

Trinh, K., Moore, K., Wes, PD., Muchowski, PJ., **Dey, J.**, Pallanck, LJ., *et al.* Induction of the phase II detoxification pathway suppresses neuron loss in *Drosophila* models of Parkinson's disease. *J Neurosci* 28, 465-472 (2008).

Dey, J., et al. (2012) Oncogenic mutation in *Smoothed* causes aberrant cerebellar development and medulloblastoma in mice (submitted)

Dey, J., et al. (2012) A novel tumor suppressor role of muscle differentiation factor, MyoD in mouse models of medulloblastoma (in preparation)

Administrative Assignments:

09/2000 – 08/2001

Editor – Department of Physiology, Presidency College, Calcutta, India

Student Publications and Departmental Magazine

09/1999 - 08/2000

Secretary - Physiological Institute, Presidency College, Calcutta, India

Organized, administered and managed academic activities of the Institute including scientific seminars, intercollegiate debates, lecture competitions and alumni liaison activities.

Personal Interests:

Piano - Completed certification courses under the Associated Board of the Royal Schools of Music, London.

Public speaking, Creative writing & Travel photography
